2012

Urban population density and environmental quality in Port-au-Prince, Haiti: a geo-statistical analysis

Myrtho Joseph
Louisiana State University and Agricultural and Mechanical College, mjose13@lsu.edu

URBAN POPULATION DENSITY AND ENVIRONMENTAL QUALITY IN PORT-AU-PRINCE, HAITI: A GEO-STATISTICAL ANALYSIS

A Dissertation

Submitted to the Graduate Faculty of the
Louisiana State University and
Agricultural and Mechanical College
in partial fulfillment of the
requirements for the degree of
Doctor of Philosophy

in

The Department of Geography and Anthropology

by
Myrtho Joseph
B.S., State University of Haiti, 1994
M.S. The University of Arizona, 2007
August 2012

DEDICATION

To God first, to my parents, my loving and supportive wife Marjorie and my wonderful children, Chris-Annie, David and Stive.

ACKNOWLEDGMENTS

Thanks to God first who gives me life and have made possible the achievement of this doctoral study. I owe the successful completion of this dissertation much to the advice, the support, the involvement, and the encouragement of several people. My profound gratitude extends first to my academic advisor, Professor Fahui Wang who has showed dedication, patience, professionalism, and a great sense of excellence and commitment to my success. Professor Wang's great sense of humor has also made our collaboration smoother. Dr Wang has successfully infected me with his viral passion for urban geography. I want to thank Professor Lei Wang who has lightened my path with his insightful advices particularly when I faced technical obstacles during my research. In the same vein, I cannot understate the sporadic but precious support of my classmate and friend Quan Tang always available when I need him, though we have been in the same boat. I am grateful for the encouragement of my colleagues Anzhelika Antipova and Yanqin Xu with whom I share the space that served like home away from home.

I am very appreciative of Dr Lam and Dr. Leitner's for their precious support and advice.

I am very thankful for the LSU Graduate School for the Huel D. Perkins Diversity Fellowship that financially supported my research from 2008 to 2012.

I want to extent my gratitude to the members of the West-Russell travel grant and the Materials award committee who, with the travel grant and the material award, has made possible the concretization of the field research in Port-au-Prince. I am grateful for the contribution of some generous donors to the field trip. They want to remain anonymous but their sensitivity and support for the cause of Haiti cannot be ignored and is much appreciated.

I also extend my deep appreciation to Ing. Anaël Hyppolite and Agr. Michel S. Azar, who adopted my cause and made all kind of arrangements to facilitate the completion of the field survey in Port-au-Prince. I am very appreciative of the staff of surveyors and data entry specialists who worked in very difficult conditions with little incentive to make the implementation of the survey a success.

Thanks to Ms Dana Sanders who has always been exemplary in her availability to provide her professional assistance.

Thanks to everyone who believed in me and have never ceased praying for this accomplishment.

TABLE OF CONTENTS

LIST OF TABLES

LIST OF FIGURES

ABSTRACT

This dissertation revolves around three issues on the urban area of Port-au-Prince, Haiti: the population distribution pattern, its estimation from remote sensing images, and its relationship with environmental quality. It follows a three-paper format. Paper 1 examines the population density pattern by the monocentric and polycentric models, based on the 2003 census data. The regression results show a poor fitting power of monocentric functions, and improved but less than satisfactory R^2 by polycentric functions. A five-sector conceptual model is proposed to capture the urban structure shaped by the absence or lack of institutional enforcement of land use regulations and urban planning. Paper 2 proposes a population estimation model based on Landsat ETM+ images that are widely available. The subpixel vegetation-impervious surface-soil (VIS) fractions derived from the Landsat multispectral bands (the mean value of houses fraction image, the mean value of vegetation and the standard deviation of vegetation fraction image) are used as predictors for urban population density. The research indicates that the geographically weighted regression (GWR) model, which accounts for spatial non-stationarity, performs much better than its Ordinary Least Square counterpart. Paper 3 uses multiple factors to assess and map the urban environmental quality (UEQ). In addition to parameters typically considered in previous studies, this study includes natural hazards and other parameters unique to Port-au-Prince. Crowdedness, waste, lack of vegetation, presence of slums and water body pollutions are considered as the most critical factors (negatively) affecting the quality of the environment in Port-au-Prince. All are exacerbated by population pressure on the resources, i.e., population density. The scores for corresponding factors are integrated together by weights extracted from a panel of local experts. The overall UEQ results are validated by field surveys. Each paper discusses important implications of major findings for public policy and planning.

CHAPTER I INTRODUCTION

Empirical studies of urban population density patterns help us understand spatial structures of modern cities. Population is at the heart of economic and social activities in a city, and there are plentiful studies of urban population density patterns in developed countries (1989). It is commonly observed that there is a negative relationship between population density and distance to gravitation point(s) called city center(s), which means that population density declines as moving away from city center(s). This function entails a trade-off between shorter travel distance and time to workplace (and higher rent) and more amenities (but longer commute to work). These amenities include larger lots size, lower crime rate, lower air pollution, lower noise level, and more greenness, etc. In other words, the structure of an urban area can be captured by its population density pattern. This pattern has also been found in some cities in developing countries such as Beijing and Shenyang in China, and Calcutta in India. However, can these models represent the urban complexion in cities of Latin America like Port-au-Prince?

Unlike cities in developed countries where options for the tradeoff are always available, the urban area of Port-au-Prince is affected by at least two major constraints. One is the limited availability of residential lands as the city is confined by the coastline on the one side and mountains on the other. The other constraint is economic means, as the city is dominated by low-income settlers whose choice of residence is dictated by their affordability and availability of space with very little concerns of commuting time or amenities. The affordability of residential lands in cities like Port-au-Prince is intimately linked to their intrinsic quality such as the environmental quality. The majority of the population is mostly low-income, and left with few choices but to share land with minimal or no amenities. As jobs are mostly in the informal sectors and unstable, commuting time is hard to plan and certainly not a priority in residential

choice. This affects density as defined by the population pressure on land. Therefore, it is not surprising that the distances from the city center and other subcenters are not as important as supposed in explaining population density in Port-au-Prince.

The shortage of quality population data is not uncommon in developing countries, and may represent a hindrance to critical planning and effective policy that govern modern cities. The increasing availability of high resolution satellite images and recent progress in remote sensing modeling have made it possible to estimate population distribution from the images. Although the models are far from surrogate for accurate counts by census, they nevertheless provide useful estimates of population pattern and may be critical in planning resource and service allocations in events such as an earthquake and other major natural disasters.

A new paradigm needs to be proposed, in this dissertation, from the perspective of urban environmental quality (UEQ). Density alone is insufficient to decipher the urban structure of Port-au-Prince. Urban environmental quality, composed of multiple factors, is considered a more comprehensive indicator that defines the urban structure of Port-au-Prince. Factors include those commonly found in the literature such as vegetation and traffic-related pollution (gas emission and noise), coastal pollution, and water pollution. Many other parameters such as susceptibility of natural disasters (flooding, landslide and coastal surge) and exposure to disamenity that are unique to Port-au-Prince are also considered. In cities in much of the world familiar to most of us, people are drawn to areas with amenities, and thus drive up land price and raise population density there. In Port-au-Prince, most residents are low-income with very little economic means, and can only afford to settle in crowded areas that are plagued by a variety of disamenity (natural disasters, pollutions, noise etc.). When a city such as Port-au-Prince without significant

development of multi-story residential buildings, this leads to a close correlation of high population density and poor UEQ score, a counter-intuitive phenomenon.

This dissertation assesses several issues in relation to population density patterns in the urban area of Port-au-Prince with GIS-based spatial analysis methods. Specifically, the objectives pursued in this dissertation are three-fold:

1. Examining the urban structure of Port-au-Prince as shaped by its population density pattern;
2. Proposing a model to estimate population from high resolution satellite imageries, and validating the model in reference to census data.
3. Assessing and integrating various UEQ factors and using the result to refine our understanding of the urban structure.

The working hypotheses for this dissertation are as follows:

1. Distance from CBD is not a significant predictor of population density in Port-au-Prince.
2. Population density can be estimated by variables derived by the V-I-S model from remote sending images, and the estimation is more accurate by the Geographically Weighted Regression (GWR) than the Ordinary Least Square (OLS) model.
3. Urban Environmental Quality (UEQ) in Port-au-Prince is population-driven, and higher population density is correlated with poorer UEQ.

The dissertation follows a three-paper format. Chapter III is based on a paper published in *Cities* (Joseph and Wang, 2010) that examines the urban structure of Port-au-Prince by its population density patterns based on the 2003 census data at the census block (Section d'énumération or SDE) and district levels. Chapter IV is based on a paper published in

GIScience & Remote Sensing (Joseph et al., 2012) that uses a combination of variables derived from a Landsat ETM+ image to estimate population in Port-au-Prince. Chapter V makes the third paper to assess and map the UEQ of Port-au-Prince. All three papers share the same issues related to the study area and data sources that are discussed in the preceding Chapter II. Chapter VI makes a summary of the findings and presents the conclusions. It also discusses the shortcomings of the research, proposes ways for future improvement, and outlines specific implications for urban planning and contributions in other domains.

CHAPTER II STUDY AREA AND DATA SOURCES

II.1 Study Area

The study area is Port-au-Prince, the administrative, commercial and political capital city of Haiti, but the second smallest city of the country. According to the fourth general population and housing census by the Haitian Institute of Statistics and Informatics (IHSI) (2006), the city had a population of over 750,000 (9% of the country's population) in a total area of 36 square kilometers in 2003. The populated urban area had 732,157 residents in about 26 square kilometers, which is 28160 people per square kilometer. Port-au-Prince is a coastal city with elevation rising from around the sea level in the northwest to over 600 meters in the southeast (Figure 1). Along with several highly populated cities around Port-au-Prince, the larger metropolitan area had a population close to 3 million. People commute daily between these cities and Port-au-Prince. Prior to the earthquake, downtown Port-au-Prince had the largest commercial center in the larger metropolitan area.

The basic geographic unit for this study is Section d'énumération or *SDE* for the purpose of statistical reporting (similar to "census block" in the U.S.). A SDE is the smallest unit in a *communal section* (similar to "county" in the U.S.). A SDE is delimited by geographic features such as waterways, mountains and roads, and generally contains 150-200 houses (IHSI 2006). SDEs are delineated by the IHSI's internal cartographic and spatial division. A maximum of five contiguous SDEs are grouped to form a *district*, which is a higher and larger spatial construct than SDE used in the census. Our study area has 670 SDEs and 171 districts. The average size of the SDEs was 0.038 km^2 with the smallest SDE of just 0.0028 km^2 and the largest SDE of 0.86 km^2. Population density varied a great deal across SDEs with an average density as high as 50,166 persons per km^2. Basic descriptive statistics for the study area are presented in Table 1.

Table 1 : Basic statistics in urban Port-au-Prince

	SDE level (n=670)			District level (n=171)		
	Area (km^2)	Population	Density (people/ km^2)	Area (km^2)	Population	Density (people/ km^2)
Minimum	0.0028	206	598	0.03	2,403	4,215
Average	0.038	1,093	59,718	0.19	5,423	50,166
Maximum	0.86	2,786	335,828	0.93	9,809	159,063
Total	25.47	732,157	28,757	25.47	732,157	28,757

Most of the SDEs had population slightly over 1,000 and area of less than 0.04 km^2. The most populous SDE had 2,786 residents, and the largest SDE in terms of area size was less than 1 km^2. The average population density at the SDE level in Port-au-Prince was as high as 59,718 persons per km^2.

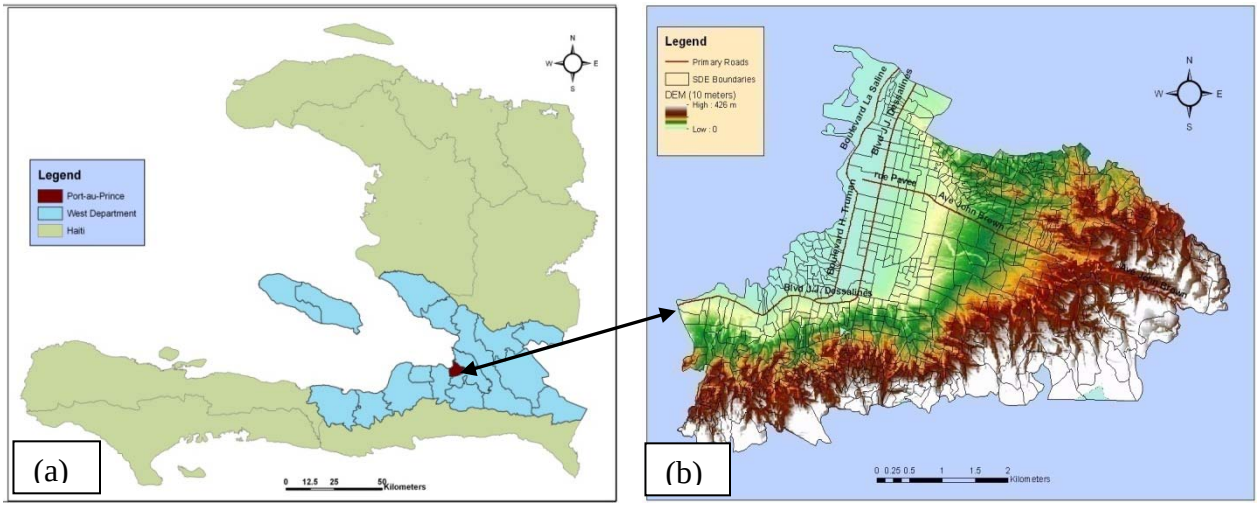

Figure 1 : Study area - Port-au-Prince, Haiti. a) Location within the West department; b) DEM

II.2 Data Sources

Demographic data were collected from the Haitian Institute of Statistics and Informatics (IHSI), which implemented the general population census of 2003. The reporting census unit is

the “Section d’énumeration” (SDE). In addition to population, the number of buildings in each SDE is also reported. However, these data were not available in GIS format. Only a PDF map and an Excel file were distributed.

A Landsat 7 Enhanced Thematic Mapper Plus (ETM+) image (path 009 row 047) was used in this research. It was obtained on March 7th 2003 from the USGS Earth Resource Observation Systems Data Center after corrections for radiometric and geometrical errors and had 2% of clouds. The image scene was rectified and registered to the boundaries of the census units (SDE). In addition, high resolution satellite images were acquired from Google Crisis Response Website (http://www.google.com/relief/haitiearthquake/geoeye.html) for reference. These images were true color and included 4-m resolution IKONOS images and 1.65 m resolution GeoEye-1 images. These images were acquired the week following the earthquake that struck the metropolitan region of Port-au-Prince on January 12, 2010. These images were used for visual inspection and referencing though changes over time and from the earthquake might have occurred.

Waterways and roads were obtained from the National Center for Geographic Information System (CNIGS) and the United Nations mission in Haiti. Other physical data such as city centers, public markets, slums, coastline, and cemetery were digitized from a topographic map published by the Hydrographic and Topographic Center of the Defense Mapping Agency and updated with the Ikonos image aforementioned. Peaks, sinks and elevation data were also digitized from the same topographic map with the contours 10 meters apart. They were used to generate the Digital Elevation Model (DEM) at 10 m resolution.

Data used for weighing the parameters and to validate the results were compiled from two separate surveys, a field survey carried face-to-face out on 407 residents in Port-au-Prince,

and an expert survey generated from Survey Monkey and distributed by email. Samples of the survey are provided in Appendix 5.

CHAPTER III POPULATION DENSITY PATTERNS IN PORT-AU-PRINCE, HAITI: A MODEL OF LATIN AMERICAN CITY?[1]

III.1 Introduction

Since the classic work by Clark (1951), population density functions have been used as an effective way to capture urban spatial structures. McDonald (1989) considers the population density pattern as "a critical economic and social feature of an urban area." Empirical research of urban population density, while plenty in developed countries, is much less in developing countries (Mills and Tan 1980). Examples of previous studies on third-world cities include Berry and Kasarda (1977) for Calcutta, India, and Wang and Zhou (1999) and Wang and Meng (1999) for Beijing and Shenyang, China, respectively. In these three cases, a negative exponential gradient similar to Western cities was observed. The main difference between them resided in the trend over time. Whereas it remained constant in Calcutta, indicating the absence of suburbanization, the density gradient became flatter over time in Beijing and Shenyang.

However, the literature on this topic is almost nonexistent in poor countries such as Haiti. One major obstacle is the lack of reliable data. While population data have become more accessible recently, Haiti does not have a spatial database system like the TIGER files in the U.S. that accompanies the release of population censuses. This research builds a Geographic Information System (GIS) at the SDE (*Section d'énumération*) level for Port-au-Prince, the capital city of Haiti, and links with the most recent census data for the study area in 2003 to examine its population density patterns. No other socioeconomic variables such as income or household size in Port-au-prince are available for our study. On the methodological front, earlier work of population density patterns is based on the *monocentric model,* i.e., how population

[1] Joseph, M. & F. Wang (2010) Population Density Patterns in Port-Au-Prince, Haiti: A Model of Latin American City. *Cities,* 27**,** 127-136

density varies with distance from one single center. Since the 1970's, more and more studies have adopted the *polycentricity* framework that recognizes multiple centers in a city (Ladd and Wheaton 1991, Berry and Kim 1993). Polycentricity recognizes secondary centers or subcenters in addition to the central business district (CBD) in most large cities. This research applies both the monocentric and polycentric models to Port-au-Prince, and analyzes the impacts of the primary center as well as subcenters on citywide population distribution.

There has been some descriptive work on urban issues of Port-au-Prince, but no systematic study of population density patterns. Are urban density patterns observed for cities in developed and/or developing countries applicable to Port-au-Prince? If they are different, what factors account for the differences? Griffin and Ford (1980, 1993) suggested a Latin American city model. In their model, the elite occupy the urban core, and the massive low-income residents settle in the periphery. As a result, high concentrations of population are found in the peripheral areas in contrast to the trend observed in cities in developed countries. Does this model fit Port-au-Prince?

This case study is not a trivial addition to the rich literature of empirical work of urban density functions. Unlike western cities with structured urban planning, the development of Port-au-Prince, though in a free market economy, has taken place under political instability that resulted in anarchy and unregulated land uses, particularly for the last two decades. The political slackness has shaped the urban landscape of Port-au-Prince, and its imprints on its population distribution need to be assessed. This endeavor has significant implications. Understanding the population distribution sets the baseline for urban planners and governmental institutions to plan and deliver basic social and environmental goods and services. It will also help inform private businesses to make the best decision in allocating their investment resources.

III.2 Data preparation

IHSI published the 2003 population and housing census in 2006 including a map of SDEs. However, no spatial data such as GIS were released. To reconstruct the GIS database for this study, we scanned the map printout, used control points to geocode the map, and digitized it into a shapefile in the ArcGIS platform. Attribute data from the census contained each SDE's name, id, other geographic delimitation (e.g., district), and demographic information such as population and housing units. The attribute data were processed, saved as a CSV file, and then joined with the newly-constructed shapefile for subsequent spatial analysis. The shapefile at the district level was created by using the "dissolve" tool in ArcGIS given the corresponding ids between SDEs and districts. Distances from each SDE (or district) to the major center and subcenters of Port-au- Prince were between its centroid and these centers. Area and population density for each SDE (or district) were also computed in ArcGIS. Figures 2 and 3 show the population density distribution in Port-au-Prince at the SDE and district levels, respectively. The high density areas are located northeast and southwest of the city center, which house some of the poorest residents that have moved to the city recently. The southeast area towards the edge of the city is on a higher ground with relatively low densities, and is occupied by upper-income residents. Some low-density spots around the city center are either commercial/industrial areas or governmental buildings.

Analysis of population density patterns begins with identifying the city center. The city center of Port-au-Prince is chosen as the intersection of two major roads, namely Boulevard Jean-Jacques Dessalines and Rue Pavée. This intersection with the busiest traffic in Port-au-Prince also anchors the roads leading to two other adjacent cities, Carrefour and Petion-Ville,

part of the larger metropolitan area. It is the commonly recognized center of Port-au-Prince in the heart of its central business district (CBD).

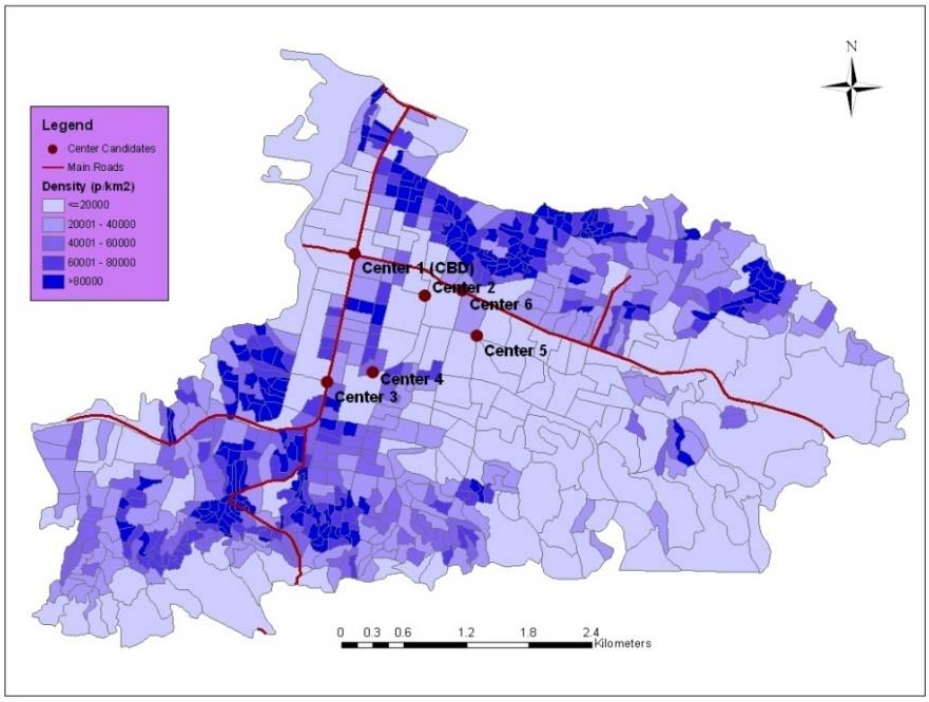

Figure 2 : Population density in Port-au-Prince at the SDE level 2003

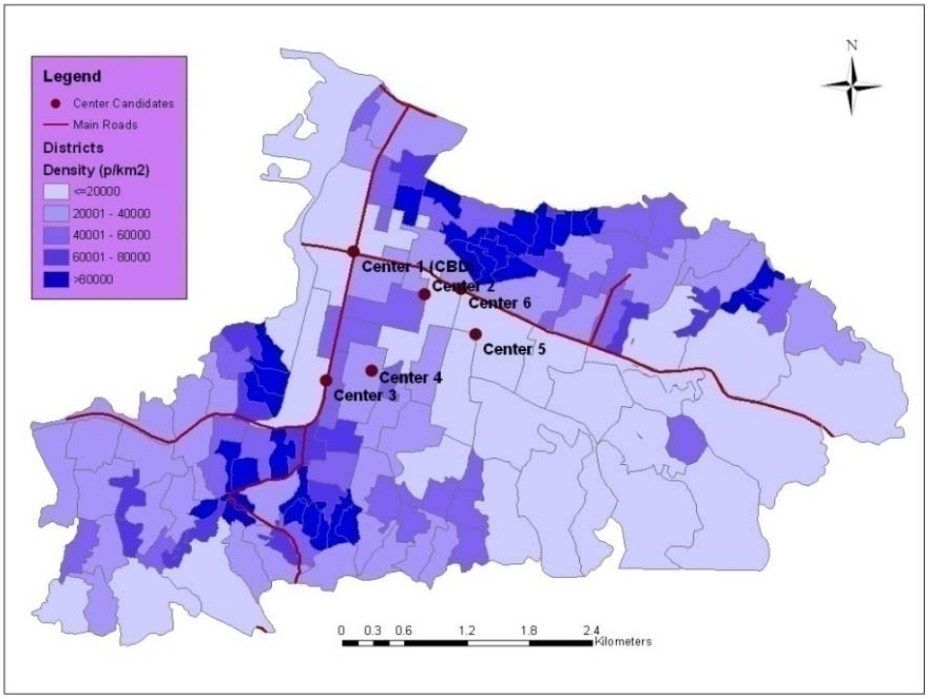

Figure 3 : Population density in Port-au-Prince 2003 at district level

In absence of local knowledge, Alperovich (1982) proposed a method to help identify the city center. The method identifies the city center as the location producing the highest R^2 in fitting the population density functions. In order to further validate the location selection of the city center, we experimented with eight other possible alternatives such as the intersection of Rue Capois at Lalue, Turgeau (College Canado Haïtien), Nazon (Lalue and Martin Luther King), Carrefour Petit Four, the National Palace, the intersection of Mgr Guilloux and Oswald Durand, and Portail Léogane. Given the small size of the study area, some of these sites are separated by less than a kilometer. The results indicated that our selection of the city center yielded the highest R^2 among the six centers with a negative density gradient. The other two centers with a positive density gradient were excluded in the analysis. The remaining six centers were also considered candidates for multiple centers in the polycentric model and will be subsequently referred to as Centers 1, 2… and 6 in the descending order of R^2 values. See Figures 2 and 3 for their locations.

III.3 Population density patterns by the monocentric model

The monocentric model assumes a city to evolve around one center, i.e., the central business district (CBD), which serves as the sole provider for employment (Muth, (1969) ; Mills, (1972)). In the vicinity of the CBD, one pays for more expensive housing, and is compensated by a shorter commuting distance to work. Therefore, everybody values proximity to the CBD, and population density is expected to decrease with distance from the CBD.

Various functions have been proposed to capture the trend of declining population density (D_r) with distance from the CBD (r) (Wang 2006):

Linear: $D_r = a + br$ (1)

Exponential: $D_r = ae^{br}$ (2)

Logarithmic: $D_r = a + blnr$ (3)

Power: $D_r = ar^b$ (4)

Polynomial: $D_r = a+br + cr^2$ (5)

Tanner-Sherratt: $lnD_r = a + br^2$ (6)

Newling: $lnD_r = a + br + cr^2$ (7)

Among the above seven functions, the exponential function fits most cities in the world the best.

To assess the possible presence of Modifiable Area Unit Problem (MAUP), the same models were applied to the data at both the SDE and district levels. The results are consistent between the two geographic units. Each model at the district level yields a greater R^2 than the corresponding model in the SDE level. This is not surprising since a district on average is composed of four to five SDEs and thus has their average (smoothed) values of distance (r) and density (D_r).

The regression results from the monocentric functions are summarized in Table 2. All functions yielded a R^2 value smaller than 0.10 with the highest R^2 in the Newling's model and the lowest in the power function. Figure 4 shows how the population density changes with distance from the city center at the district level, and a trend line of polynomial function is used to capture the general pattern. Evidently, urban densities in Port-au-Prince do not closely follow the general trend of declining density with farther distance from the city center. One may describe the trend as lower densities near the city center, increasing up to 2 kilometers, and then decreasing toward the edge. While this indicates a weak association between population density and distance, the t-values in most models are indeed statistically significant and represent the expected negative correlation between them.

III.4 Population density patterns by the polycentric model

The monocentric functions assume that population densities are identical at the same distance from the city center regardless of directions. The lack of fitting power of the monocentric functions leads us to look for alternative models. Polycentric functions consider more than one center from which densities vary with distances (Small and Song 1994). The underlying rationale is the necessity for residents to access several centers including the CBD and sub-centers for services and activities. There are different assumptions about the influences of multiple centers, ranging from perfectly substitutable to completely complementary (Heikkika et al. 1989). This paper tests two most plausible assumptions.

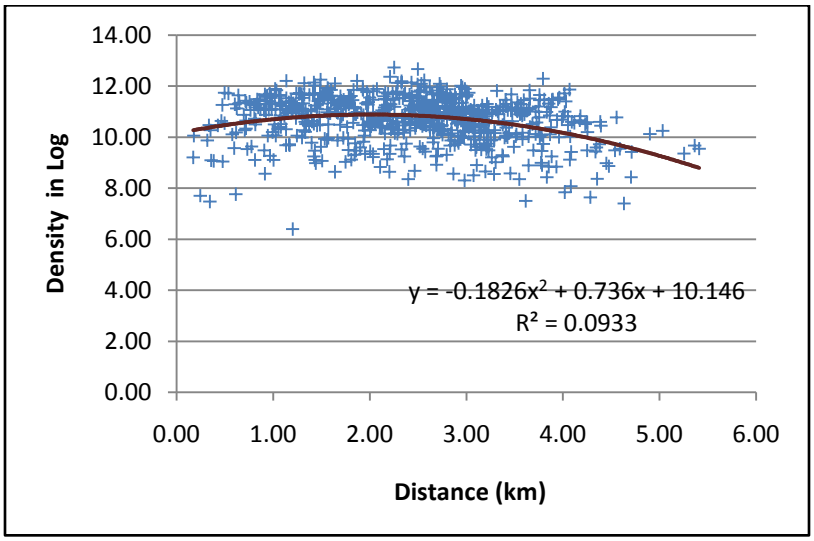

Figure 4 : Population density at the district level fitted by a polynomial function

The first argues that the influences are complementary and that access to all centers is required. In this case, the polycentric density is defined as the product of the monocentric exponential functions, i.e., *multiplicative effects* (McDonald and Prather 1994). The model's logarithmic transformation is written as:

$$\ln D = a_0 + \sum_{i=1}^{n} b_i r_i \qquad (8)$$

where D is the population density of an area, r_i is the distance between the area and each center i (= 1, 2 …), and a_0 and b_i are parameters to be estimated.

The second proposition assumes the polycentric density as the sum of center-specific monocentric functions, i.e., *additive effects* (Griffith, (1981); Small and Song, (1994)). Based on the exponential density function, the polycentric function is written as:

Table 2 : Regression results for the monocentric density functions

	SDE level (n = 670)				District level (n =135)			
	a	b	c	R^2	a	b	c	R^2
Linear	77111 (18)***	-7203 (-4.3)***		0.027	65307 (9.0)***	-6232 (-2.3)*		0.036
Exponential	11.05 (123)***	-0.16 (-4.6)***		0.030	10.98 (61)***	-0.175 (-2.6)**		0.047
Logarithmic	65023 (22)***	-6943 (-2.1)*		0.007	54127 (11)***	-5140 (-1.0)		0.007
Power	10.70 (175)***	-0.12 (-1.8)		0.005	10.65 (87)***	-0.12 (-1.0)		0.007
Polynomial	44195 (5.6)***	25373 (3.8)***	-6666 (-5.0)***	0.063	29686 (2.3)*	29390 (2.6)**	-7355 (-3.2)**	0.106
Tanner-Sherratt	10.95 (191***)	-0.04 (-6.1)***		0.053	10.88 (95)***	-0.05 (-3.5)***		0.086
Newling's	10.14 (64)***	0.74 (5.5)***	-0.18 (-6.8)***	0.093	9.82 (31)***	0.97 (3.6)***	-0.24 (-4.4)***	0.167

Note: t values are in parentheses; *** significant at 0.001, ** significant at 0.01, * significant at 0.05.

$$D = \sum_{i=1}^{n} a_i e^{b_i r_i} \qquad (9)$$

where D and r_i are the same notations as in equation (8), and a_i and b_i are parameters to be estimated.

As explained earlier, we had six candidate sites for multiple centers. These sites are the intersections of major roads that attract significant commercial activities. After numerous

attempts, the additive effect model in equation (9) would not converge with five or more centers. Therefore, only centers 1-4 were included in the regression analysis, and the results are presented in Table 3.

The multiplicative effect model in equation (8) yielded R^2 = 0.095. Note that first two centers had positive density gradients (b_1 and b_2), against the intuition of distance decay effect. The other two centers had negative gradients that were statistically significant. The additive effect model as in equation (9) had R^2 close to 0.20. All four centers had negative gradients that were statistically significant. The results indicate that the additive effect model better captures the population density pattern in Port-au-Prince.

Table 3 : Regression results for the polycentric models at the SDE level

	Multiplicative Effects	Additive Effects
a_0	10.113 (61.37)***	
a_1		-355890 (-9.33)***
b_1	2.306 (6.71)***	-0.685 (-7.36)***
a_2		-296943 (-9.41)***
b_2	1.643 (5.34)***	-1.196 (-7.02)***
a_3		530005 (8.42)***
b_3	-3.676 (-6.27)***	-0.497 (-14.13)***
a_4		-67259 (-3.64)***
b_4	-0.173 (-2.74)**	-1.650 (-2.66)**
R^2	0.095	0.199

Note: t values are in parentheses;*** significant at 0.001, ** significant at 0.01, * significant at 0.05.

III.5 A model of Latin American City?

As illustrated in Figure 5, the Griffin-Ford model for Latin American's cities includes five constructs (Griffin and Ford, (1980, 1993). The *CBD* is the commercial center and the primary location of employment and entertainment for the city. The *spine/sector*, a commercial zone, is a longitudinal extension of the CBD surrounded by the residences of the elite and the upper-middle class. This area is marked by the presence of natural and man-built amenities for the wealthy. The *zone of maturity* hosts a relatively stable population in constantly improving residences. The *zone of in situ accretion* is a transitional zone between the periphery and the zone of maturity, with modest houses and others in building process. Not all area in this zone has adequate public infrastructures. Finally, the *squatter settlements zone* houses the poor, many of whom have recently arrived from even poorer rural areas. Housing quality in the zone is undesirable with minimal public services.

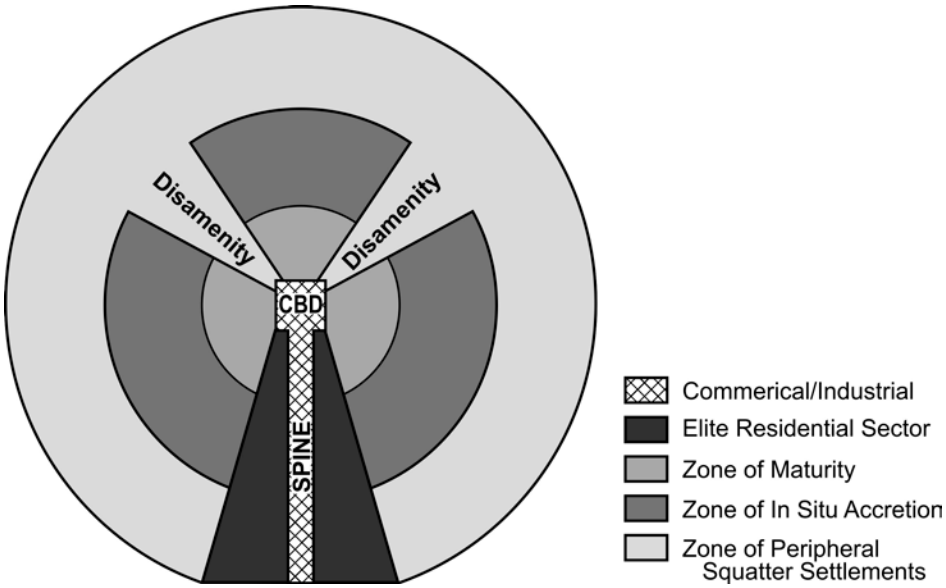

Figure 5 : A generalized model of Latin American city structure (based on Griffin & Ford, (1980))

Port-au-Prince bears some resemblances to the Griffin-Ford model in several aspects: primarily the role and location of the CBD along with the commercial spine, and the squatter

settlements on the edge of the city. The CBD in Port-au-Prince is the convergence point of main transportation activities with heavy traffic in daytime, but becomes empty after sunset. Governmental offices and major private commercial buildings dominate the landscape of the CBD and the commercial spine with a multitude of small retail and service stores. One main scene, common in Latin American cities, is the presence of widespread street merchants. However, in contrast to the Griffin-Ford model, areas adjacent to the commercial spine in Port-au-Prince do not possess the amenities that attract the upper-middle class resident. It could be more likened to the zone of maturity, with average housing and public services. Housing and population density in this area is stable and unlikely to change barring major urban renovation projects. There are also variations within the area in different parts of the city.

The elite and the upper-middle class are located in the east and southeast areas with natural vegetation and high-quality housing despite steep topography. The areas are provided with mandatory public services, in contrast to no or minimal services for the zone of squatters with similar topography. The lots in the areas are also bigger than those in the transitional zone. Despite steep slopes in the areas, the land price is driven up by a high demand for housing and diminishing land availability. While the housing is similar to those in suburban areas in western cities, the areas are purely residential with no retail stores in the vicinity.

Areas of squatter settlements have some of the highest population and housing densities, and also account for the highest percentage of population in Port-au-Prince. This zone is not necessarily limited to the peripheral areas as suggested by the Griffin-Ford model, rather widespread in places short of infrastructures and public services with complex topography. Residents are drawn to the areas for availability of open space or low-price land, proximity to the CBD or the commercial spine, and convenience of access to public transportation. Some of the

residents have to travel a long distance to work outside of the city. Some pockets of high densities are less than 1.5 kilometers southwest of the CBD and close to the sea. These shantytowns have recently been built on former landfills prone to flood and high tide. Major high-density concentrations are in northeast and south-southwest areas at two to three kilometers from the CBD. There is also a small high-density "island" in the southeast area, surrounded by upper-middle class housing. This small pocket is close to a ravine, unattractive for others and occupied by squatter inhabitants. The low population density in the south-southeast edge is rather attributable to the topographic conditions that have hindered its development.

Port-au-Prince also has an area similar to the zone of maturity in the Griffin-Ford model but not in the same morphologic regularity. It reflects an upward socioeconomic mobility of low-income to the middle class, replacing long-established residents that moved out of Port-au-Prince or emigrated to North America or Europe. This area, not purely residential, is located eastward from the CBD. Private schools, medical clinics and other retail services mingle in these neighborhoods.

III.6 Five conceptual zones in Port-au-Prince

A conceptual model (Figure 6) is designed to further advance our understanding of urban structure in Port-au-Prince. Based on our field work and review of satellite images of the city, we identified five zones on the district map. These five zones are a combination of zones in the Burgess's (1925) concentric model and sectors in the Hoyt's (1939) model. Therefore, we use the term "zone" and "sector" loosely and interchangeably in the following discussion.

The first sector is the *commercial* quarter (see Figure 7) and radiates from the city center outward in all direction up to about 1.5 kilometers along the axes of main streets. The seaport at the northwest corner is Haiti's largest in term of commodity throughputs. The average population

density of over 50,000 people per square kilometer in this sector is attributable to the concentration of long-time low-income households in this sector, most of whom rely on the informal commerce for a living. This sector also includes main public administration buildings, public parks and market places.

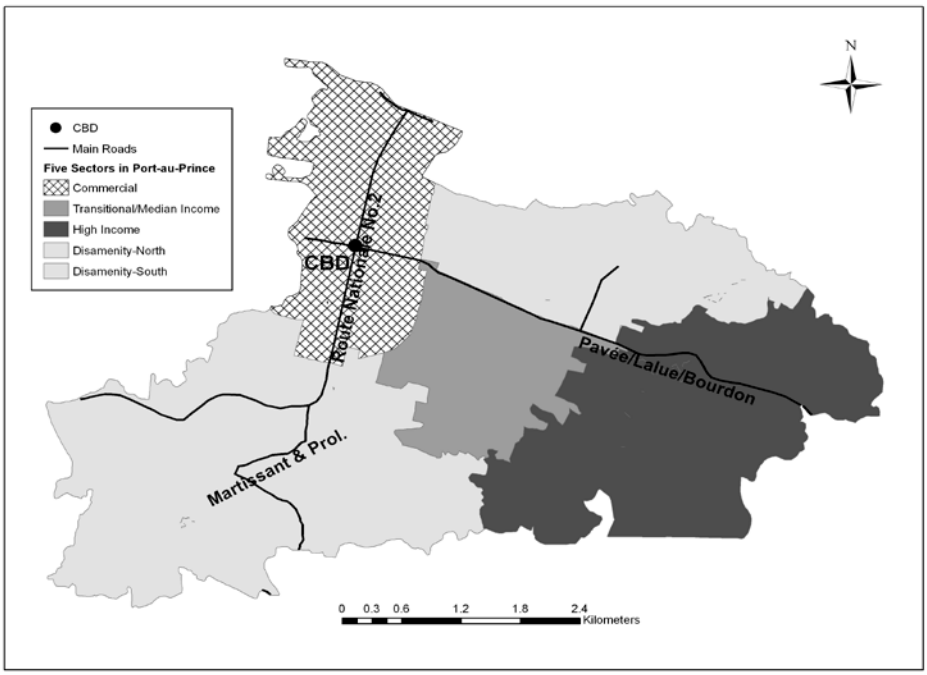

Figure 6 : Five conceptual zones in Port-au-Prince

The second sector is a *transitional* zone between the commercial and the residential areas with mixed land uses (see Figure 8), bearing some resemblance to the zone of maturity in the Griffin-Ford model. Activities in the sector range from groceries to retail stores, services and schools, buffered along the main streets. Housing quality in this sector is better than zone 1. Better amenities are found toward the edges of the city, and thus it is difficult to draw a clear boundary from sector 3 in some areas. The population density is slightly higher than sector 3.

The third sector is the *high-income residential* (see Figure 9) with an average density of about 25,000 persons per square kilometer. It is located relatively far from the city center in the southeastern region of Port-au-Prince with high elevation and often difficult terrain. The sector is

occupied by high-income minorities with best amenities (large lots, less vehicle traffic, rich vegetation, etc.) with no or minimal commercial activities. As explained previously, this area is punctuated by a small pocket of slums in the middle, which carries a high density of near 93,000 in two SDEs.

Figure 7 : Port-au-Prince CBD

Figure 8 : Transitional zone in Port-au-Prince

Sectors 4 and 5 are termed "*disamenity-north*" and "*disamenity-south*" (see Figure 10), separated by the transitional sector. The disamenity-south sector is in the south and southwest

areas, and the disamenity-north sector is in the north. They share many characteristics: lack of basic services and amenities, unpaved or poorly maintained roads, high population density, difficult topography, poor sanitation, and most prone to natural disasters.

Figure 9 : High-income residential area in Port-au-Prince

Figure 10 : Disamenity zone in South Port-au-Prince

Figure 11 shows the average population density in each zone declining in the order of disamenity-north, disamenity-south, commercial, transition and high-income zones. The lackluster fitting power of the monocentric models can be easily explained by the higher

densities in the two disamenity zones on the city's outskirt than the central commercial zone at the heart of the city. A regression model with dummy variables is constructed to test whether population density indeed varies significantly across different zones.

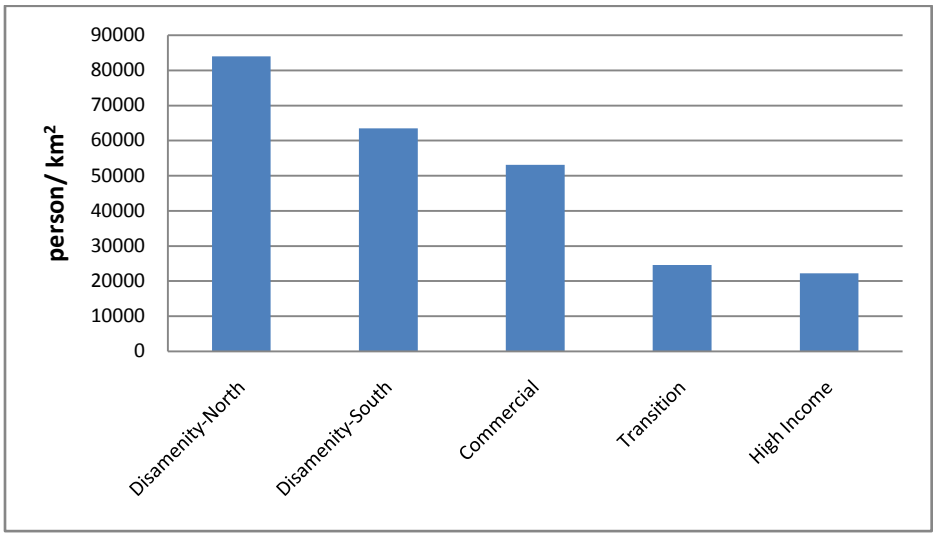

Figure 11 : Average population density by sector

Four dummy variables (x_2, x_3, x_4 and x_5) are used to code each SDE that falls within one of the five zones. The *commercial sector* (zone 1) is used as the reference zone coded as $x_2 = x_3 = x_4 = x_5 = 0$. The *transition sector* (zone 2) is coded as $x_2 = 1$ and $x_3 = x_4 = x_5 = 0$, the *high-income sector* (zone 3) as $x_3 = 1$ and $x_2 = x_4 = x_5 = 0$, the *disamenity-north sector* (zone 4) as $x_4 = 1$ and $x_2 = x_3 = x_5 = 0$, and the *disamenity-south sector* (zone 5) as $x_5 = 1$ and $x_2 = x_3 = x_4 = 0$. A regression model can be constructed as below to test whether and how the population density varies significantly across the zones (Wang 2006):

$$D = c_1 + c_2 x_2 + c_3 x_3 + c_4 x_4 + c_5 x_5 \qquad (10)$$

We tested the regression model (10) by defining the dependent variable D as both the population density and its logarithm in each SDE. The results are presented in Table 4.

From Table 4, the logarithmic model (R^2 =0.252) outperforms the plain density model (R^2 =0.186). The intercept c_1 indicates the average density (or its logarithm) in sector 1 when x_2

$= x_3 = x_4 = x_5 = 0$, and coefficients c_2, c_3, c_4 and c_5 represents the density (or logarithm of density) difference between sector 1 and sectors 2, 3, 4 and 5, respectively. All coefficients are statistically significant, and validate the conceptual model for the urban structure in Port-au-Prince. In both models, the highest coefficient is c_4 (indicating the highest density) in the disamenity-north zone, and then c_5 (second highest density) in the disamenity-south zone, and both c_4 and c_5 are positive (indicating higher densities than the reference zone, i.e., the commercial zone); the negative c_2 and c_3 indicate that the transition and high-income zones have lower densities than the reference (commercial) zone, and the more negative c_3 than c_2 shows the lowest density in the high-income zone. The regression analysis not only confirms the findings from Figure 11 but also shows that the density gaps are statistically significant across the five zones.

III.7 Conclusions

Port-au-Prince has experienced tremendous growth in recent years because of migrations from rural areas and other cities. As the capital city of Haiti, centralization of political power, public services and economic activities helps propel its growth. The political transition from a dictatorship to succession of short-lived governments has left strong imprints on the recent development of Port-au-Prince. Political instability has undermined the governmental power to manage land development and natural resources. For the last 20-25 years, many shantytown neighborhoods have been erected on marginal lands by taking advantage of the institutional volatility and some natural barriers. These barriers take one or more of the following forms: high slopes, proximity to floodplains and rivulets, and adjacency to municipal waste conducts and the sea. The informal housing, known as *bidonvilles* (in former French colonies), has some common features: no tenure security, lack of basic infrastructures, being dominated by substandard

dwellings, and occupying areas unsuited for land use regulations and ill-fitted for development (Pamuk 2006). “The bidonvilles are anarchically sprawling in Canapé-Vert, in Bourdon, and Carrefour-Feuilles… And although since 1940 the lawmakers have declared these areas protected, the law has never been made functional” (Métropole 2003). That is to say, these squatter zones of high population density are not necessarily “developed” for easy access to employment in the city center but rather because of availability of non-regulated marginal lands.

The urban structure in Western cities and elsewhere (e.g., cities in China) is shaped by market forces or government planning strategies (Feng, Wang and Zhou 2009). However, Port-au-Prince has very little planning, and land use irregularity is the norm. Leapfrogging causes a patchwork development process on the urban periphery, and leads to the formation of a “discontiguous entity” (Crowley 1998). In addition, lower-status socioeconomic groups have more restricted activity space, and their ‘‘cognitive maps’’ may not be as far reaching as those better off (Lynch 1960). In a city with the largest segment of population living in the substandard squatters, not all residents have the mobility to reach what the city has to offer. Therefore, the distance from the CBD does not play an important role in shaping the density patterns as much as in cities of developed countries. This explains the poor fitting power of monocentric functions and less than satisfactory R^2 by the polycentric functions. After all, the very foundation for any density functions is the assumption that residents value the access to the center(s) of a city for jobs or other activities.

Like many cities in developing countries, *suburbanization* is taking place in the larger metropolitan area of Port-au-Prince. The process has been fueled by the deterioration of living conditions near the city center due to crowdedness and institutional carelessness. The impact is felt beyond the administrative limit of the city. The recent development of adjacent cities with

more open land and better amenities has been partially supported by this flight of median-to-high-income classes from Port-au-Prince. The displacement creates a void, quickly being filled by residents of low-to-median income, who could not afford in the past. The city is becoming "a conglomeration of nondescript office buildings, slums, old Victorian houses with 'gingerbread' trim, modern cement block houses, and million-dollar homes" (Denis 2009).

Future work will advance the study in several directions. First, the study area can be expanded to a bigger region in order to better understand the interaction between the city and its surrounding rural areas. The second issue is to consider all land uses. Population density merely reflects the residential land use. Other land uses (e.g., commercial, industrial and public) interact with residential and influence its density pattern. The third direction is to collect data of more demographic and socioeconomic variables so that more meaningful social areas can be identified. Finally, data of more than one census year will help us examine the changes over time and possible forces behind the changes.

CHAPTER IV USING LANDSAT ENHANCED THEMATIC MAPPER PLUS IMAGERY FOR POPULATION ESTIMATION WITH GEOGRAPHICALLY WEIGHTED REGRESSION IN PORT-AU-PRINCE, HAITI[2]

IV.1 Introduction

Analysis of population density patterns is fundamental in urban studies. As population serves as both supply (labor) and demand (consumers) in an economic system, the distribution of population represents that of economic activities (Wang 2006). In addition, urban population is an important parameter for urban environment (Benn 1995, Sutton et al. 2001). Reliable population data are essential for effective planning in resource allocation and disaster preparation. However, such data are often not available at adequate geographic scales or not updated in a timely fashion in developing countries. The problem is particularly troublesome in Haiti. The last 2003 census was carried out after over twenty years from the previous one. This results in a loss of one decennial of demographic data. In addition, even the most recent census does not accompany with any spatial database system like the Topologically Integrated Geographic Encoding and Referencing (TIGER) files for the U.S. census. The database is published in a spreadsheet along with a map in PDF format showing the delimitation of the census units, but the digital version of the database is not available to the public. In the wake of 2010 Haiti Earthquake this information deficiency did not facilitate an objective evaluation of the affected population particularly in the most vulnerable zones. This situation prevented the institutions to deploy appropriate relief operations where most needed, and the estimation of casualties were just speculation. We found that it was critical and urgent to develop a model that

[2] Joseph, M., L. Wang & F. Wang (2012) Using Landsat Imagery and Census Data for Urban Population Density Modeling in Port-au-Prince, Haiti. *GIScience & Remote Sensing,* 49**,** 228-250.

can provide information about the population at detailed level for Port-au-Prince, yet the next census expected in 2013 may be jeopardized because of financial constraints.

The success of remote sensing analysis in deciphering the biophysical characteristics of urban ecosystems has provided a basis for the study of urban morphology, biophysical systems , and human systems (Ridd 1995). Population estimation is one of the specific domains that have taken advantage of the application of remote sensing through direct visual interpretation of analogue images (e.g. dwelling counts, measurement of homogenous areas or urban areas, and categorization or generalization of land use and) or digital image analysis for the generation of explanatory variables to include in regression analysis. Remote sensing (RS) has been used to estimate human settlement patterns when census or surveyed data are not available (Harvey 2002b). While an accurate estimate of urban population remains a challenge, some basic understanding of population patterns by RS may still prove to be very useful, especially for emergency planning or post-disaster reconstruction in underdeveloped countries such as Haiti.

Major techniques for population estimation by RS include the traditional dasymetric mapping (Holz, Huff and Mayfield 1973, Langford and Unwin 1994, Fisher and Langford 1996), regression models (Shroeder 1990, Langford, Maguire and Unwin 1991, Yuan, Smith and Limp 1997, Sutton et al. 2001, Harvey 2002b, Qiu, Woller and Briggs 2003, Wu and Murray 2007) and geostatistical models (Paez, Uchida and Miyamoto 2002, Wu and Murray 2005, Lo 2008, Harris, Fotheringham and Charlton 2010, Joseph and Wang 2010a, Lloyd 2010, Qiu, Sridharan and Chun 2010).

The use of remote sensing imagery for population estimation has recently gained momentum with the increasing availability of high resolution images. Several sensors have been used to this end with performance and accuracy commensurate with the improvement of sensors.

In their seminal review of usage of remote sensing to estimate population, Wu et al. (2005) reports early applications of aerial photographs to count dwelling units through visual interpretation by Green (1956) applying the method proposed by Porter (1956), Hsu (1971), Collins and El-Beik (1971), Dueker and Horton (1971) and (Forster 1985). Tobler (1969) used satellite imagery in 1969 to directly correlate population and urban areas with the aid of images from the Gemini space flight program (Wu et al. 2005). Photographically-generated residential land use types were also used to estimate population counts (Anderson and Anderson 1973, Kraus, Senger and Ryerson 1974). To alleviate the time-consuming method of dwelling unit count, Lo (1988) adopted a raster approach to extract density of residential building with aerial and space photographs

Since the launch of Landsat 1 the first reported use of a modern sensor was by Lo and Welch (1977) who applied Landsat Multispectral Scanner (MSS) images from 1972 to 1974 to correlate populations and classified urban areas of Chinese cities through a function referred to as the allometric growth model (Wu et al. 2005). Subsequently Iisaka and Hegedus (1981) extracted mean reflectance values of the four MSS bands as surrogates in population estimation regression.

Since then, taking advantage of the increasing availability of higher resolution images, population estimation models have also been derived from different types of sensors such as Landsat Thematic Mapper (TM) (Langford et al. 1991, Yuan et al. 1997, Harvey 2002a, 2002b, Wu and Murray 2005); Landsat Enhanced Thematic Mapper (ETM+) (Li and Weng 2005, Lu, Weng and Li 2006, Wu and Murray 2007); high resolution QuickBird imagery (Galeon 2008, Garrison 2010); IKONOS (Liu 2003, Sengupta et al. 2003, Liu, Clarke and Herold 2006); high resolution multi-spectral SPOT image (Weber, Hirsch and Serradj 1994, Lo 1995); imaging radar

systems (SAR) (Henderson and Xia 1997); nighttime urban light images (Sutton 1997, Sutton et al. 1997, Dobson et al. 2000, Prosperie and Eyton 2000, Sutton et al. 2001, Lo 2001, 2002); Light detection and ranging (LIDAR) point cloud data (Wu, Wang and Qiu 2008, Fang, Harini and Yongwan 2010). Lu et al (2010) found that combining two different sensors, QuickBird and LIDAR data, greatly improved population estimation models over other models based on spectral data.

It is generally accepted that the urban population density is positively related to the intensity of human modification to the earth surface, namely the land use and land cover (LULC). However, land use classification is improperly used as an indicator of population. Jensen (1983) contends that the process of creating LULC types induces loss of biophysical information. Moreover, Webster (1996) argues that land use is not directly linked to information about housing and its utilization in population models can create estimation errors. Recent efforts in population estimation have seen the use of the Vegetation-Imperviousness-Soil (VIS) urban model (Ridd 1995, Wu 2004, Lu and Weng 2006, Weng and Quattrochi 2007) to quantify human disturbance to the natural land covers (Li and Weng 2005, Wu et al. 2005, Lu and Weng 2006, Wu and Murray 2007, Morton and Yuan 2009). Ridd (1995) established the V-I-S model in which an urban environment can be characterized by its biophysical composition in terms of vegetation, impervious surface, and soil. An impervious surface consists of materials that prevent water to infiltrate the soil (Ridd 1995, Ji and Jensen 1999). Impervious surface fraction provides the proportion of a pixel made of impervious material and preserves considerable amount of information about housing density (Ji and Jensen 1999). The VIS model has recently gained more popularity because of its potentiality to provide context for population distribution.

However, to the best of our knowledge, no studies have been reported using VIS to estimate population for cities in the developing world such as Haiti.

Another issue with population estimation methods concerns the assumption of stationarity implied by global regression models such as the Ordinary Least Square (OLS) method. Most studies on population estimation assessed the OLS model as a starting point of their analysis (Sutton et al. 1997, Harvey 2002b, Qiu et al. 2003, Li and Weng 2005, Lu and Weng 2006, Wu and Murray 2007). OLS assumes the normal distribution of the dependent variable and independence among the observations and/or the residuals. When these assumptions are not satisfied, the estimation of the coefficients can be biased. For instance, the presence of autocorrelation in the data may lead to wrong conclusions on the relationship between the dependent and the independent variables (Qiu et al. 2010). In short, global models cannot handle the problem of spatial non-stationarity (Langford 2006). Some suggest that regional regression fitted independently for each sub-region or analysis unit can provide greater estimation precision (Yuan et al. 1997) by taking into account in their measurement the fact that the social processes vary from one place to another (Fotheringham, Brunsdon and Charlton 2002). The Geographically Weighted Regression (GWR) (Fotheringham et al. 2002, Huang and Leung 2002) takes into account local variations and aptly deals with the issue of spatial autocorrelation, and thus improves the accuracy of population estimation over the global OLS model. The use of the GWR has emerged as a promising technique in improving population estimation (Yu and Wu 2004, Langford 2006, Lo 2008).

This research aims to construct a population regression model for Port-au-Prince by RS data. Specifically, based on the Landsat ETM+ data, we use the urban VIS model to extract explanatory variables and the GWR method to capture spatial variability in the influence of each

variable on population density. The model has potential for future uses of estimating population patterns in Port-au-Prince or areas of a similar setting in absence of census data. Such data will be useful to support research and planning in disaster management, mitigation and post-disaster recovery.

IV.2 Data processing

The IHSI released the population (and housing units) data and a map of SDEs, but no spatial data in GIS or other socio-demographic information. To reconstruct the GIS database for this study, we scanned the map printout, used control points to geocode the map, and digitized it into a shapefile in the ArcGIS platform.

In order to match with the 2003 census data, the Landsat 7 Enhanced Thematic Mapper Plus (ETM+) image (path 009 row 047) on March 7 of 2003 was obtained from the USGS Earth Resource Observation Systems Data Center (http://landsat.usgs.gov/index.php). Landsat 7 ETM+ was the only sensor for which high resolution images were available for the area of study for the period the census was implemented. This specific image was chosen for its lowest percentage of cloud cover (2%) with high quality. It was right before the failure of the scan line corrector of the ETM+ on May 31th 2003, and thus acquisition of any ETM+ images afterwards was not feasible. The image already had the radiometric and geometrical corrections completed. For additional reference, high resolution satellite images of this area were obtained from Google Crisis Response Website (http://www.google.com/relief/haitiearthquake/geoeye.html). These color images include 4-m resolution IKONOS images and 1.65-m resolution GeoEye-1 images. These images were acquired in the week after the Haiti's earthquake on January 12, 2010. Although there were significant changes after 2003 particularly from the earthquake, the images were useful for visual inspection and reference for our analysis.

Following the procedure described in Wu and Murray (2003), we processed the Landsat ETM+ image to obtain the V-I-S fraction images by using the Linear Spectral Mixture Analysis (LSMA). This algorithm decomposes the images into a number of components called endmembers after eliminating noise such as the effect of water. Endmembers are a combination of spectra made of pure land cover types, and each endmember corresponds to a pure land cover. Endmembers were located by visual examination of scatter plots for spectral information of an image's band combinations (Rashed, Weeks and Gadalla 2001). Three processes were performed in LSMA: (1) using the maximum noise fraction (MNF) transformation, which is a cascade principal component (PC) transformation, to guide the selection of endmembers from the reflectance image, (2) computing the pure pixel index (PPI) in aid of the selection of endmembers after 15,000 iterations at a threshold of 2.5, and (3) using the N-Visualization tool in the ENVI software to define the endmembers by selecting the corner pixels in the n-dimensional feature space.

Three endmembers were identified by examining the spectral curves and locations of the endmembers in high resolution images, as plotted in Figure 12(a). The linear unmixing algorithm produced three fraction images of endmembers and one image of the root mean square error (RMSE) of the least square fitting. Two constraints were applied to the least square fitting to ensure that the fraction of each endmember is positive and that the sum of them equals to one following the procedure developed by Chang & Heinz (2000). The fraction images of the three endmembers are displayed in Figure 12 (b) – (d). The residuals of the linear unmixing are expressed in Root Mean Square Error (RMSE) in Figure 12(e). The mean RMSE is 0.017, better than the value reported in (Wu and Murray 2003).

IV.3 Defining variables in regression models

As suggested by the VIS model, urban population density can be predicted by variables related to the fractions of vegetation, residential houses and concrete pavement (impervious surface), and soil captured by remote sensing data. This section discusses the definitions of these variables for subsequent regression models.

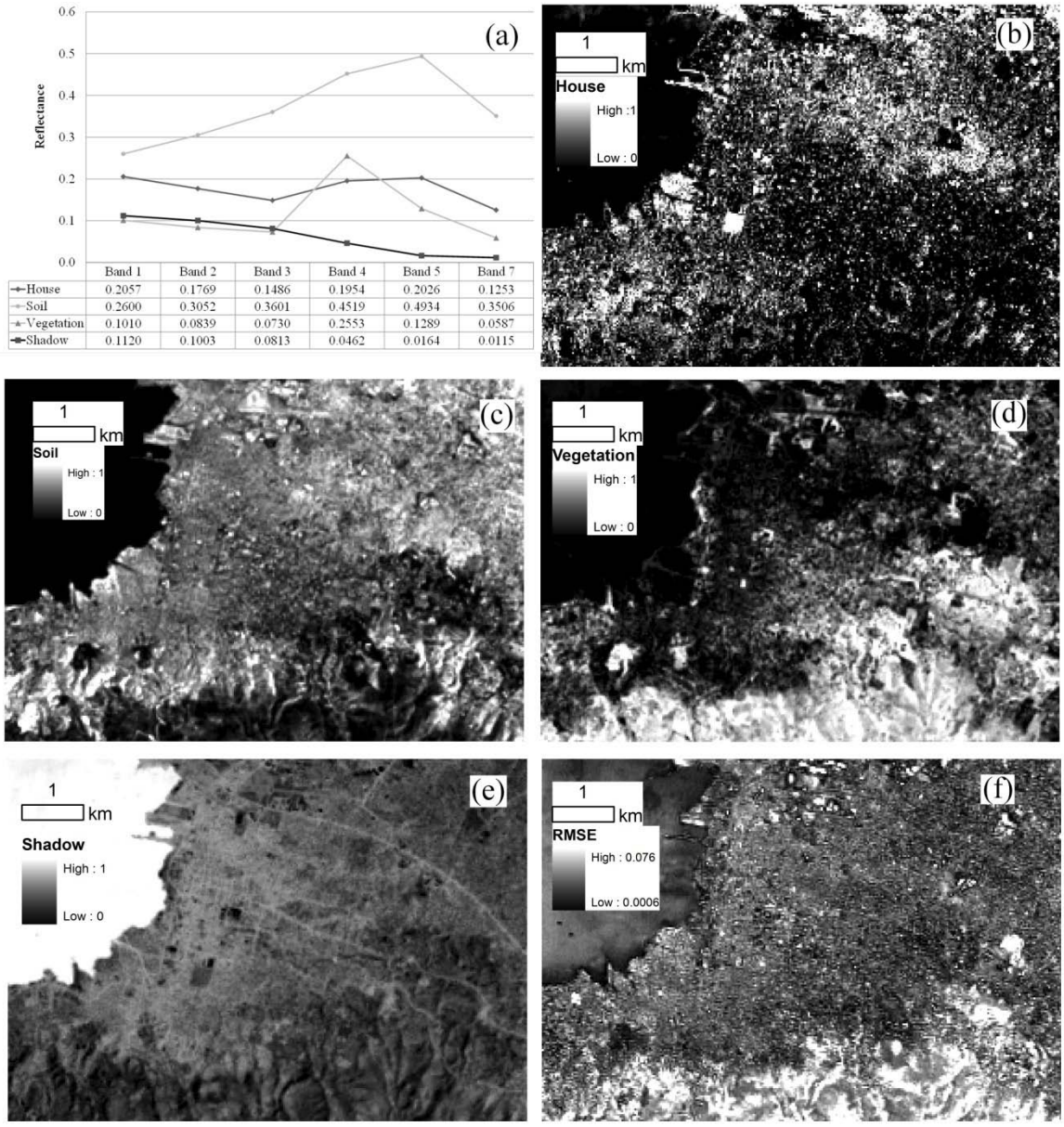

	Band 1	Band 2	Band 3	Band 4	Band 5	Band 7
House	0.2057	0.1769	0.1486	0.1954	0.2026	0.1253
Soil	0.2600	0.3052	0.3601	0.4519	0.4934	0.3506
Vegetation	0.1010	0.0839	0.0730	0.2553	0.1289	0.0587
Shadow	0.1120	0.1003	0.0813	0.0462	0.0164	0.0115

Figure 12 : a) Spectral reflectance curves of the endmembers from the Landsat ETM+ image, (b) – (e) Fraction images of each endmember (house, soil, vegetation, and shadow), (f) RMSE of the fully constrained linear unmixing calculation

IV.3.1 Population density and its transformation

Population density, as the dependent variable in regression models, is measured as the number of people per km^2 at the SDE level. Several transformations on population density have been used in the literature to maximize a model's fitness. Transformation is recommended for datasets with increasing residuals for larger values of the dependent variable or when the standard deviation is proportional to the mean value (Keene 1995). This trend in the residual happens because the change in the dependent variable represents a percent of the value instead of an absolute value (Hopkins 2000). The logarithmic (log) function transposes non-uniform residuals to uniform residuals and provides the optimal estimate of percent change. In other terms, the log transformation weighs observations according to a ratio scale and lessens problems related to percent changes from baseline. Therefore, models derived from log-transformed absolute values are likely fit for the data better and mitigate the problem of underestimation or overestimation reported for most linear population estimation (Keene 1995, Hopkins 2000). The logarithmic transformation is also used in modeling the spatial pattern of population density decay with distance from the city center (Clark 1951).

Others suggest the square root transformation. The Box-Cox function provides a valid approach of integrating these transformations (Keene 1995), as expressed below:

$$Z = \begin{cases} (y^{\lambda} - 1)/\lambda & (\lambda \neq 0) \\ \log(y) & (\lambda = 0) \end{cases},$$

where y is the original data, and λ is the power to which y is raised in order to normalize its distribution. When λ = 0, a log transformation is required; when λ = 0.5, a square root transformation is recommended; and when λ =1, no transformation is necessary.

Figure 13 plots the frequency distributions of population density in the study area, and those of post-transformations. The positive skewness of the original data indicates the need of

data transformation. Either the log or the square root transformation converts the data closer to normality (median slightly larger than mean in both). Both transformations were assessed at the early stage of our analysis, and the log transformation was chosen for a slight advantage in fitness of the models. By doing so, the change in the dependent variable represents a percent of the value instead of an absolute value.

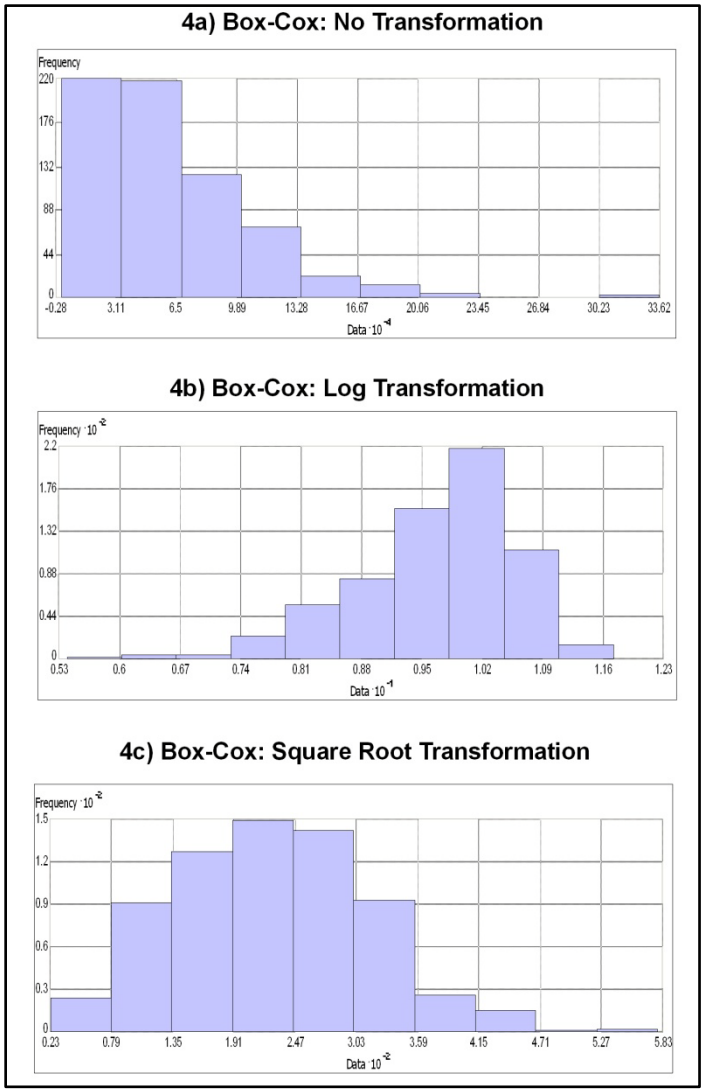

Figure 13 : Box-Cox transformation of population density: a) Strong positive skewness of original data (median < mean), b) Log transformation, c) Square root transformation.

IV.3.2 Defining explanatory variables

All explanatory variables were based on the Landsat ETM+ images, and were aggregated to the SDE level to match with the census data. In addition to the means of three endmembers (vegetation, houses, soil), we tested the standard deviation of vegetation as an indicator for vegetation's spatial continuity. In a typical urbanized area in a developing country such as Port-au-Prince in Haiti, it is commonly observed that a high population density tends to be associated with less and highly-fragmented vegetation. The standard deviation of vegetation fraction captures the degree of variation in vegetation cover across image pixels within a SDE. If the standard deviation is low, the area may be highly vegetated with small fragments of built-up areas or low vegetation cover in a high density residential area. A high standard deviation of vegetation cover represents possible fragmentation of both vegetation and residential areas, which corresponds to low population density residential areas (e.g., the mountainous area to the south).

IV.3.3 Selecting explanatory variables

In order to help select variables in regression models, we began with simple bivariate correlation analysis between logarithm of population density and each measure of fraction variables. Table 1 reports the correlation coefficients and the significance level of each variable.

All explanatory variables extracted from the RS data correlate with population density with statistical significance, but the strength of correlation varies. The mean of vegetation fraction has a strong negative correlation with population density (r=-0.74). The standard deviation of vegetation fraction also has a negative correlation with population density (r=-0.66). Areas with a higher vegetation fraction or a higher-fragmented vegetation cover encompass fewer buildings thus lower population density. Soil fraction abundance has the weakest

relationship with population density, and its coefficient even has an unexpectedly positive sign. One likely explanation is the unique linkage between soil fraction and population density in the study area because of the presence of bare soil (unpaved streets) in high-density squatter areas and reflectance from buildings made of makeshift materials in these areas. Residential houses, directly representing impervious surface fraction, has a moderate correlation coefficient of 0.47 with an expected positive sign. We suspect that the complexity of building structure in the study area might have dampened the contribution of this variable in estimating population.

One concern inherent to a multivariate regression model is the issue of collinearity among explanatory variables as some of the explanatory variables may correlate with each other and contain duplicated information. Multi-collinearity leads to erroneous estimates of coefficients and corresponding standard errors in the regression model and thus misinterpretation of influence of each explanatory variable. Multicollinearity affects the ability to generalize the model (Shroeder 1990). Advances in statistical software enable us to compute several indicators for diagnosis of multicollinearity such as the tolerance value, the Variance Inflation Factor (VIF), and the condition number (*K*).

The tolerance value represents the proportion of variability exclusively accounted for by an independent variable, and is equal to the result of subtracting from one the squared multiple correlation between a specific independent variable and the other independent variables involved in the regression ($1 - R^2$) (Norusis 1983). VIF, considered as the most reliable indicator to assess multicollinearity, is the excess of variance associated with each variable when multicollinearity is present in the regression (Shroeder 1990). VIF indicates by how much multicollinearity degrades the precision of the model (Fox 1984) and is equal to the inverse of the tolerance number:

$$VIF = \frac{1}{1 - R^2}$$

The other indicator, condition number (*K*), is generated from the eigenvalues that are issued from factor analysis. The condition number is formulated as the square root of the proportion of the largest to the smallest eigenvalue:

$$K = \sqrt{\frac{\lambda max}{\lambda min}}$$

in which λmax and λmin are the largest and the smallest eigenvalues issued from the collinearity diagnostic statistics. A greater probability of collinearity is associated to smaller eigenvalues. A common rule of thumb is: (1) a tolerance value equal or less than 0.01, (2) VIFs of 10 or higher, and (3) a condition number *K* greater than 15 are sources of concerns for multi-collinearity. If *K* is greater than 30, there are definitely serious reasons to be alarmed (Shroeder 1990, Simon 2004, Weng and Quattrochi 2007).

Table 4 presents the multi-collinearity diagnostic result for the chosen model after we experimented with numerous plausible combinations of explanatory variables. The model is free of any apparent concerns for multicollinearity. The selected explanatory variables include the mean value of houses, the mean of vegetation and the standard deviation of vegetation.

Table 4 : Multi-collinearity diagnosis for the OLS model

Variables	Collinearity diagnostic			R^2	F
	Tolerance	VIF	Condition number		
Mean_House	0.72	1.4	11.6	0.45	181.0
Mean_Veg	0.29	3.5			
Stdv_Veg	0.33	3.0			

IV.4 Model estimation and assessment

In order to develop the model for estimating population density as well as validate it, the study area was divided into two datasets. The whole area of 670 SDEs was randomly divided into a training data set and a validation data set, each with 335 SDEs.

IV.4.1 OLS regression

An Ordinary Least Square (OLS) regression model was first fitted, and the result for the training area is written as:

$$\begin{array}{l} \text{Log(Dens)} = 11.17 + 3.21\ \text{Mean\_House} - 4.03\ \text{Mean\_Veg} - 1.68\ \text{Stdv\_Veg} \\ \qquad\qquad\quad (107.4)\ \ (3.2) \qquad\qquad\quad (-10.07) \qquad\quad (-1.74) \end{array}$$

where the corresponding t-values in parentheses indicate that the first two explanatory variables are statistically significant at 0.01, but not the variable Stdv_Veg (standard deviation of vegetation). The model yielded a $R^2 = 0.62$. Both the positive sign of Mean_House (mean of house fraction) and the negative sign of Mean_Veg (mean vegetation fraction) are expected. Although the variable Stdv_Veg is not significant, it has the expected negative sign.

IV.4.2 Geographically weighted regression

In an OLS model, the coefficient of each explanatory variable is assumed constant across the whole study area. However, the measurement of the relationship is affected by variability over space, termed “spatial non-stationarity” (Lo 2008). In our study area, the spatial non-stationarity might be associated with different land use and land cover types and various stages of urban development in different parts of the city. Additional causes of non-stationarity may include spatial variability of classification errors and aggregation of data from satellite images to SDEs (Lo 2008). The geographically weighted regression (GWR) method (Shroeder 1990,

Fotheringham et al. 2002) can be used to mitigate the problem. The mathematical expression of the GWR regression is as follows:

$$Y_i = a_{io} + \sum_{k=1}^{n} a_{ik} x_{ik} + e_i \qquad (1)$$

where *k* indexes the explanatory variable *x* and its corresponding coefficient *a*, and *i* indexes the location (i.e., i = 1, 2, …, 335 of SDEs in our study). For instance, a_{ik} is the estimated coefficient of *k*-th variable at location *i*. Similarly, the GWR model is to explain the logarithms of population density by three remotely-sensed predictors (*k* = 1, 2, 3): the mean values of the fraction image of the houses endmember, the mean value of vegetation and the standard deviation value of vegetation.

The estimator for this model takes into account measurements of the independent variables not only available at the location *i*, but also is equally conditioned on the relative location of *i* to other observations nearby based on a weighting schema. Observations closer to a point *i* considered are given more weights than neighbors farther apart. A spatial kernel, fixed or adaptive, is used to establish a limit to the number of neighbors around the point considered. For an evenly distributed dataset, a fixed kernel is recommended; otherwise, an adaptive kernel is used. Given the irregularly distributed configuration of the data used in this study, an adaptive kernel with 30 nearest neighbors was applied, as suggested by the GWR tool. The GWR produces parameter estimates for each point considered and thus accounts for the spatial non-stationarity in each predictor's influence on population density.

The GWR model also yielded an adjusted R^2=0.80, a significant improvement over the OLS model with R^2 = 0.62. In addition, the corrected Akaike's Information Criterion (AIC) index is used to measure the relative performance of a model. The AIC is a natural way to compare complex models with prior distributions in that it is based on the posterior distribution

of the log-likelihood, following the Bayesian model framework built by Dempster (1974). The AIC builds a trade-off between the data fit of the model and the complexity of the model. A smaller AIC value indicates a better data fit and a less complicated model. The GWR's AIC = 466, smaller than the AIC=562 by the OLS. Therefore, the GWR outperformed the OLS in fitting the training data set.

IV.5 Validation of the models

The above discussion on R^2 and AIC examines the fitness of a model on the training data set, which does not necessarily converts to its prediction power. A model may score in high fitness and accuracy values in the testing area, but fail to reproduce the same results in the validation area. The extensibility of a model is its ability to demonstrate stability (robustness) by providing similar estimation results when applied to a different spatial or temporal context.

The performance of a model can be evaluated through several characteristics such as bias, consistency, accuracy, validity, and robustness (Harvey 2002a). The presence of bias in a model is indicated by the consistent underestimation or overestimation of the dependent variable. Variability or conversely consistency refers to the range of values of the estimation error for individual cases, large or small. Bias and variability are two components or cause of inaccuracy in the estimates. In this study, these three aspects together are measured by two indicators: the mean absolute proportional error (mean % error or MAPE) and the median absolute proportional error (median % error). The robustness of a model is tested by the application of the estimation coefficients to the validation area.

The relative or proportional estimation error is expressed as

$$R_{Ek} = \frac{P_{Ek} - Po_k}{Po_k} * 100$$

where R_{Ek} is the relative error for case k; P_E is the population estimate from a model; and P_O is the true population obtained by census. Then, the mean % error (MAPE) is defined as follows

$$Mean\ \%\ error = \sum_{k=1}^{n} \frac{|R_{Ek}|}{n}$$

The median % error is the 50th percentile of the ordered n values of $|R_{EK}|$, where n represents the total number of observations in the data set. The mean and median % errors are used together because of the distorting influence of a few outliers on the mean (Harvey 2002a, Lu and Weng 2006).

In addition, the overall estimation bias (Total Relative Error) is assessed such as

$$R = \frac{(P_E - P_O)}{P_O} * 100$$

where P_E and P_O represent the total predicted population and the total observed population, respectively, for the area considered.

To validate a model, the regression result based on the training data set is applied to the validation data set. The GWR algorithm includes a feature that permits estimating coefficients at locations with no data, such as SDEs in a validation set (Fotheringham et al. 2002). To this end, the algorithm interpolates the fitted GWR coefficients to the known locations of the validation area using the parameters provided (such as kernel type, bandwidth method, distance, and number of neighbors) to launch the regression. Figure 14b displays the predicted population density by the GWR, in comparison to the observed population density in Figure 14a. Overall, the two maps exhibit a strong consistency across the study area, and most SDEs stay in the same density classification. This suggests that in general the model performed well in reproducing and predicting population density in the study area.

The differences between observed and estimated densities are residuals. Residuals by GWR are shown in Figure 15, and by OLS in Figure 16. The light colors point out to low residuals while the darker colors of both spectrums indicate either overestimation or underestimation. Our discussion here focuses on Figure 15. Largest over-predicted densities are mostly located in the south-southwest and northern-northeastern regions, which are characterized by very high population density, poor housing conditions, unpaved streets and abrupt terrain (Joseph and Wang, 2010). Most cases of large underestimation by RS signals are also located in areas where housing density is extremely high and correspond to small census units. Some cases of underestimation were also observed south-southeast of the city center. This area is host to some public parks, government buildings and a mix of commercial-residential housings where many people lived there in contrast to expectation or the model's prediction. Conversely, estimated census tracts were observed along the spines going from north of the city center eastward, and south of this road eastward (in the neighborhood of Lalue, Ave John Brown). Since the model correlates the presence of man-built structures with high density, this commercial area had few residents living there, and thus was over-predicted by the model. Note that the residuals by GWR shown on Figure 15 do not exhibit obvious clusters, whereas the residuals by OLS in Figure 16 displays clear clusters of ovepredictiion mainly in the commercial and the transition zones in the northwest area and underprediction in high density areas in the south.

Table 5 presents the performance indicators of the OLS and GWR. The advantages of the GWR model are clear with a significant higher accuracy in population estimates. Understandably, the errors in the validation area are higher than those in the training area. The mean (MAPE) and median proportional errors for the validation area by GWR were 40.4 and

27.3 respectively, higher than 26.1and 19.8 for the training area. The total relative error was equal to 8.1% in the validation area compared to 2.8% for the training area. A large discrepancy was noticed in the minima (0.01 and 0.1) and the maxima (314 and 513.5) of the mean proportional error between the training and the validation areas. Since the selection of the training and the validation areas were randomly made, we suspect that this difference in the mean and the median is inherent to the specific characteristic of the SDEs in each dataset. Overall, the difference is not substantial enough to undermine the robustness and validity of the model.

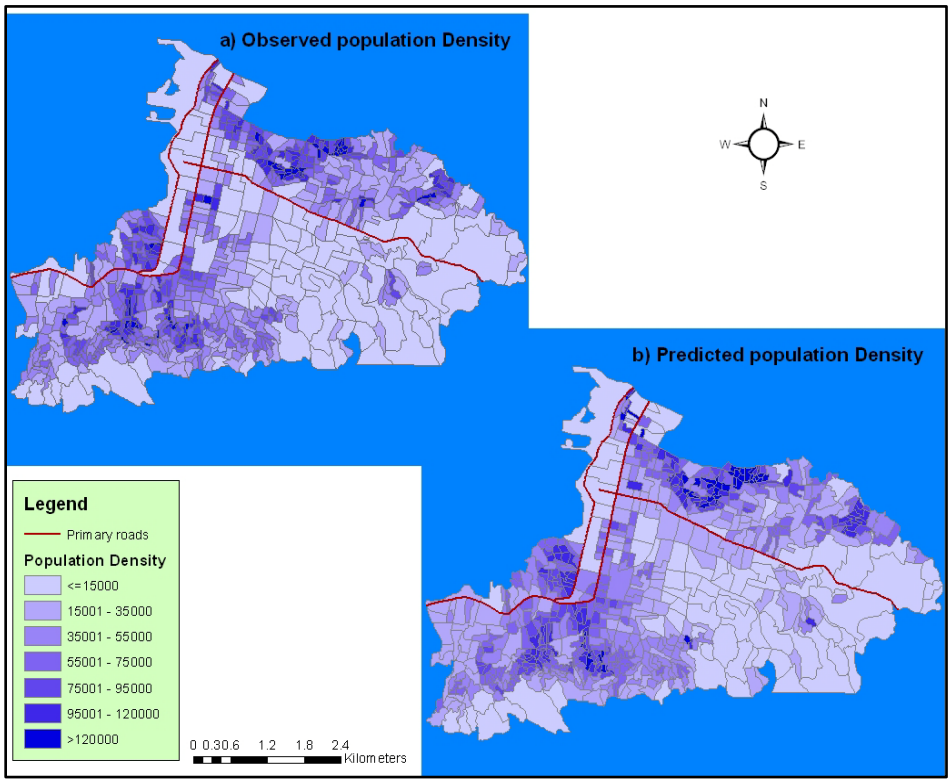

Figure 14 : Observed vs. predicted population density from GWR

IV.6 Spatial variability of linkage between RS signals and population density

By analyzing the spatial variations of GWR coefficients, we can develop a better understanding of the urban development, living environment quality, and spatial segregation of population in Port-au-Prince.

Table 5 : Indicators of regression model performance

Model	Data set	Mean % Error	Median % Error	Total % Error
OLS model	Training Area (n=335)	54.4	32.0	11.1
	Validation Area (n=335)	83.9	30.8	24.9
GWR model	Training Area (n=335)	26.1	19.8	2.8
	Validation Area (n=335)	40.4	27.3	8.1

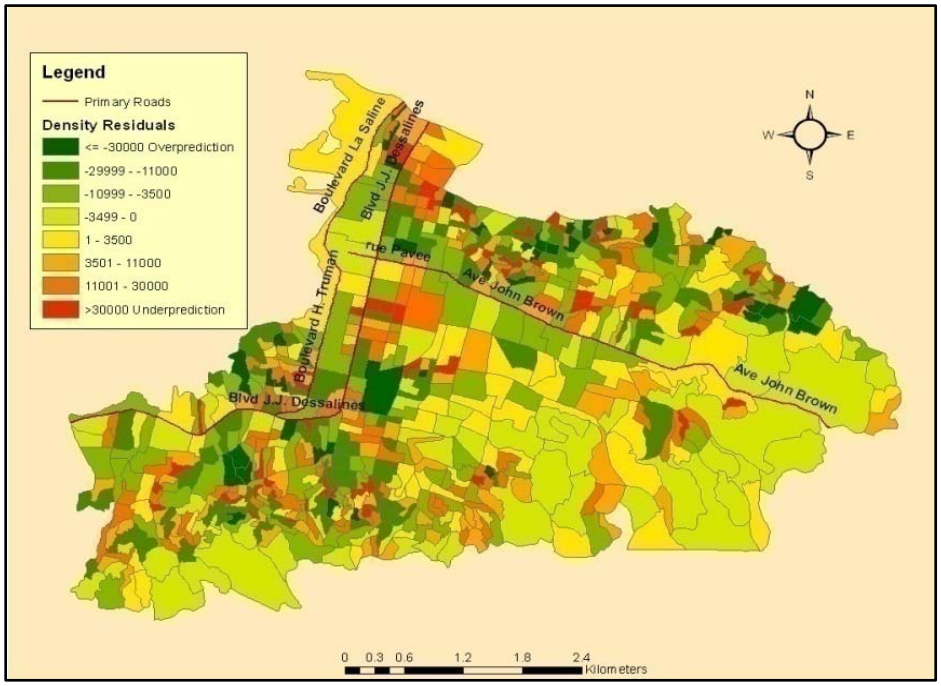

Figure 15 : Estimation residuals by GWR

The spatial variations of regression coefficients in the GWR model are mapped in Figures 17-19. Both the sign and value of each of the three coefficients vary over space, and indicate high spatial non-stationarity. The coefficients for mean fraction image of houses ("Mean_House") exhibit high positive values in the south-southeast area but negative in the northwestern corner as well as the northeastern area (Figure 17). The southeastern region had more vegetation cover than anywhere else in the study area with relatively scarcely distributed

residential houses and thus the population prediction model put heavier weight on the housing land identified from the remote sensing image. The opposite can be said for the north areas of high population density. In other words, the housing coefficient represents the potential of the land in supporting more population growth.

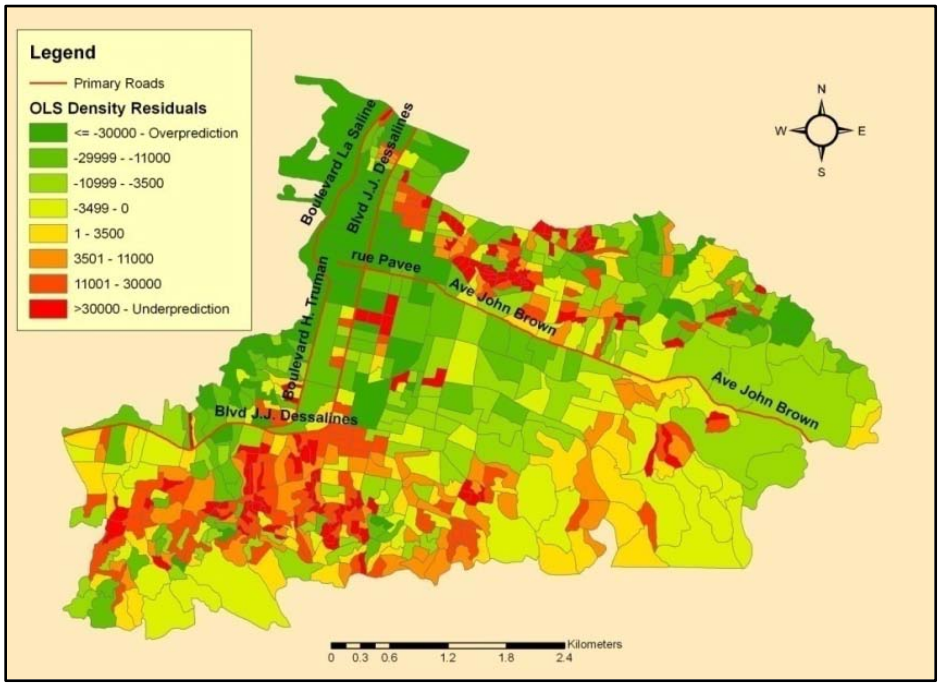

Figure 16 : Estimation residuals by OLS

Figure 18 displays the pattern of the coefficients for “Mean_Veg” (mean fraction image of vegetation). The coefficients decline towards the east and southeast (higher elevation areas). The lowest (negative) values are observed in the northwestern tip of the area with little vegetation present. That is to say, on top of the overall negative relationship between Mean_Veg and population density, the effect is amplified by even more negative coefficients in high-vegetation (low-population-density) areas and positive coefficients in low-vegetation areas.

Figure 19 depicts the variation in the coefficient estimates for “Stdv_Veg” (standard deviation of vegetation fraction). The coefficients range from the lowest (-80.5) in the northwest region to the highest (13.5) in the southeast. The pattern is in a strong contrast to Figure 18 for

"Mean_Veg". The southeast area has higher vegetation (and thus higher Mean_Veg) implying that it is less fragmented (and thus lower Stdv_Veg). Therefore, the model honors more on the spatial fragmentation (e.g. by changing land from vegetation to houses) of residential houses and vegetation cover than the amount of vegetation. The land to the north-east has little vegetation (Figure 12d) cover within the built-up area. Thus, increasing the spatial fragmentation of vegetation (e.g. by planting more trees) is not appreciated by the model.

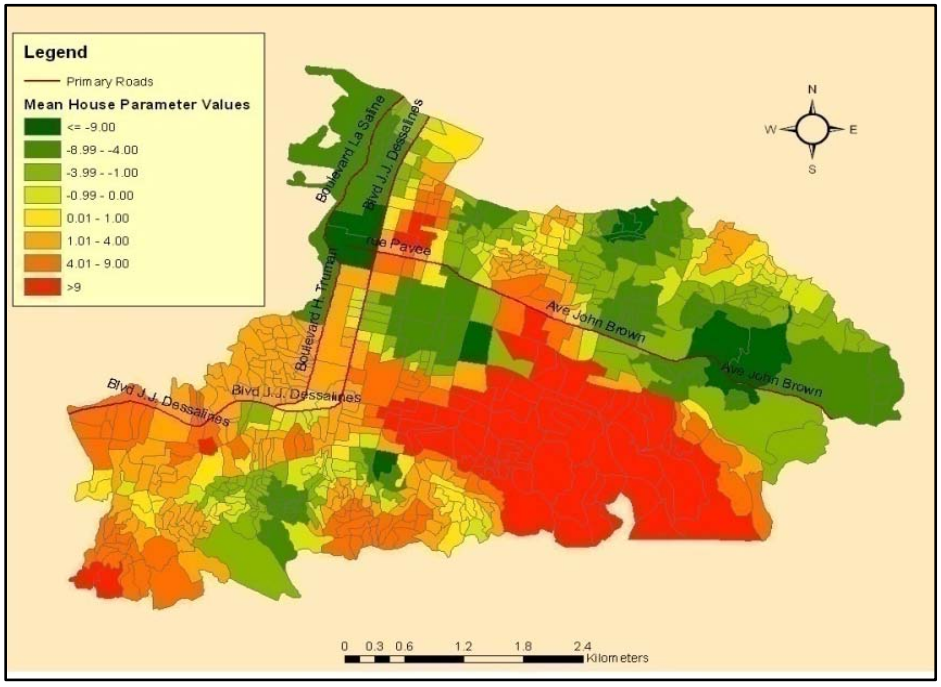

Figure 17 : Spatial variation of coefficient for mean fraction image of houses in GWR

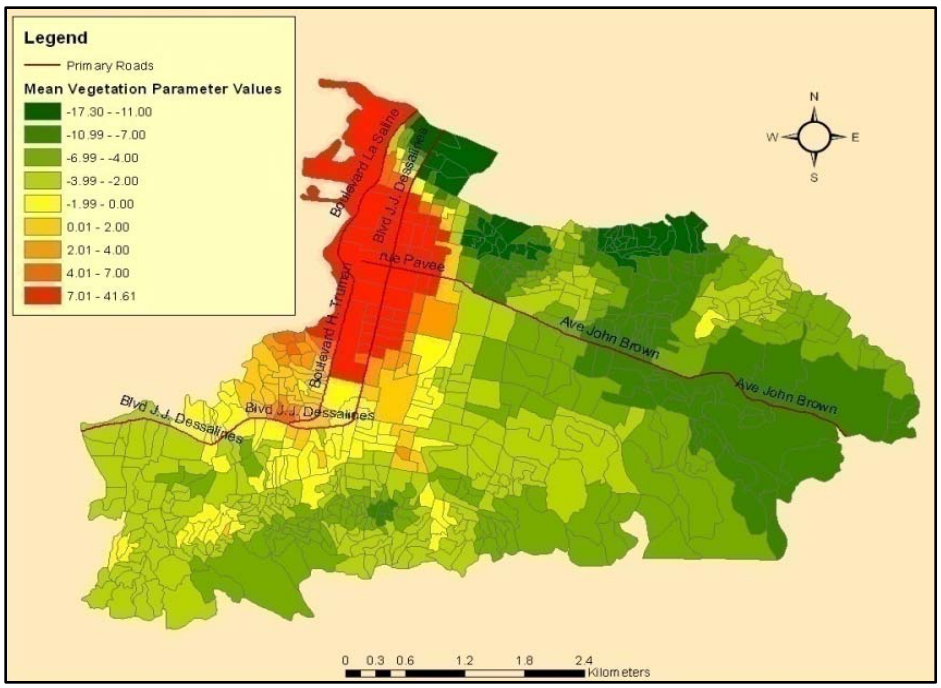

Figure 18 : Spatial variation of coefficient for mean fraction image of vegetation in GWR

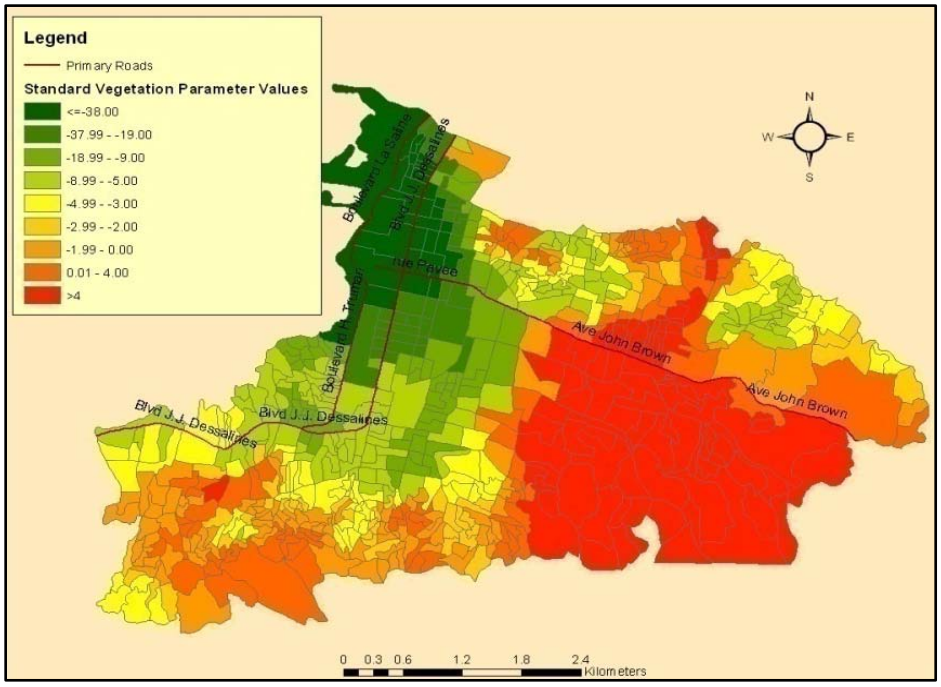

Figure 19 : Spatial variation of coefficient for standard deviation of vegetation in GWR

IV.7 Summary and concluding comments

This paper has attempted to identify a suitable model for population estimation from remote sensing image in Port-au-Prince, Haiti. Explanatory variables used in the regression were

fraction images extracted from Landsat ETM+ images by spectral mixture analysis. These variables at the pixel level from remote sending image were aggregated to the SDE level to match with the population data from the census. Our initial models tested a wide range of explanatory variables related to the fractions of vegetation, impervious surface and soil, and standard deviation of vegetation. Based on various diagnosis statistics for multi-collinearity, three variables were kept: the mean value of houses, the mean of vegetation and the standard deviation of vegetation. The dependent variable was defined as the logarithms of population density in order to improve the model's fitting power. An OLS regression model was tested and achieved a R^2 of 0.62. Due to spatial non-stationarity, the geographically weighted regression (GWR) was employed to permit the variation of each coefficient across the SDEs, and generated an adjusted R^2=0.80. The AIC for the GWR was also smaller that the AIC for the OLS, and thus the GWR was a better model considering both the data fit and the model's complexity.

By randomly splitting the study area into a training data set and a validation data set, we were able to assess the accuracy of these models. Based on the indicators such as mean proportional errors, median proportional errors and total relative errors, the advantages of the GWR model was further validated. A number of conclusions can be drawn from the study. First, urban population density can be estimated from fraction images extracted via spectral mixture analysis with reasonable accuracy. Secondly, the logarithm transformation of population density yielded better fitting power than the square root transformation or population density itself. Thirdly, not all endmembers from RS data and their related statistics (mean, standard deviation) contributed to the explanation power of the regression models. Finally, the GWR regression was a better model than the OLS in terms of a better fit for the training data set (even after accounting for the model's complexity) as well as a higher accuracy for the validation data set.

The results show the promise of using remote sensing data to estimate urban population density in a region of a developing country. This is particularly important for a country the study area such as Haiti, which was anticipated to conduct its next national census in 2013 but seems unlikely to take place since much of the attention in the aftermath of the earthquake has been focused on reconstruction efforts with no plans of implementing a national census. Updated information about the distribution of population is crucial in planning for service delivery and other purposes in Port-au-Prince and beyond.

CHAPTER V ASSESSMENT AND MAPPING OF URBAN ENVIRONMENTAL QUALITY IN PORT-AU-PRINCE, HAITI

V.1 Introduction

The world is undergoing an unprecedented process of urbanization. According to the Economic and Social Affairs division of the United Nations, over sixty percent of the world's population is expected to settle in urban areas by 2030 (UN 2003). The internal structure of a city, particularly in developed countries, is hardly random and conforms to some stunning regularity (Stutz and Warf 2007). However, the expansion of urban population in countries of the less-developed world has taken place in absence of required development of services and facilities in order to maintain the urban environment adequate and healthy (Hardoy, Mitlin and Satterthwaite 2001). The inadequate management of the impacts of rapid urbanization results in deterioration of the human health, the environmental quality, the quality of life and the urban productivity of the residents, mainly the poorest (Leitmann, Bartone and Bernstein 1992).

There is a rich body of literature on studies of quality of life (QOL), which have turned toward urban areas mainly because of the increasing urbanization trend observed lately and the concomitant alteration of the living conditions. The domains of QOL encompass physical, material, environmental, emotional, social, behavioral, psychological, and spiritual aspects, and can be approached objectively or subjectively across different cultures and disciplines (WHOQOL-Group 1995, Testa 1996, Cummins 1997, Felce 1997, Haas 1999, Hagerty et al. 2001, Janse et al. 2004). The measurement of these domains may include indicators as broad and diverse as health, physical environment, natural resources, personal development, security, socio-economic status, psychological elements, housing, neighborhood conditions, demographic status, and education (Dahmann 1985, Bonaiuto et al. 1999, Haas 1999, Mitchell, Namdeo and Kay 2001, Kjellstrom 2007, WHO 2007, Fleury-Bahi, Félonneau and Dorothée 2008, Hur and

Morrow-Jones 2008, Rehdanz and Maddison 2008, Walton, Murray and Thomas 2008, Hur, Nasar and Chun 2009, Metropolitan-Studies-Group 2010). In the (Mercer 2011) report, the concept QOL is based on objective and unbiased measurements that target the mesosystem and macrosystem levels as conceptualized by Schalock (1996).

The implementation of effective policies should take into consideration the multidimensional aspect of QOL and furthermore be built on a spatial approach. More specifically, sound environmental policies need to identify places of high exposure to harmful environmental conditions, followed up by actions to protect the affected populations. The goals are first, in the long run, to bring up corrective actions to deteriorated neighborhoods; second to slow the process of declining environmental quality; and third, prevent further similar environmental issues. In that vein, Lo and Faber (1997) underline the necessity for planners and government agencies to continually evaluate the quality of life of the jurisdiction under their control in order to ensure the delivery of services to the population and to identify areas with problems. In poor countries with limited financial resources needed to mitigate these problems, it is even more crucial to focus the attention on areas where the problems are most severe and likely to worsen in order to prevent further degradation of the environment and the impairment of life conditions. The assessment of environmental quality at a detailed spatial resolution is of utmost importance in urban planning as it will help determine the degree of severity, affected areas, stakeholders and related corrective actions. The ultimate goal is to enhance environmental health and promote social and environmental justice and sustainability.

Urban environmental quality (UEQ) represents one dimension of the broader concept QOL (1998). UEQ is more concerned with the physical, material domain of QOL. However, while the factors within this domain are objective or tangible, their assessment may be based on

facts (objective) or perception (subjective). Previous studies of UEQ included factors derived from different sources such as census, satellite data, physical data, and environmental data. UEQ embodies the interplay of many interrelated parameters from different spheres such as the domestic environment, the public environment, the physical environment, and even the atmosphere (Tzeng et al. 2002, Nichol and Wong 2005). Some studies integrate social environment, economic environment and residential environment (e.g. Bonaiuto et al. (1999), Bonaiuto et al. (2006), Lotfi and Solaimani (2009), Rehdanz and Maddison (2008)). The present study focuses the parameters from the physical and the public environment. The list of factors include vegetation density, greenness, NDVI, leaf area index, heat island intensity, impervious surface temperature, population/household density, aerosol optical depth, building density, building height, noise, air pollution, land use/land cover, water quality, land quality, drainage facility, solid waste, park, open spaces, accessibility to roads, etc. (Lo and Faber 1997, Bonaiuto et al. 1999, Tzeng et al. 2002, Jensen et al. 2004, Kelay 2004, Nichol and Wong 2005, Sanesi et al. 2006, Li and Weng 2007, Rehdanz and Maddison 2008, Nichol and Wong 2009, Rahman et al. 2011). The list is contingent to data availability and adjustable according to the specific environmental context of the study area. Most UEQ studies have given much attention to manmade and technologically-generated environmental hazards, but much less to natural hazards. Natural hazards trigger environmental degradation and destroy the resources of the natural systems. Left unsolved, landslides and flooding, among other hazards, can potentially sink urban centers into environmental chaos (Nyambod 2010). Among the exceptions are Majumder et al. (2007) that included flashflood as a factor in assessing the UEQ of Chittagong Metropolitan City in Bangladesh, and Romero et al. (2012) that considered exposure to flood and waterlogging in the assessment of urban environmental segregation in Santiago de Chile.

Information on location, probability and anticipated impacts are useful to assess impacts to the urban systems (Heiken, Fakundiny and Sutter 2003).

This study is built upon the existing literature on UEQ, with an emphasis of natural hazards that are critical to the residents in our study area. The objective is to integrate some unique factors in Port-au-Prince with other commonly-used physical and demographic parameters in previous studies, and develop a comprehensive measurement of environmental quality in Port-au-Prince. Population density is examined with relationship to various UEQ factors. Results are used to refine the five-sector conceptual model developed previously in Chapter III.

V.2 Parameters of urban environmental quality

The variables used in this study are derived from high resolution remote sensing images, census data and GIS-processed physical parameters. Factors affecting environmental quality are grouped according to their sources and the nature of their contributions to the general UEQ. The first group, subdivided into two subgroups, belongs to the physical environment and addresses environmental amenity (vegetation, greenness or green areas), or environmental disamenity (pollution) such as gas emission and noise from traffic, pollution from water bodies and the sea coast, pollution from solid waste and dusts. The second group is from the public domain and encompasses, in addition to crowdedness, factors that are unique to Port-au-Prince. Those factors are: public markets, slums, and cemetery. Finally, the last group contains three natural hazards, including flooding, landslide susceptibility, and coastal surge.

Due to the deficiency of spatial data for the study area and because of the limited resources, some potential factors that typically impact UEQ could not be included in the implementation of the model. This is the case of trashes dumped on the streets in open sky and

dusts from poorly paved and unpaved roads. Their prediction over space and time was simply not possible. The following parameters are objective in the sense that their assessment did not rely upon individuals' perception. However, their measurement includes subjective methods induced by the utilization of ordinal scales based on proximity. There is not much support from the literature as to the exact distance threshold to use for the proximity parameters. The thresholds used are experimental and arbitrarily chosen by lack of better choice. Nevertheless, the degree of impact assigned to each threshold is logical and is consistent to Tobler's First Law of Geography regarding the influence of distance on relationship (Tobler 1970). A list of parameters and sub-parameters along with their operationalization can be found in Appendix II.

V.2.1 Group 1: Physical domain factors

V.2.1.1 Environmental amenity: Greenness/Vegetation

Within the physical or environmental domain green space in urban areas embodies a fundamental element contributing to the quality of the environment and has been incorporated in most studies. Green spaces provide many tangible and intangible benefits. Vegetation within an urban area understandably represents a great amenity that makes life more enjoyable and more pleasant for many reasons such as mitigation of heat waves and positive impact on the health and the emotional well-being of citizens (Li et al. 2005, Sanesi et al. 2006, Lafortezza et al. 2009); correction of air–temperature exchange and provision of shade to create a comfortable environment for people (Nikolopoulou and Steemers 2003, Shashua-Bar and Hoffman 2003, Gomez, Gil and Jabaloyes 2004); promotion of accelerated recovery from surgery and relief from stress, and the restoration of the cognitive capacities (Ulrich 1984, Kaplan 1995, Bonaiuto et al. 1999, Bonaiuto, Fornara and Bonnes 2003, Hartig 2004, Hartig and Cooper-Marcus 2006).

Greenness was extracted from a Landsat Enhanced Thematic Mapper Plus (ETM+) image processed with the Vegetation-Imperviousness-Soil (VIS) model using the Linear Spectral Mixture Analysis (LSMA). For more details about the procedures see (Joseph, Wang and Wang 2012). The continuous values were converted to an ordinal scale from 1 to 4 using the natural breaks Jenks classification scheme (Jenks 1967). The natural breaks (Jenks) classification method, among the most popular used in GIS software (Osarangi 2002, Longley et al. 2005) is deemed appropriate for rearranging similar values (ESRI 1996) and leads to a relatively low loss of information compared to other classification techniques (Osarangi 2002). Unless indicated, the same categorization procedures used for greenness were also utilized for the other parameters for similar operation.

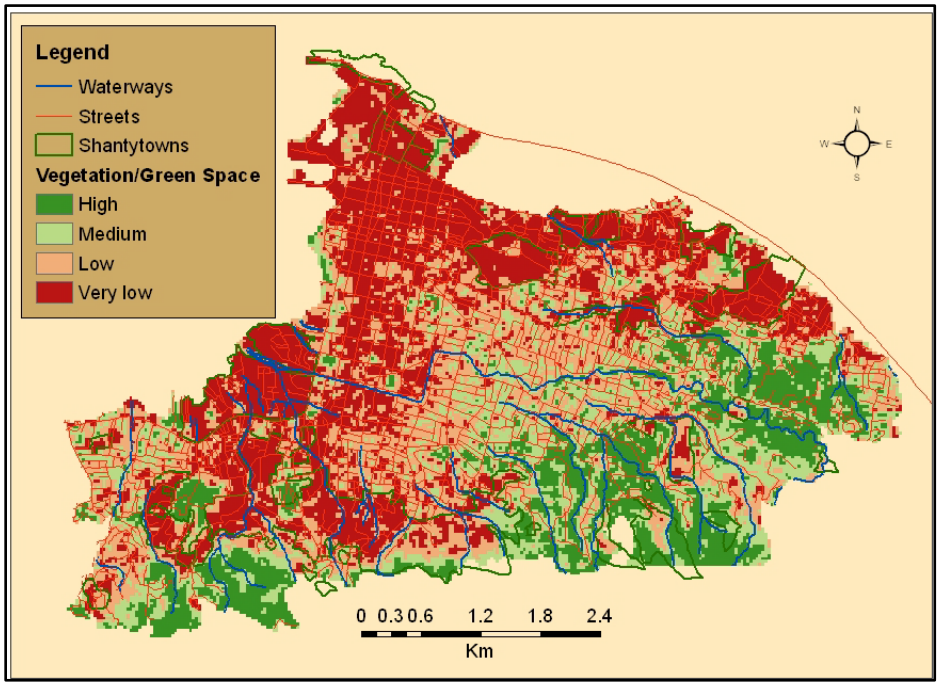

Figure 20 : Distribution of greenness in Port-au-Prince. More vegetation spotted at the south-southeastern edge of the city.

According to experts vegetation represents the most significant feature after crowdedness and waste that affects UEQ with a score of 11.2%. This score represents the average weight of vegetation obtained as the ratio of the total score attributed to vegetation by the sixteen experts to

the total combined score for all the parameters. It is important to mention that the scores for crowdedness and waste were redistributed to the other parameters proportionally to their original score. Figure 20 displays the vegetation cover map resulting from the VIS/LSMA process. The bulk of greenness available is mostly found in the south-southeastern edge of the city. While the southeastern part of the city corresponds to the neighborhoods of the upper-income residents, the south portion is more related to remote and less accessible areas with steep slopes that slow the advance of squatters. The presence of vegetation in some way improves the environmental quality of this zone in spite of the presence of derisory houses.

About eighty eight percent (88%) of the population live in neighborhoods with low to very-low green spaces and most of the slums are included in this vegetation-deprived region. Some dark spots of low to very low green cover are noticed in the southeastern zone. This is due to recent extension of the city mostly by squatters who systematically get rid of the vegetation in order to build their houses, inducing higher risks of erosion and landslide. Another striking but not unforeseen contrast is the density of population between areas with lowest and densest green cover with 66,737 versus 16,709 people per square kilometer, respectively. This underscores the pressure of population on the natural resources and the impact of high population density on UEQ.

V.2.1.2 Gas emission and noise from traffic

As sub-products of the physical environment both noise and air pollution contribute to deteriorate the quality in the surrounding neighborhoods (WHO 1998). Van Leeuwen et al. (2006) underlines the reliance of good quality of life of people living in large cities on the quality of the urban environment. Identified as the main sources of air pollution in urban cities, motor vehicles generate carbon monoxide, hydrocarbons and nitrogen oxides. These major air

pollutants are the main environmental-related causes of lung malfunction, lung cancer, cardiovascular diseases, respiratory symptoms, stroke, neurobehavioral problems, premature mortality, and possible exacerbation of asthma, (Richman 1994, Venn et al. 2000, Venn et al. 2001, Jerrett et al. 2002, Maheswaran and Elliott 2003, Nafstad et al. 2003, Greene and Pick 2006). In addition, studies have demonstrated that noise pollution has adverse effects on health as well. These include high blood pressure, speech interference, sleep hindrance, fatigue, headache, gastro-enteric disorders, loss of appetite, depression, and irritation. Noise pollution interferes with other relaxation activities in the neighborhood and causes discontent with the nearby environment (USEPA 1981, Yoshida et al. 1997).

Many studies incorporate air pollution and noise pollution as main contributors of a low environmental quality (e.g. Dahman (1985), Dike (1985), Giannias (1996), the Ontario Social Development Council (1997), Shafer, Koo Lee and Turner (2000), Rehdanz and Maddison (2008), Nichol and Wong (2009), Schweitzer and Zhou (2010), etc.).

Models of exposure to air pollution include parameters as broad and diverse as proximity to high traffic roads, traffic counts, emission and pollutants data, road type, traffic density, traffic frequency, vehicle type, land use, meteorological and atmospheric conditions, building height, presence and type of buildings, etc. (English et al. 1999, Elliott et al. 2001, Hoek et al. 2001, Hoek et al. 2002, Langholz et al. 2002, Wilhelm and Ritz 2003, Ferguson, Maheswaran and Daly 2004, Schikowski et al. 2005). All modeling approaches but the proximity model requires data about the level of pollutants concentration or health outcomes information that is not readily available and for which the implementation is very costly. Given the limited purpose of the current study the proximity model is indicated in spite of its drawbacks. These drawbacks include the lack of scientific base for the choice of the maximum distance and the different

thresholds within this distance. They are chosen arbitrarily and not supported by existing literature. The application of the proximity approach can result in misclassification. (Jerrett, Arain and Kanaroglou 2005). Finally, it is difficult to determine potential and future exposure (Zou et al. 2009).

Some studies assess distance to roads from a precise location of the exposed subjects, schools or residences (van Vliet et al. 1997, Wilkinson et al. 1999, Janssen et al. 2001, Venn et al. 2001, Hoek et al. 2002). Other studies calculate distance from census units centroid (Maheswaran and Elliott 2003), or establish a buffer around the roads or around the residences (English et al. 1999, Sahsuvaroglu et al. 2009). Distance to roads is used in conjunction with traffic density, building density, and elevation. Based on air emission dispersion models and previous studies of exposure assessment (Verluis 1994, English et al. 1999, Hoek et al. 2001, Sahsuvaroglu et al. 2009) a maximum distance of 200 meters was considered with three threshold values of 50, 100 and 200 meters. Traffic density data is not readily available. This information was generated based on road type (primary, secondary, and arterial street) adjusted with information drawn from a panoramic view of the traffic volume at peak hours obtained from a Google Earth image of Port-au-Prince. The impervious fraction generated from the same procedure described earlier for vegetation was used as surrogate for building density. An impervious fraction represents the fraction of impervious material included in a pixel and that holds information about the density of houses (Chapter IV, page 33-34). These different sub-parameters affecting gas emission were integrated through weighted linear combination using the weights obtained from the expert opinion survey. The experts' survey included one section to evaluate the weights of the four sub-parameters mentioned above affecting air pollution from and three others affecting noise nuisance from traffic.

Heavier traffic generates more pollution and vice-versa. Denser buildings trap and prevent pollution dispersion, and higher elevation is usually associated with more air scattering resulting in lower pollution levels.

Statistical and mathematical models associated to on-site measurements of noise levels include predictors such as wind velocity and direction, traffic speed, lane width, roadway width, number of lanes, traffic volume and composition, road gradients, road surface, and physical barriers (Ali and Tamura 2003, Calixto, Diniz and Zannin 2003, Pamanikabud and Tansatcha 2003, Banerjee et al. 2008). As for the air pollution the purpose of this paper is beyond the scope of measuring noise pollution but rather to determine exposure levels. Thus an experimental distance of 500 meters to roads with increments of 100, 300, and 500 meters were combined with traffic density and buildings density data to generate the noise exposure surface. With the same causal relationship used for gas emission pollution, these sub-parameters were combined according to the same procedure utilized for air pollution. Separate weights were obtained from the experts for distance, traffic density and building density.

Gas emission from traffic was ranked sixth over 11 factors investigated in the expert-opinion survey. Gas emission is exacerbated by the lack of regulations of traffic or the reinforcement thereof and by the too large fleet of cars exceeding the capacity of the roads. This is directly linked to the large population concentrated in Port-au-Prince. No regular and comprehensive inspection for gas emission is conducted by the service of transportation over the vehicles fleet, though many vehicles use diesel at a cheaper price than gasoline with the gasoline having a negative effect on the quality of the environment. In addition, the vehicles fleet mostly includes used car imported from the United States that do not comply with the standards applied in the United States. Lastly, regular maintenance of vehicles is rather atypical. The map in Figure

21 depicts areas affected by different pollution levels from gas exhaust. Worst conditions (high to very high) of gas emission pollution affect 66% of the entire population for a corresponding average density of 62,000 people per square kilometer. The population density in low to moderate pollution is only 55,333.

Noise pollution comes right after gas emission pollution in the experts' survey but it severely affects slightly more people than gas emission from traffic (67%). As for gas emission, noise pollution is density-dependent as areas more severely distressed include higher population density than areas with low to moderate noise pollution: 64,000 versus 52,000. The map of exposure to noise pollution is displayed in Figure 22.

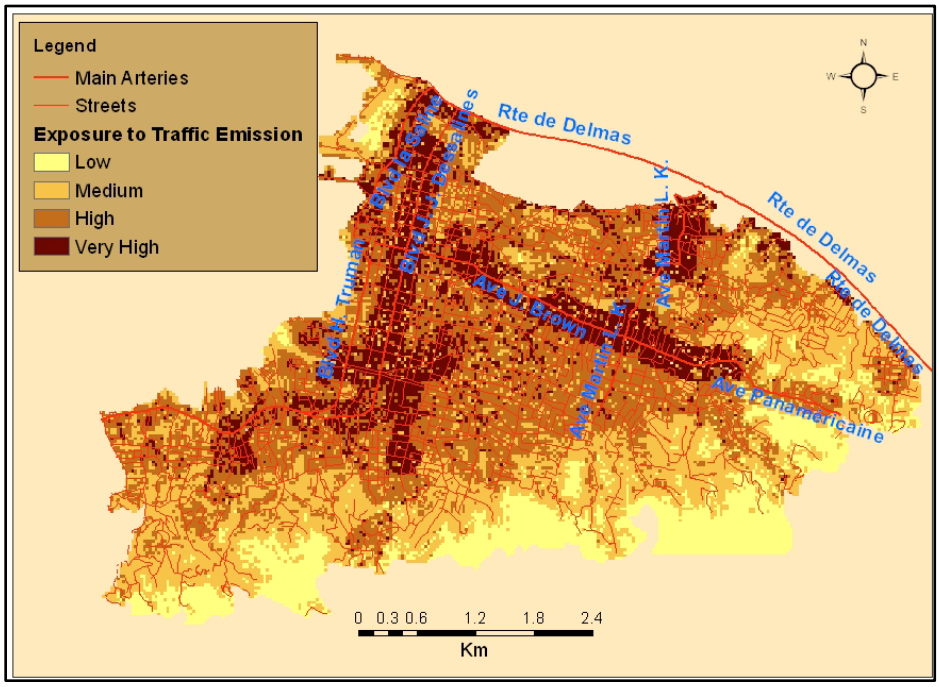

Figure 21 : Exposure to gas emission from traffic

Typically, noise nuisance from traffic originates from vehicles' engines and is exacerbated by the unrelenting use of horns by drivers. In addition to these sources, loud music in certain traffic circles, notably the axes Carrefour-Downtown and Carrefour-Feuilles-Downtown significantly contribute to increase the noise burden. The high decibel level in these

autobuses is used as a strategy to attract customers, particularly the youngest. The higher the noise level, the more likely and the more quickly the seats are filled-up. This has had serious consequences on passengers who are unable to receive or place a call because of music interference. One expert mentioned protestant churches' worship or prayer services and night clubs as additional sources of noise nuisance.

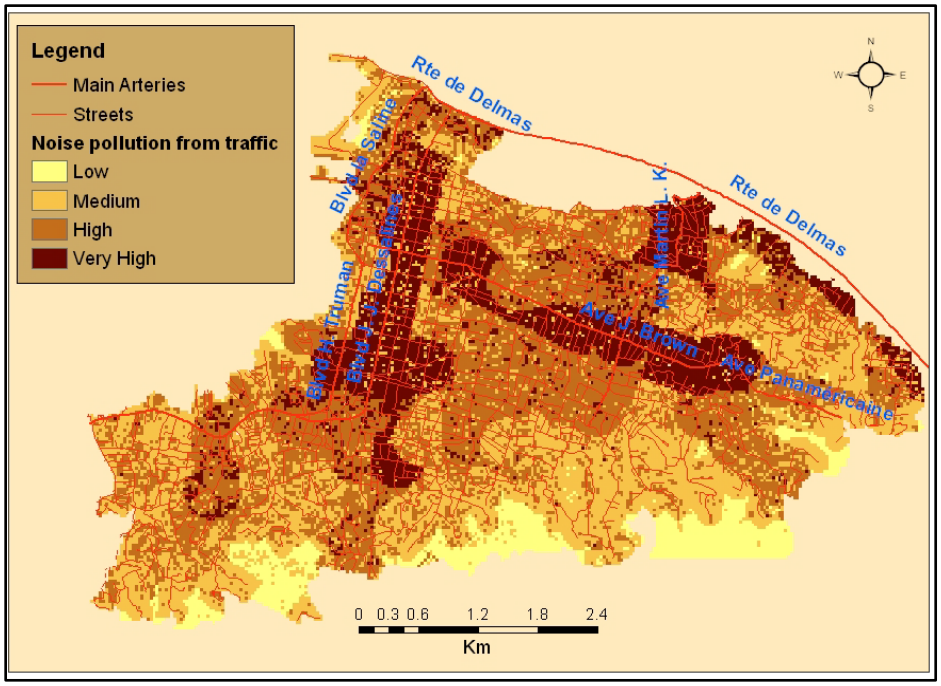

Figure 22 : Noise pollution exposure from traffic

V.2.1.3 Pollution from waterways

Dikes, waterways, and rivulets impinge on the physical environment in several ways. They transport solid sediments and trashes containing polluted agents and discharging bad smell to the surrounding environment. Stagnant water triggers breading of mosquitoes, which serve as vectors for malaria (Dike 1985). This has the potential to physically affect the health of the residents and the aesthetical impression of a neighborhood (Tzeng et al. 2002, Majumder et al. 2007, Rahman et al. 2011). Very often in Port-au-Prince no distance isolates polluted waterways

from people's residences, increasing the vulnerability of the residents and particularly women and children. At low altitude and gentle slope, the conditions are even more severe.

To estimate pollution originating from water bodies, a Euclidean distance was generated from the waterways and reclassified into distance thresholds of 0-100, ≥100 -200, ≥200 -300 meters and beyond. Distance was combined with other parameters like elevation, slope, and housing density (Number of houses per square kilometer). Worst cases of exposure to pollution from water courses were identified closer to water ways, at lower altitude, gentle slope and high habitat density. These parameters were integrated using raster map algebra.

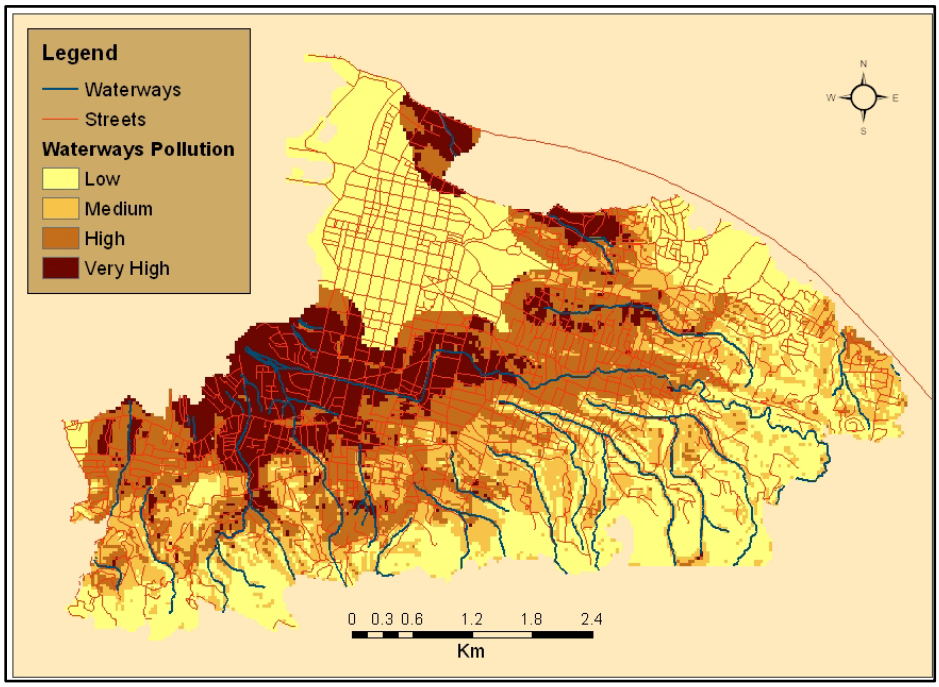

Figure 23 : Pollution from waterways

The darkest color on the map in Figure 23 portrays areas were worst cases of pollution from watercourses occur. Two slums (ironically called Cité Leternel and Cité de Dieu – standing for City of the Lord and City of God) are entirely located in areas with very high risk of water pollution. Water pollution is considered by the experts as the third most important UEQ factor with an average weight of 10.12% just behind vegetation and slums. Nevertheless, there is part

of this pollution that has not yet been accounted for. It relates to the many channels that are part of the drainage system filled with stagnant water, clogged with sediments, domestic residues, plastic bottles, plastic bags, and other solid wastes.

Water pollution affects about 54% of the population, especially in areas where the population is more concentrated. The average population density at high and very high risks of water pollution is over 70,000 people per square kilometer, while the population density in the remainder of the area is only 48,000.

V.2.1.4 Pollution from the seacoast

Typically, the seacoast is an attractive place for relaxation, meditation, and recreation of urban residents. In fact, in the past (before 1986), Port-au-Prince's boulevard Harry Truman along the seacoast was a very attractive place for tourists. However, the inefficient planning and management of the seacoast caused its surrounding environment to become unappealing and not suitable for touristic activities. For example, the most prominent slums are erected on landfill and previously open areas illegally occupied by low-income squatters close to the seashore (UNEP 1996). This statement, however, cannot be generalized to all Haiti's coastal cities or the entire extent of the coasts. By contrast to Port-au-Prince other coastal cities for which landfills and open space are not available don't face with the same issues of coastal pollution. The north section of Cap-Haitian's boulevard, the second largest city of Haiti illustrates well this fact (See Figure 32 in Appendix 1).

The seacoast is now the ultimate repository of domestic and industrial waste, solid residuals, and even human refuse. Solid waste in the form of plastic bags, rags, used tires, cans, and bottles are sinks for mosquitoes breeding, which eventually spread malaria and dengue.

Exposure to pollution located on the seashore is dependent upon distance combined with other parameters such as land use, housing density, and proximity to the waterways' mouth. A distance of up to 1,000 meters from the seacoast was computed with thresholds of 300, 500, 700 and 1,000 meters. Higher housing density intensifies pollution; residential land use exacerbates coastal pollution more than its commercial counterpart due to the discharge of human and domestic wastes to the sea. Furthermore, since the waterways carry polluting materials to the sea, sections of the shoreline located near a watercourse were considered more vulnerable.

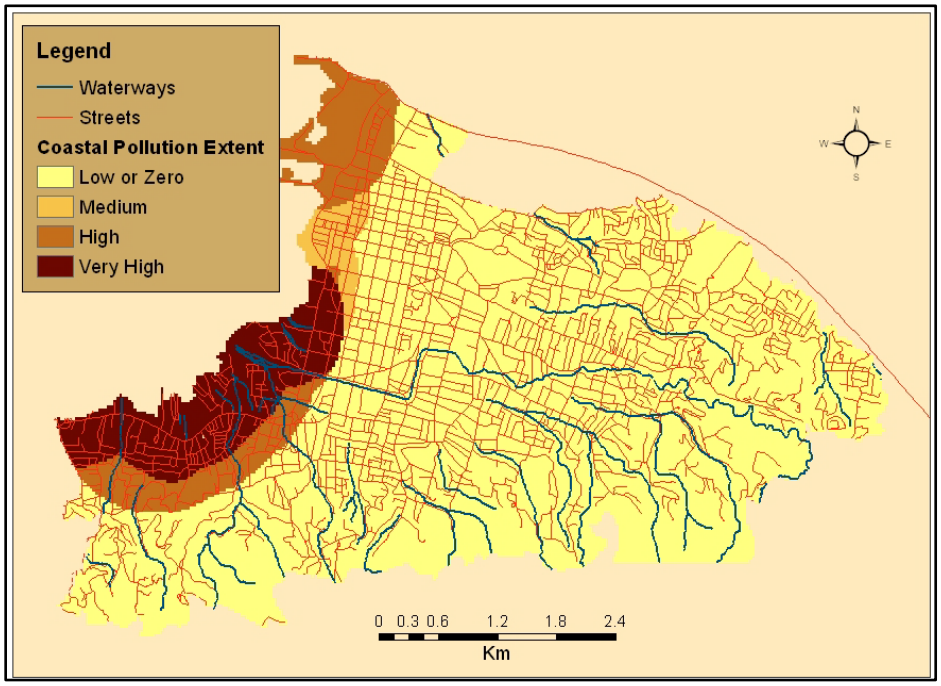

Figure 24 : Extent of coastal pollution

Figure 24 shows that areas more severely affected by coastal pollution are located along the southeastern tip of Port-au-Prince, which feature the presence of the two slums aforementioned. The population affected by high and very high exposure to coastal pollution is roughly 138,000 representing approximately 19% of the entire population. This factor was classified fifth for its weight in environmental quality immediately after flooding and before traffic pollution.

V.2.2 Group 2: Public domain factors

V.2.2.1 Public marketplaces

Market places include traditional markets located indoor and clearly identified, and ambient markets that typically take place either preeminently in specific areas or just randomly on the streets. However, either because the capacity inside the buildings is exhausted or because merchants are looking for more exposure of their goods, rarely have the limits of these building contained the merchants. As a result, the markets extend beyond their assigned physical boundaries and generate multiple environmental problems. The impact of public markets on environmental quality has not been previously reported in the literature, probably because the impact of public markets is specific to urban areas in developing countries. Nevertheless, indoor public market places and informal street markets are potential sources of waste and affect the aesthetic and the sanitation conditions of neighborhoods in which they are located. These markets inhabit unspeakable deleterious hygienic conditions that are either harmful to the attendants or people living in their proximity. Evidences suggest that the degradation observed in the urban environment is closely related to activities of the informal economic sector of Port-au-Prince (Howard 1998). Due to inadequate rubbish collection service, these markets are sinks for agricultural and food-related solid waste that decompose rapidly under the sun and are hosts to and attract mosquitoes that can transmit diseases to residents living nearby. In addition, they generate offensive stench that spreads to the neighborhoods and are a source of noise during the day. Another hazard associated to street markets is their imbrications with traffic that very often induces injuries and deadly accidents. Not to mention the impediment to pedestrian circulation and, in case of emergency, a hindrance to fire department and police actions to bring relief.

While indoor markets were digitized as polygons, ambient markets were identified with high resolution aerial images and Google Earth images and digitized as lines. Euclidean distance to markets was computed on both features and subsequently combined to retain the locations indicating the worst case scenarios.

Public markets have recently increased with the escalating rural-to-urban migration, political instability, and compression of jobs in the formal economy particularly in the assembly industry. Attempts to suppress markets with coercive actions have been a failure, because the socioeconomic forces that influence the evolution of the markets are ignored. Although the experts rank this phenomenon as among the four least important environmental problems, over 150,000 people (21% of the entire population) are affected at high to very high exposure levels with a corresponding population density of 69,000 people per square kilometer.

V.2.2.2 Cemetery

While in developed countries a cemetery is a sacred and secure place that poses no problem for the immediate environment, the main cemetery of Port-au-Prince is not a peaceful sanctuary for the deceased. Sanitation conditions inside the cemetery are very precarious and are mainly affected by overcrowding, the inappropriate disposal of the corpses and vandalism. Because the hosting capacity of the cemetery is overwhelmed and as a result of vandalism, often dead bodies are left exposed to the open sky for a long time. Many instances have been reported where debris of coffins and remains of cadavers are left outside allowing the wind, runoffs and mosquitoes to spread bad smell and infectious agents throughout the surrounding neighborhoods. The bad condition of the environment around the central cemetery of Port-au-Prince is at least affecting those living in the vicinity. To illustrate the situation prevailing in the cemetery an image is exhibited in Figure 33 in Appendix 1.

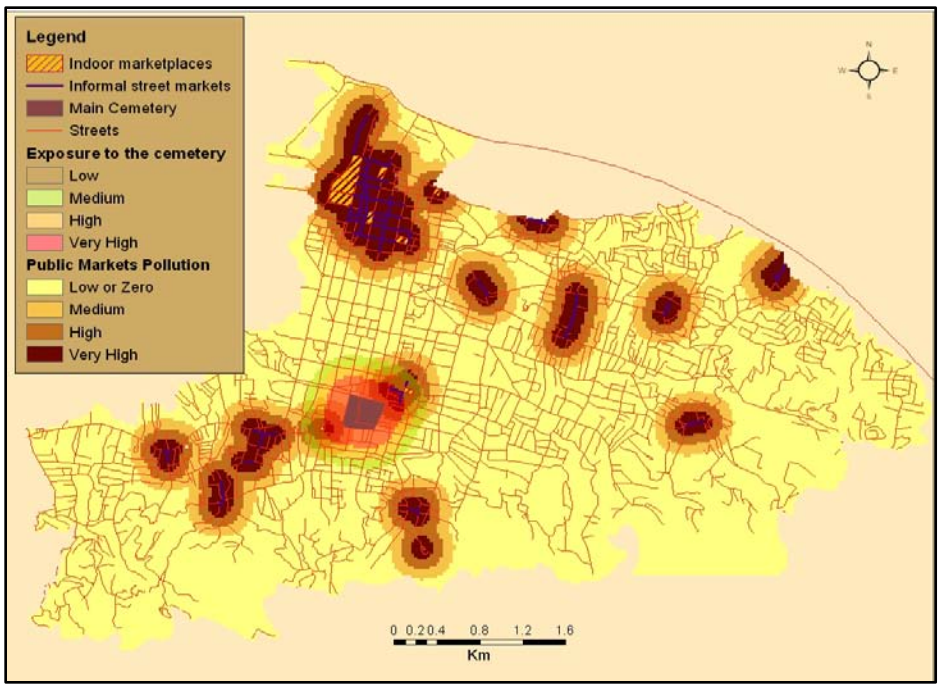

Figure 25 : Exposure to public markets and cemetery pollution

A Euclidean distance was computed from the cemetery and distance thresholds of 200, 300 and 400 meters were adopted. Problems from the cemetery are the least-weighted non-natural environmental hazards for Port-au-Prince according to the experts' survey. Cemetery had an average weight of 7.1% in the experts' survey and affects 25,000 people (3.4%). The extent of exposure to cemetery pollution is displayed in Figure 25 along with public market pollutions.

V.2.2.3 Slums/informal settlements

Slums feature many environmental features that unquestionably create conditions for a deteriorated urban quality. Hardoy and Satterthwaite (1991) point out three problems affecting the neighborhood environment in which many poor households live. These include dangerous sites, household garbage not collected and inadequate infrastructure. They enlighten the situation as follows:

> *...These are large clusters of illegal housing on dangerous sites, for instance on steep hillsides, floodplains or desert land,… around solid waste dumps, beside open drains and*

sewers, or in industrial areas with high levels of air pollution. They also develop in sites subject to high noise levels, for instance close to major highways or airports.

Other risks associated with poor infrastructure comprise flooding, waterlogged soil, and dormant pools, which can transmit diseases. People with lower income choose to live there not being unaware of the danger but because the location of these sites meets more urgent lodging needs. Hence a slum is by itself a direct indicator of poor environmental quality.

The slums were digitized with the combination of a 1994 topographic map and a more recent orthophoto (2005). In addition to the areas within the slums, selected buffers of 100 and 200 meters were also included. Adjustments were made for location, size and level of deprivation in amenities of the communities. For instance, a slum community located on the seashore faces different adverse conditions than another built on the hill. A larger slum is likely to host more problems (e.g. access, concentration, and sanitation) than a smaller one. Obviously, a slum with fewer vegetation cover is worse off than one with higher rate of greenness.

Among the parameters distressing the urban environment of Port-au-Prince slums were ranked second with an average weight of 10.2% on the experts' scale. At the time of the last census (2003), the southernmost space now occupied by shantytowns was not a very populated area. More recent aerial images indicate significant squatter in progress. The next census will need to redefine the SDE borders and include these recently populated areas. Over 64% (almost 471,000) of the population lived in areas defined as shantytowns with a population density of around 73,500 people per square kilometer versus 35,400 for the remainder of the study area. If the 200 meters buffer is excluded the population density within the slums exceeds 83,000 people per square kilometer and the house density is estimated at 14,700 houses by square kilometer. The spatial extent of slums in Port-au-Prince is shown in Figure 26.

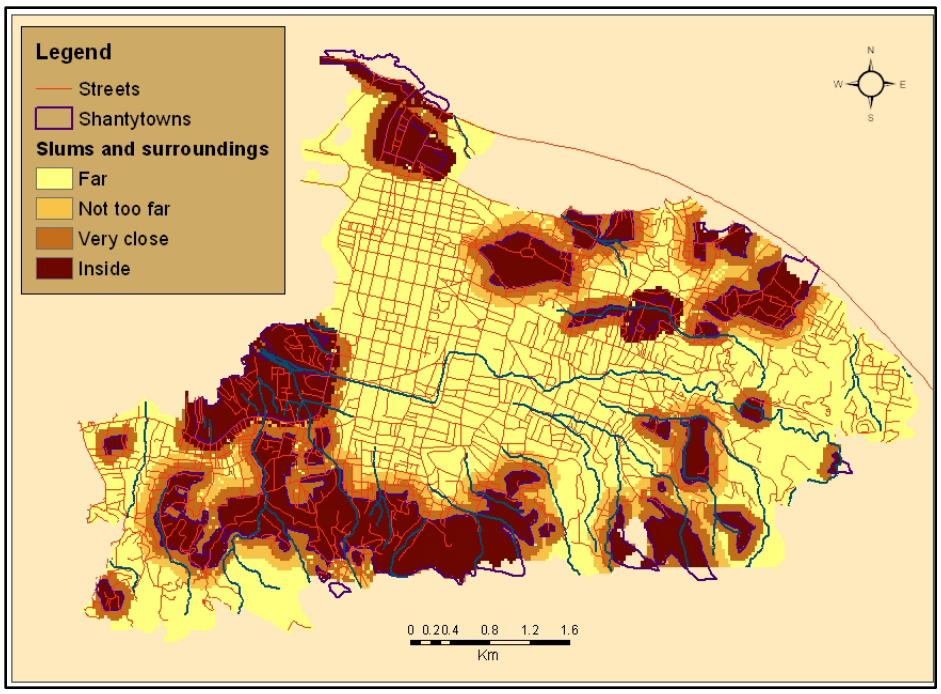

Figure 26 : Slums and immediate surroundings

V.2.2.4 Crowdedness

Overcrowding is another intervening factors that has been assessed as determinant of the conditions of a neighborhood (Amerigo and Aragones 1997, Chan 1999, Cramer, Torgensen and Kringlen 2004, Fleury-Bahi et al. 2008, Hur and Morrow-Jones 2008, Walton et al. 2008). The relationship between population density and environmental externalities can be easily understood when considering issues with rubbish collection, traffic jam, and constant pressure on the natural resources. Cramer et al. (2004) found that the general quality of life decreases as a result of an increase in population density. Higher population density is correlated with the occurrence of more negative events and a higher density also negatively affects the perception of neighborhood quality. Another impact of density (compactness) is perceived on health and materialized by a higher exposure to and human inhalations of pollutants (Marshall et al. 2005, Schweitzer and Zhou 2010). In the context of Port-au-Prince population density and crowdedness are used interchangeably because of the negative consequences associated with population density.

Since it is assumed that population density underscored UEQ, population density was left apart and was not included as a parameter in the processing of the model. Population density will be used to test the relationship between population density and the different parameters intervening in UEQ.

Crowdedness was ranked in-tandem with waste as the top two problems that affect environment quality in Port-au-Prince.

V.2.3 Group 3: Natural hazard domain factors

Previous UEQ studies usually fail to include the component natural hazards as a contributing factor of environmental quality. The safety and security aspects, when referred to in the study of urban environmental quality, have been linked to man-made features along with other socio-economic characteristics, but not to natural hazards. The impact of hazards such as landslides and floods on land and neighborhood values have been investigaged. Some studies have found negative correlation while others did not find any significant correlation (Babcock and Mitchell 1980, Tobin and Montz 1988, 1990, 1994, Schaefer 1990). Coastal populations are much at-risk as proven by the deadly events occurred in the last 10 years and these risks are heightened by sea level rise as a result of global climate change (Tralli et al. 2005). In Port-au-Prince these events are aggravated by some anthropogenic components such as accelerated tree-cutting on high slopes, the obstruction of the drainage network, and the low rate of water infiltration due to urbanization (road and residential constructions) (Howard 1998, Mathieu et al. 2000). Recently, many flashfloods have paralyzed activities in the metropolitan area and offered a repugnant spectacle for the environment. People living in the proximity of the sea face risks of tsunamis and coastal surge (though the perception of tsunami is very low in Port-au-Prince because no recent events have been reported). The residents' perception about the safety of a

residential location is affected both by the impact of recent events and the potentiality for the occurrence of further events. Therefore natural hazards cannot be understated.

V.2.3.1 River and flash flooding

Flood hazard models are built with variables such as elevation, land cover information, and water bodies (Islam and Sado 2000). The assessment of flood hazards can also take advantage of the ability of remote sensing technologies to identify flooded areas (Islam and Sado 2000, Tralli et al. 2005). Absence or lack of detailed data limits the ability to include all the fundamental variables suggested by the hydrologic modeling system (HMS) developed by the Hydrologic Engineering Center of the US Army Corps of Engineers (Peters 1998) or the model developed by HAZUS-MH Level-2 (Scawthorn et al. 2006), which requires topography-related and hydrologic information. The non-availability of some data to include in a model impose a trade-off between sophistication and simplicity regarding the accuracy of the outputs (Bates and De Roo 2000). The Stream Flow Model (SFM) 3.3 flood model, a semi-distributed hydrologic model assuming uniform flood heights along the stream channel is particularly suited for the monitoring of flood where adequate hydrologic data are not available (Artan, Restrepo and Asante 2002, Gall, Boruff and Cutter 2007). A semi-distributed model is a conceptual model in which a watershed is further divided into several sub-basins (Guleid et al. 2007). A similar approach was used by De Roo et al. (De Roo et al. 2007). In a study funded by the Oxford Committee for Famine Relief Great Britain assessing natural hazards and risks affecting Haiti, a height of 6 meters was used above the rivers to model flooding. This height represented the minimal for the entire country (Mathieu et al. 2000). The modeling of the floodplain for Port-au-Prince is a modified version of the SFM 3.3. It takes into account the fact that the study area is not crossed by any major river. Most importantly, the actual state of the waterways is such that

they are usually loaded with sediments and solid waste that can cause an event or lesser magnitude to raise water level above the river bed and generate flooding.

To begin with, a water surface was created with height of the river derived from the DEM. Second, a grid of 30x30 meters was generated to which the mean elevation from the DEM surface was added. This represents the terrain elevation at each cell of the grid. These two steps enabled the computation of the elevation difference between the river at its flooding level and the surrounding terrain. However, to ensure that only areas closer to the river were included, distance from each cell of the grid to each point of the river was computed. Combining several distance thresholds to rivers, elevation, and height difference, queries were applied to determine locations at risk of flooding at several levels. The resulting map is displayed in Figure 27.

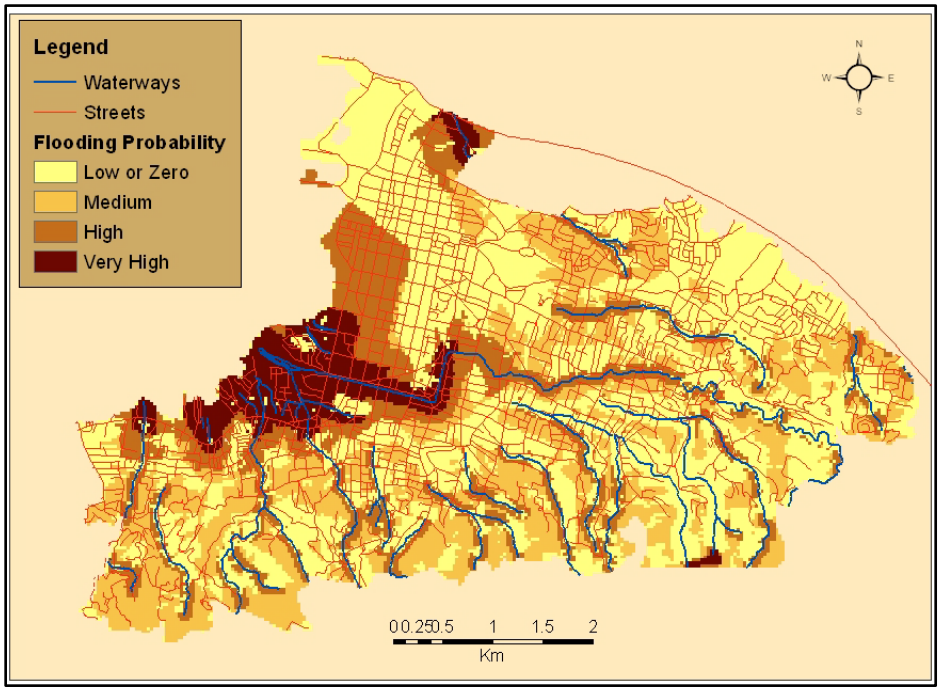

Figure 27 : Flood probability for a 100-year event

According to the experts, flooding ranks as the top natural hazard affecting the urban environment in Port-au-Prince. Areas with highest probability of flooding correspond to the location of the shantytowns “Cité Leternel” and “Cité de Dieu”. Other vulnerable regions include

the gorges neighboring the waterways in Bourdon where people have decided to build their houses in spite of recent reported casualties from run-off and flash flooding events. Twenty six (26%) percent of the population representing about 190,000 people is exposed at high and very high risks if an event capable of producing flows from three to five meters were to occur. The obstruction of the channels by sediments and trashes can easily force flows out of the canal beds even with the occurrence of an event of lesser magnitude than a 100-year flood.

V.2.3.2 Landslide

The occurrence and probability of landslides are influenced by as many and diverse event-controlling parameters as past occurrence of events, slope, landform, illumination, aspect, elevation, rainfall, plan curvature, profile curvature, soil type and surface land use, proximity to the road network, and the hydrological profile (Irrigaray Fernandez et al. 1999, Ayalew, Yamagishi and Ugawa 2004, Young, Kil Jin and Choi 2010, Kelly 2010). Ayalew et al. (2004) acknowledge that, while the inclusion of all the variables can increase the accuracy of landslide susceptibility models, as a minimum requirement a model must include the topographic attributes.

The Mora-Vahrson (1994) method to assess natural susceptibility to landslide hazard was utilized in an analysis of multiple natural hazards study for the Haiti in 2010 (MULTI-MENACE-HA 2010). This method superimposes several characteristics intrinsic to slope failure such as geology/lithology, topography, humidity, seismic activity and rain intensity. However, this approach is more appropriate for macro-zonation of landslide hazard than for determining the predisposition of a micro-zone such as Port-au-Prince to landslide. Detailed geology for the area is missing, along with most of the data needed for the other indicators. Ayalew et al's (2004) suggestion is retained to include parameters such as slope gradient (greater than 20%),

proximity to roads (50 meters), proximity to waterways (50 meters), and housing density (greater than 5000/km^2). These parameters were combined with the Local Cell Statistics tool using the "minimum" operand.

Landslide susceptibility was ranked in 9th position by the experts. The occurrence of landslides has increased over the last decade due to anarchical constructions on steep slopes and along the rivulets in unstable soils. Forty two thousand (42,000) people lived in areas with high and very high susceptibility of landslides. Areas susceptible to landslides are displayed in Figure 28 along with coastal flood hazard.

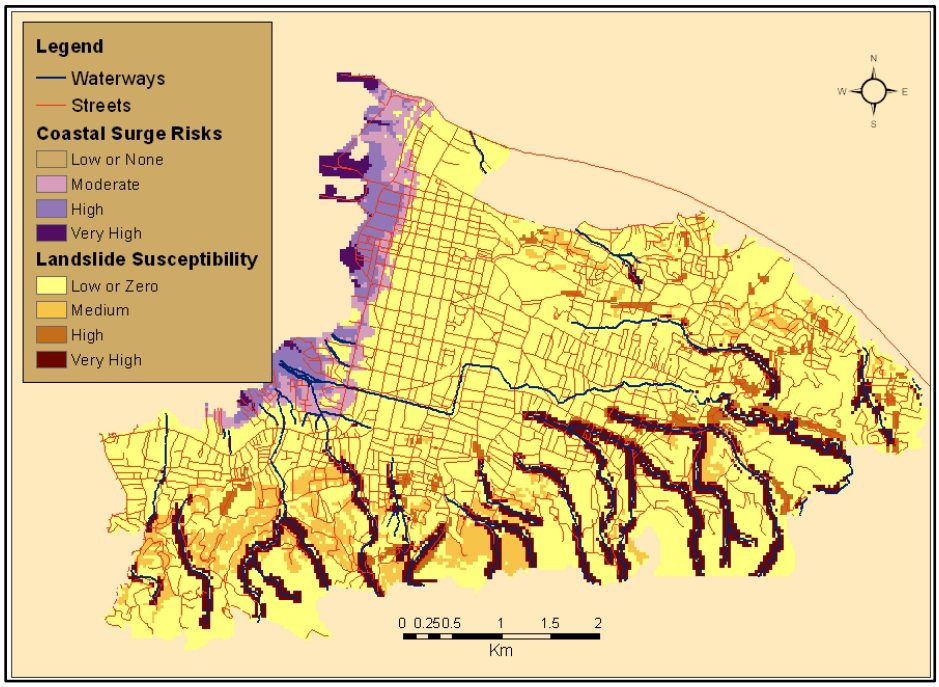

Figure 28 : Costal flooding and landslide susceptibility in Port-au-Prince

V.2.3.3 Coastal flood hazard (Wave surge)

The assessment of coastal flooding takes into account the flood depth above ground determined by deducting the ground surface from the flood surface (Scawthorn et al. 2006). Considering an event that would generate waves that are five meters above ground, four

thresholds of risks based on classification of elevation by natural breaks (Jenks) were generated. The resulting surface is displayed in Figure 28 along with coastal flooding.

Sea surge does not appear to be a vital concern for residents in Port-au-Prince. Ranked last by the experts, it affects only 3% of the coastal population. That includes mainly three shantytowns located on the coast, the seaport and a portion of the commercial centre (downtown).

V.2.4 Summary of the parameters

A summary of the average weight scored by each parameter in the experts' survey along with their corresponding population density is displayed in Table 6. Crowdedness and waste are not displayed in the table since they were not included in the model. However, they were ranked first and second most important parameters affecting UEQ. After redistribution of their scores proportionally to the initial weight of the other parameters, vegetation, slums, waterways pollution, flooding, sea pollution, and gas emission exposure were, by descending order, the six most important parameters included in the UEQ model. From a brief examination of the column with population density it can be inferred that higher population density is related to lower UEQ levels and vice-versa. This is true for all the parameters except for public markets, cemetery and wave surge. The point biserial coefficient can be used to validate the correlation observed.

The point biserial coefficient is a special case of the Pearson's moment correlation coefficient that is designed to test correlation between one dichotomous variable (e.g. low and high UEQ) and an interval or ratio variable (e.g. population density) (Shaw and Wheeler 1994). For all the 11 parameters the Pearson correlation coefficient generated from the point biserial application yielded -0.42. This indicates that as UEQ decreases population density increases. The lower population density associated with lower UEQ for the three parameters aforementioned

may be directly related to their small geographic extent that does not include other very populated neighborhoods. High population density in these outside-neighborhoods serves as outliers that offset the effect of inside-neighborhoods with high population on the trend observed. After removing these three variables the Pearson coefficient increased to -0.63, significant at the 0.01 confidence level.

Table 6 : Weight and population density by parameter of the UEQ model

Parameters	Experts' weight	UEQ level	Population density
Vegetation Cover/ Greenness	0.1121	Low-Very Low	66,737
		Moderate - High	16,709
Shantytowns	0.1019	Low-Very Low	35,416
		Moderate - High	73,458
Waterways pollution	0.1012	Low-Very Low	70,393
		Moderate - High	47,901
Flooding	0.0965	Low-Very Low	60,855
		Moderate - High	59,337
Sea Pollution	0.0949	Low-Very Low	61,230
		Moderate - High	59,395
Gas Emission from traffic	0.0942	Low-Very Low	62,311
		Moderate - High	55,333
Noise pollution from traffic	0.0918	Low-Very Low	63907
		Moderate - High	52,064
Public Markets	0.0872	Low-Very Low	57,306
		Moderate - High	69,016
Landslide Susceptibility	0.0802	Low-Very Low	61,477
		Moderate - High	59,594
Cemetery	0.0716	Low-Very Low	53,159
		Moderate – High	59,920
Wave Surge	0.0685	Low-Very Low	52,694
		Moderate – High	59,934

V.3 Integrating factors for UEQ assessment

Several obstacles may arise with the integration process of the individual parameters affecting UEQ. Those include the difference in spatial extent, the non-uniform scale measurement (ordinal or continuous) and the difference of spatial units (Pixel, SDE, buffers) (Lo and Faber 1997, Nichol and Wong 2009). To circumvent these difficulties, the parameters were converted to raster format with a unique pixel size of 30 meters over the full extent of the area, and then integrated with weighted raster overlay.

The weighted linear combination technique (WLC) used by Ayalew et al. (2004), a process similar to the Analytical Hierarchy Process (AHP) (Saaty 2005), was applied for the overlay operation. To determine the weights, an online survey (sample is provided in Appendix V-a) was distributed at the secondary-level to 40 pre-identified experts of which 16 completed and returned their survey. The professional profile and the educational background of the experts are also provided in Appendix V-b. The experts assigned a number from one to ten to all the 13 potential parameters listed in the questionnaire with one meaning unimportant and 10 extremely important. To standardize the weights, the sum of the answers for a parameter was divided by the total score for all the parameters. However, since crowdedness and waste was not included in the final model, their scores were redistributed proportionally according to the initial respective weight of the other 11 parameters. This procedure generates a weight between 0 and 1for each parameter with the sum of the weights equals to one. The weight can also be expressed as a percentage. For example, the total score attributed to vegetation by the 16 experts amounted to 144. The score for the eleven parameters and for all the experts totaled 1285. The average weight of vegetation was found by dividing 144 by 1285, which yields 0.112 or 11.2%.

After additive linear combination of all the parameters with their respective standardized weight as coefficient (see Nichol and Wong (2009)) the GIS overlay results in a single composite UEQ for each SDE according to the following formula:

$$UEQ = \sum_{1}^{n} W_i F_i$$

Where n= the number of parameters, w_i the percentage of variance or weight of factor i as indicated by the experts; and F_i = factor i.

The entire process was performed within the Model Builder environment in ArcMap (See flow chart in Appendix III (IIIa & IIIb) and the Python codes in Appendix IV). For mapping purposes, the whole UEQ range was reclassified into four classes using the quantile technique. The quantile classification scheme was retained for its ability to establish a balance in the distribution of the features among classes. Brewer and Pickle's (2002) surveying many respondents to evaluate seven classification methods, found that the quantile technique was more appropriate for conveying patterns of mapped rates. This technique, while retaining a similar number of features in each UEQ class allowed visualizing areas with concerns more than did other classification methods.

The map in Figure 29 depicts the composite UEQ at pixel level. The darkest color in the southwest and the northeast where the lowest urban environmental quality conditions are spotted correspond to the location of the two disamenity zones north and south identified in Chapter III. The east-southeastern edge displays the highest UEQ, consistent with the location of the residences of the upper-income sector. For once, dark colors characterizing areas with low to very low UEQ appear in the commercial zone.

Over 682,000 people (93%) fall within the ranges of moderate to very low UEQ. The corresponding population density is 63,200 people per square kilometer. The exclusion of the

"moderate" category would increase the population density to about 74,250 for a proportion of 62% of the population. This indicates that not far from two-third of urban residents of Port-au-Prince are exposed to or living in worst environmental conditions. At the opposite end, only 50,000 people live in areas with high UEQ with a corresponding population density of about 15,500. This clearly emphasizes the weight of population pressure on environmental quality.

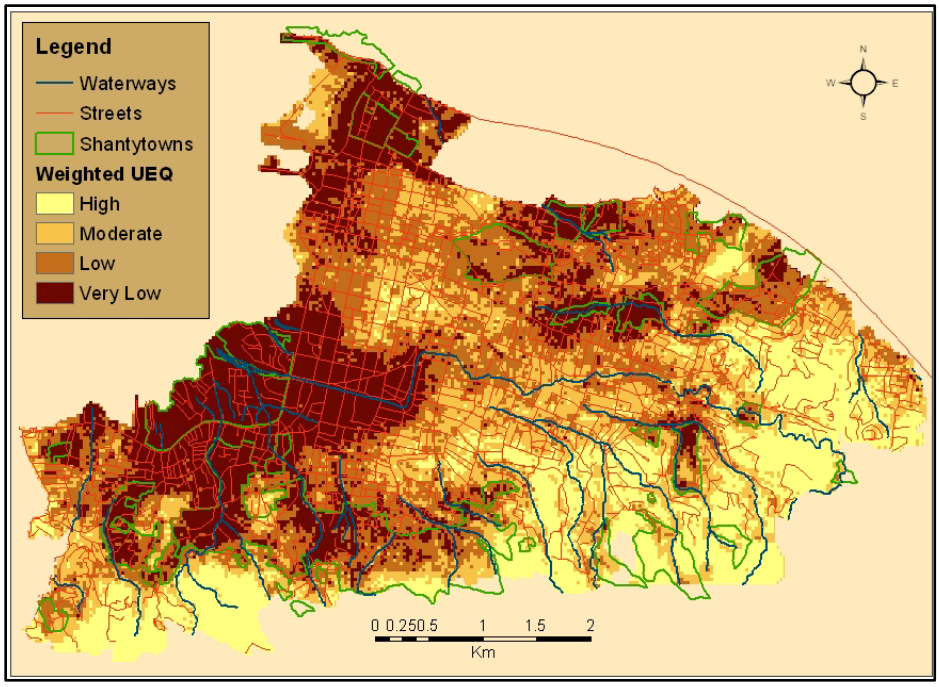

Figure 29 : UEQ index for Port-au-Prince at pixel level (30m)

The test of the relationship between population density and UEQ was tested over the ranked values of population density and UEQ with Gamma and Somer's D statistical parameters. High population density was expected to be found in areas with lowest UEQ. While Gamma tests the symmetrical measure of association between two ordinal variables, Somer's D is an asymmetric extension of Gamma that incorporates the number of pairs not tied on the independent variable. Field (2005) recommends to use Gamma and Somer's D for the directional relationship between two ordinal variables. Values of Gamma and Somer's D range between -1 and 1. Whereas values closer to 0 indicate a weak relationship, values near -1 or 1 indicate strong

negative or positive relationship, respectively. Gamma and Somer's D are given by the following formulas:

$$Gamma(\gamma) = \frac{P - Q}{P + Q}$$

$$Somer'sD = \frac{P - Q}{P + Q + T_{\gamma}}$$

Where P = number of concordant pairs

Q = number of discordant pairs

T_{γ} = number of ties in the dependent variable

For a dependent variable Y and an independent variable X a pair is termed *concordant* if the subject ranks higher on both X and Y. A pair is *discordant* if the subject ranks higher on X but lower on Y (Agresti 2002).

The test of the relationship between the ranked values of population density and UEQ ranked values (both ranked with Natural Breaks) achieved a Gamma value of -0.54 and a corresponding Somers's D value of -0.37. Both statistics were significant at 99% confidence interval and suggest a moderate inverse relationship between population density and urban environmental quality. Highest population concentrations are likely to be found in areas with degraded urban environmental standards and areas with be best environmental amenities are occupied by less dense population.

The other goal pursued in this paper was to evaluate, based on the UEQ index, the prospect of refining the five-sectors model conceptualized by Joseph and Wang (2010b). In fact, the previous model was oversimplified with the categorization based only on land use and visual inspection of a high resolution image. In addition, the model was aggregated at SDE level, implying homogeneity within a SDE and ignoring possible differences inherent to variation in

the physical environment and population distribution. This paper offers the benefits of a finer study unit and a more comprehensive assessment through the integration of a mosaic of indicators.

The new structure was derived by combining the UEQ scores at SDE levels, population density and the previous sector structure, all converted to grids with the weighted overlay tool. Population density, UEQ, and the original sector were assigned an arbitrary weight of 0.5, 0.3, and 0.2, respectively. The resulting raster in Figure 30 was then aggregated to seven large polygons (Figure 31) through manual digitization.

The new structure introduces a new conceptual sector termed “in situ accretion”, in reference to the Latin America cities model proposed by Griffin–Ford (1993). This sector, located at the edge of the city, hosts houses comparable to the shantytowns and possesses little or no infrastructure. The lands have been freshly occupied, and squatter is still ongoing. Another characteristic of this sector embodied by the other inland in situ accretion zone is the high vulnerability of the houses. They are built on marginal lands, on the hills, and in floodplains. The transitional zone and the residences of the upper income shrank because of the presence of the in situ zone of accretion in Bourdon’s Valley and Canapé-Vert. The commercial sector could be divided into the formal sector (south) and the informal (north). However, the informal section was rather linked to the disamenity zone north, which also contains slums at the northwestern tip of Port-au-Prince. The disamenity zone south still holds but it is stripped off of the southwestern most portions that now become the sector of “in situ accretion”.

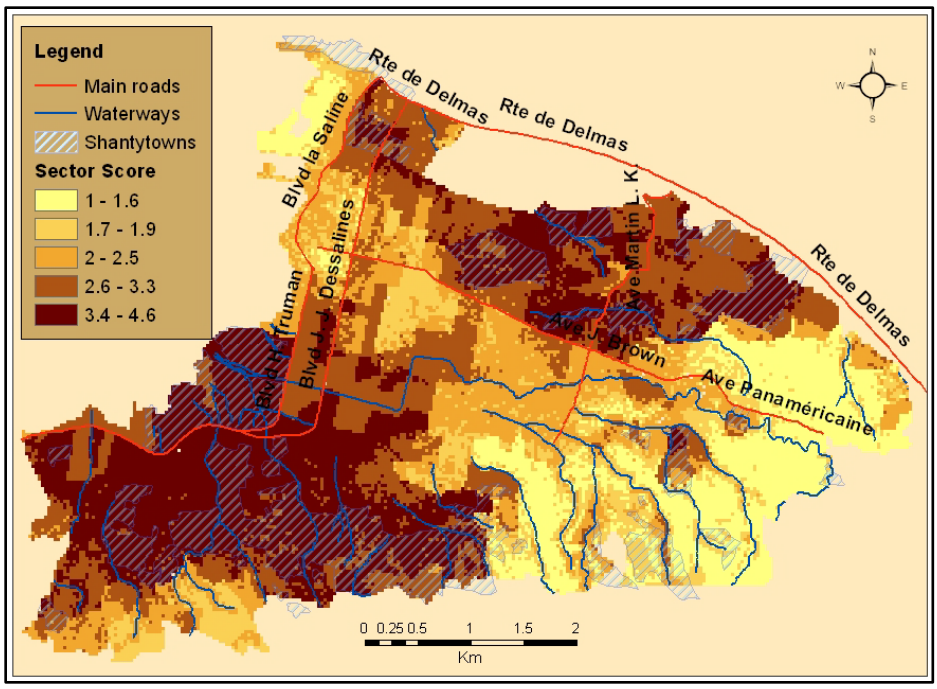

Figure 30 : Refinement of the sector model at pixel level

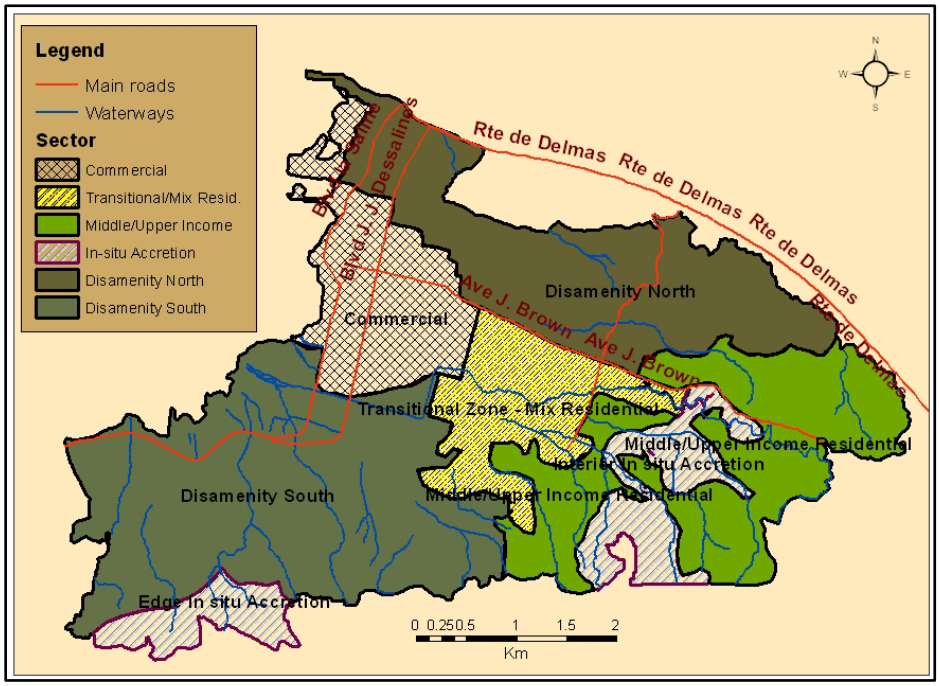

Figure 31 : Refinement of the sector conceptual model for Port-au-Prince

V.4 Validation of UEQ by field survey

V.4.1 Implementation of the survey

To assess the accuracy of the UEQ index and validate the results a face-to-face survey was administered to 407 individuals selected by random stratification from 10% of the SDEs (67) under the constraint that each SDE was represented by six to seven respondents in each stratum extracted from the five sectors identified in Joseph and Wang (2010). The strata were chosen so as to ensure representation in the survey of respondents from the different sectors. The respondents were asked first, to evaluate the general environmental quality in their respective neighborhood; and second, evaluate the contribution to environmental quality of each parameter in their neighborhood. A sample of the survey is provided in Appendix V-c (English) and Appendix V-d (French). The range of values varied on a scale of 1 to 5, with 1 standing for the worst case scenario and 5, the best case. To standardize the range of values of the UEQ model (one to four) and that of the survey (one to five), the highest values of the survey four and five were combined into four, which means high UEQ.

Due to theft risks for the GPS equipments, the surveyors were advised not to use the GPS units to collect the geographic location of the respondents. Therefore, information about the specific location of the respondents was not available. The scores at individual level were aggregated to SDE by retaining the highest frequency of responses (majority) within a SDE.

The responses to the survey indicate that more than 60% of the population was living in low to very low urban environmental conditions. When residents living in moderate situation are added to this number, the total represents over 90%. Only 10% of the population was living in good to very good conditions. These numbers in general reflect the results of the model.

V.4.2 Accuracy tests

Two types of control were applied to test the accuracy of the model. First, we looked at independence between the prediction of the model and the actual data collected on the field. The strength of the relationship was tested with two correlation measures, including Spearman's rho (ρ) and Kendall's tau, both used for testing ordinal relationships (Shaw and Wheeler 1994, Higgins 2003). Spearman's rho is comparable to the Pearson product moment correlation coefficient. It only converts the data to ranks before calculating the coefficient. The formula of Spearman's rho is as expressed below:

$$\rho = 1 - \frac{6 \sum D^2}{N(N^2 - 1)}$$

Where D = the difference between the ranks of corresponding values of the UEQ of the survey and the UEQ of the model, and N = the number of pairs of values (67). Spearman's rho takes values between -1 and 1. Values closer to one indicate strong correlation.

For the UEQ index, Spearman's rho was equal to 0.27 (in absolute value), significant at the 95% confidence interval, which points to a weak but significant association between the results of the survey and those of the model.

Kendall's tau also tests the strength of relationship between ordinal variables. However, it offers the advantage over Spearman's rho to be able to interpret its value as a measurement of the probabilities of observing *concordant* and *discordant* pairs (Shaw and Wheeler 1994). The formula of Kendall's tau is:

$$\tau = \frac{2P}{\frac{1}{2}n(n-1))} - 1$$

In which P is the sum of cases ranked after the given item by both rankings, and n represents the number of paired items.

Kendall's tau absolute value of 0.31, significant at 99% confidence interval, substantiates the weak-to-modest relationship between the survey and the model's results. It indicates that there is over 30% chance that the correspondence between the results of the model and the field survey does not follow a random process but about 70% chance that the ranks issue from the model are assigned randomly when compared to the perceptions collected from the field survey.

The second type of control assessed accuracy comparing the prediction of the model to the survey results on a case by case basis. Exact match and closely match ranked cases from both sources were added up. Closely match cases are considered particularly between low and very low and between moderate and high UEQ because the difference between these categories may be fuzzy. The classification method used does not establish a clear and definite division of the values. In addition, the judgment of different respondents even within the same SDE might not entirely help grasp the contrast among adjacent classes (e.g. low and very low or moderate and high).

Twenty nine (29), representing 43.3% of the 67 SDEs exactly matched the predictions of the UEQ model. Thirty (30), or 44.8% other SDEs were classified in adjacent UEQ levels. The addition of close matches and exact matches represent about 88% of the SDEs, meaning that 88% of the SDEs might have been more or less correctly classified. This can be considered an important achievement of the model in terms of accuracy.

The same association test was performed for each individual parameter of the model. The results are displayed in Table 6. Only four parameters of the model have significant bivariate correlations (as indicated by Spearman's rho and Kendall's tau, which both have a value over 25%). The correspondence matrix points toward an improved performance of the model. Five parameters achieved at least 40% of cases that exactly match while nine out of the 11 parameters

have at least 70% of cases exactly or closely matched. This was consistent with Spearman and Kendall's statistics.

Table 7 : UEQ model and lay-persons survey results comparison

Parameters	Spearman's rho	Kendall's tau	% of Exact match	% of Close match	Total exact & close match
Traffic air pollution	0.28*	0.25*	25.4	46.3	71.7
Vegetation cover	0.36**	0.32**	40.3	43.2	83.5
Traffic noise	0.06	0.055	29.8	40.3	70.1
Water pollution	0.08	0.07	17.9	44.8	62.7
Shantytowns	0.27*	0.24*	23.9	47.8	71.7
Flooding	0.19	0.17	23.9	47.7	71.6
Public markets	0.08	0.07	26.9	37.8	64.7
Landslide	0.14	0.14	70.1	25.4	95.5
Sea pollution	0.22	0.21	68.7	23.9	92.6
Coastal surge	0.40**	0.40**	95.5	3.0	98.5
Cemetery	0.23	0.23	81.0	17.9	98.9

** Correlation is significant at the 0.01 level (2-tailed); * Correlation is significant at the 0.05 level (2-tailed).

V.5 Discussions and conclusions

While attempting to replicate a phenomenon of the real world, a model must incorporate to the extent possible all or most relevant predictors that influence the phenomenon under study. This endeavor may be restrained by the availability of reliable data. When ordinal data is applied in the analysis, the outcome depends on measurements based on a series of logical assumptions, but not necessarily scientifically established. The proximity analysis is a case in point. The use of divergent methods will yield different outcomes and conclusions. It is however essential to conduct a field study to validate the findings of the theoretical model.

Since urban environmental quality is a geographical phenomenon by nature, overlooking some site-specific parameters would result in under-specifying the model. Likewise, some factors that work for one place may be redundant or irrelevant in another location. The experts

were in agreement with the choice of parameters included in the model. Although public waste and dust were dropped from the model due to measurement issues and unavailability of data, other parameters fully or partially embodied the extent of these two parameters. For instance, dust can be geographically covered by air pollution from traffic; and waste could be represented by public markets, river pollution, coastal pollution, and slums.

The model built in this research achieved an overall average Urban Environmental Quality Index for Port-au-Prince of 2.17 on a scale whose minimum is 1.25 (high UEQ) and maximum 3.2 (low UEQ). The corresponding median value is 2.12. Not surprisingly neighborhoods with the highest UEQ are located on the east and southeast edges of Port-au-Prince, which corresponds to the residences of the upper-income people and the less accessible zones (south-east) due to high elevation and difficult terrain. The latest has not suffered yet from the full extent of population pressure like the other slums. The existence so far of some vegetation cover and their location far from features of the public domains and pollution sources boosted their UEQ rank. However, this situation can quickly change if nothing is done to stop the ongoing squatter process in this region as revealed by recent high resolution images.

Neighborhoods with the lowest UEQ carry a host of environment problems ranging from pollution to natural-related hazards. But most importantly their exposure is underlined and aggravated by the highest housing and population densities. They are located in the southwest and the north regions of Port-au-Prince corresponding to the two disamenity sectors (south and north respectively). The northwestern tip, part of the commercial sector, also is included among the SDEs with lowest UEQ. This is due to the presence of a large strip of public markets (formal and informal) with advanced degraded conditions (e.g. Marché Croix des Bossales) and a slum

(Wharf Jérémie). Coastal pollution, water pollution, lack of vegetation, and flooding are the other environmental problems that plague these neighborhoods.

Though not purposefully integrated in the model, population density is a central parameter for a more accurate UEQ that captures details that the other surrogates fail to embody. Several SDEs of the northeastern section of downtown or the commercial sector display high UEQ while in reality these neighborhoods are adjacent to the north disamenity zone known for its low living standards as confirmed by the field survey. This area is spared of the impact of several parameters that lack of vegetation, pollutions from traffic, and public markets alone could not offset.

The statistics in Table 6 portraying the prediction accuracy of each model's parameter may reveal several aspects with regard to the perception of the population about urban environmental quality. First, there might be a distortion from the respondents induced by a too microcosmic view of the definition of neighborhood that is different and much smaller than a SDE. This might have affected the response given for a specific parameter. For instance, a respondent living in a neighborhood doted of some trees in his neighborhood might attribute a rank of moderate to very good for greenness while, in fact, based on the 30x30 meters processed image, the percentage of vegetation ranks the SDE as having a low UEQ. On the other hand, if a localized feature affects negatively his/her immediate residence, a respondent would tend to generalize the issue to the entire SDE. This stereotype tendency may even imply greater impact for large SDEs affected by the ecological fallacy problem. Second, an environmental issue such as landslide has very localized extent that barely extends to an entire SDE. If a respondent's neighborhood is not particularly impacted by this problem, he tends to provide answers that show his lack of awareness or concern while the issue is objectively and spatially assessed by the

model. This creates a discrepancy between the two. Another source of discrepancy explained by the high percentage of closely matched cases lies in the ranking process, completely subjective from the respondents, semi-objective from the model. Yet the surveyors might have contributed to the subjectivity by personally interpreting the respondents' thought or if their judgment is influenced by their own observation of the state of the environment at the location of the survey. Finally, there is the generalized tendency of respondents in Haiti, particularly those with less formal education to be pessimistic in providing answers regarding the conditions of their environment. This stems for a strategic behavior that consists of providing careful answers that leave windows of opportunities open in the case that the goal of the survey is the future realization of some improvement projects. Overall, the perception of the individuals verbalized in the field survey corroborates the objective assessment of the model.

Through the integration of factors from the physical environment, the public domain, and natural hazards, this study confirmed the multidimensional characteristic of urban environmental quality. The most important factors affecting UEQ are, according to the experts, crowdedness, waste, greenness, shantytowns, and different sources of pollution. The study also indicates that natural hazards are not to be ignored in the assessment of UEQ for Port-au-Prince. As anticipated, UEQ is a population-driven phenomenon. Areas with highest population densities are those with worst urban environment conditions. This is also substantiated by all the parameters except proximity to cemetery and coastal surge. The model elucidates the types of environmental issues that areas even smaller than a SDE face with and it puts in evidence "problem-neighborhoods" (Adrianse 2007), to which the attention of urban planners should focus. Finally, the UEQ enabled to refine the sector model, pointing to the existence of a new

sector similar to the in situ accretion zone of the Latin America cities model (Griffin and Ford 1993).

The UEQ model could be improved in several ways. First, more empirical researches are needed in order to include sub-parameters and proven objective measurements. For instance, the component building height could be incorporated in the determination of gas emission and noise pollution from traffic. It could be measured with LIDAR data contingent availability. Aerial photos taken after landslide and flood events could be used to delimit more accurately landslide susceptibility and floodplains. Direct measurement, whenever possible, is always better than approximation.

Second, it is imperative that the other critical parameters such as waste, highly ranked by the experts, and dust are integrated in the model. Further research needs to determine methods for their measurement. For instance, the component soil in the VIS fraction could be used as surrogate for dust after combinations with road and housing features.

Third, the field survey needs to follow the same ordinal scale than that used in the model to avoid any ambiguity. In addition, in spite of the difficulty to use mobile GPS to record the location of the respondents, this information could be useful for a more precise comparison between perception and objective measures. Lastly an odd number of surveys per SDE would facilitate generalization better than an even number.

The UEQ model offers several practical applications. First, by identifying the specific environmental causes and targeting the locations of the problems, policy-makers are provided with information on where to concentrate their improvement efforts and in what sector. Second, the results call to the adoption of policies to prevent further resources depletion and ensure environmental sustainability. Ongoing squatters and encroachment of the lands are identified in

areas very prone to natural hazards. Loss of lives and assets can be avoided with the adoption of appropriate measures in these fragile areas. Third, the causes to the urban environmental problems investigated here are multi-faceted. They have to be dealt with a consortium of stakeholders including several governmental entities, non-governmental organizations, donors, the private sector, but more importantly the communities directly affected. It cannot be emphasized enough that urban planning is made for people of the communities and with people from the communities. Only their involvement early in the planning process until the implementation can ensure durability and effectiveness of development and improvement projects. Because they live in the communities and face the problems every day, members of the communities are expert in their own way. Their input must not be disregarded. First they need to acknowledge the problems their community is facing with; second they need to appropriate the problems by having a sense of ownership and pride of their community. This will stimulate their interest for involvement in improvement activities implemented in their neighborhood.

Finally, the results invoke adopting a sector-oriented approach in regard of each of the parameters investigated. This will allow focusing and concentrating energy and resources to solve one problem at a time instead of investing limited resources to solve several problems while not reaching any concrete results.

CHAPTER VI CONCLUDING COMMENTS

This chapter presents a summary of the results and discussions articulated in previous chapters. Port-au-Prince, the capital of Haiti is the study area about which this dissertation was implemented. The urban area of Port-au-Prince, the second smallest city in Haiti, comprises a very high population density that makes it one of the most overcrowded cities in the world. This high density is mainly associated to massive rural-to-urban migration mainly associated to the decline of the agricultural sector and an effort of development of the manufacture. This considerable movement of the population toward the capital has occurred in a context of overwhelmed urban resources (including natural and infrastructure) and exhausted reception capacity. The political vacuum and/or instability of the last 30 years have furthermore exacerbated the issue with the failure of the governments to have a global planning vision and to regulate the lands. Consequently Port-au-Prince has suffered countless issues among which an unarticulated urban structure and panoply of environmental problems. This dissertation targeted three goals:

1. Examine the urban structure of Port-au-Prince in comparison with that of cities in developed countries;
2. Given the context of data availability constraints revealed in this research, the second objective was to elaborate a model to estimate population at census level using remote sensing imageries;
3. Assess and map urban environmental quality in Port-au-Prince and refine the sector model elaborated while attempting to address the first objective.

VI.1 Objective 1

Chapter III addressed the first objective by examining the population density pattern of Port-au-Prince through two theoretical models: the monocentric structure and the polycentric structure. These models predict an inverse relationship between population density and distance decay from city center(s). This type of relationship is termed density function. For the monocentric structure that assumes the existence of one city center serving as the main provider of services and jobs for the whole city in a context of market economy, population density decreases from this city center to its edge. Several mathematical forms of the density function where tested for Port-au-Prince based on 2003 census data. None of the mathematical forms of the monocentric model examined yielded significant results that validated the expected negative exponential density pattern for Port-au-Prince as indicated by the low coefficients of regression (R^2). The density pattern was also investigated with the polycentric structure, which at the opposite of the monocentric counterpart, assumes the existence of several city centers from which population density declines. Though the correlation measures improved, they were not satisfactory enough to validate the anticipated negative density gradient.

These results indicated that Port-au-Prince urban structure does not conform to the configuration empirically proven for cities in developed and developing countries. This counterintuitive result is mostly explained by the failure of governments to apply proper planning and land use regulations. Consecutively empty spaces and marginal lands have been filled out by substandard dwellings that don't respect any urban land use and zoning principles. Thus density patterns observed in Port-au-Prince have little to deal with the specific location of and distance from city center(s). The structure bears some resemblance with that observed for cities in Latin American countries with some differences.

Finally, a model was proposed, which attempted to reproduce the socio-functional characteristics of Port-au-Prince with five geographic sectors including a commercial center, a transitional zone mixed with businesses and the residences of low to middle income, the residences of the upper-income people, and two zones of disamenity mainly characterized by the presence of shantytowns.

VI.2 Objective 2

Chapter four dealt with the second objective of this dissertation consisting in elaborating a regression model to estimate population. To this end, a high resolution LANDSAT ETM plus image was used along with census data for 2003. The V-I-S methodological approach was privileged for its ability to link spectral information from remotely-sensed images to human-built characteristics of the landscape that embody population density. The LSMA procedure was applied to derive fractions of image's components from which surrogates were generated for correlation with census data.

Multicollinearity tests were performed on several potential explanatory variables to ensure non-redundancy or over-specification of the model and retain only the non-correlated variables. The three retained variables were mean value of house fraction, mean value of vegetation fraction and standard deviation of vegetation fraction. Population density, the independent variable was transformed into different mathematical forms including logarithm and square root to increase model's fitness. The logarithmic transformation, which produced new absolute values that are likely fit and mitigate the problem of underestimation or overestimation was demonstrated to be more appropriate for such task. In addition, the Geographically Weighted Regression model, a local model that assumes non-stationarity of social processes and admits spatial variations was used as an alternative to the global Ordinary Least Square model.

The GWR model achieved a satisfactory correlation coefficient of 0.80, a large improvement over the OLS model as indicated by a smaller AICc value. The model was internally validated based on the training data set with a mean proportional error of 26.1% and a total proportional error of 2.3%; and externally validated on a validation sample with a mean proportional error of 40.4% and a total proportional error of 8.1%.

VI.3 Objective 3

To achieve the third goal, a set of parameters derived from existing literature pertaining to Urban Environmental Quality (UEQ) to which was added some study area-specific parameters and three natural hazards was aggregated by Weighted Linear Combination in a spatial analyst environment. Each parameter was assigned a weight acquired from local experts through an online survey. An individual-based field survey was conducted to validate the results achieved by the model.

The respondents to the expert's survey confirmed the relevance of the parameters chosen to include in the model and they classified crowdedness, waste, vegetation, slums and water pollution as the five most relevant factors affecting environmental quality in Port-au-Prince. Most of the parameters were found to underscore population density. Areas most affected by environmental problems were also those with highest population density. This UEQ-Density relationship was substantiated by several association tests such as Spearman's rho and Kendal's tau. These two tests added to an accuracy matrix were also used to determine how close the predictions of the model were to the respondents' perception of the reality. Forty three (43%) of the UEQ cases were accurately classified and over 88% of the cases were approximately classified. However, taking each parameter individually, Spearman's rho and Kendal's tau

results showed some substantial discrepancies that might have revealed a lack of awareness from the population about certain environmental problems that plague their neighborhood.

The UEQ model was finally applied to refine the sector model proposed in chapter III. One new sector, likened to the in-situ accretion sector of the Griffin-Ford model for cities in Latin America, emerged. Moreover, by taking into account more specific characteristics that the model in Chapter three failed to consider, the location and the size of each sector was adjusted. Overall, about two-third of Port-au-Prince's population are living under worst environmental conditions.

VI.4 Contributions of the research

The contribution of Chapter IV is straightforward. The model proposed can be used to estimate population in non-census years as well as for areas with similar patterns where census data is not available.

The following considerations concern both Chapter III and Chapter V.

Most of the environmental problems Port-au-Prince is facing with are demographic by nature, related to the too much pressure of the population on the resources. Policies that the government and law makers adopt of fail to adopt potentially impact the structure of cities. These policies determine the location, the distribution and other patterns of physical features found in an urban area. One of the main incidences is manifested on how population is distributed across the city. When population settlements are not spread according to the respect of urban zoning and land use principles, many environmental consequences result.

The research calls to the adoption of policies and actions with potential result in two prospects: corrective and preventive.

VI.4.1 Corrective measures

The current state of the environment in Port-au-Prince needs to be redressed with specific actions aimed at lessening the impact on the residents' health and well-being as well as decreasing the number of individuals more deeply affected (currently two third according to the UEQ assessment). This represents a big challenge to the extent that this requires undoing the existing structure at a huge social and financial cost. But this is an imperative intervention.

Specifically, the government and urban planners need to intervene in the following areas:

- Adopt land use and zoning regulations capable of transforming the conditions of identified neighborhoods from worst environmental conditions to a decent a livable situation for humans;
- Create buffer zones along the gorges near the waterways and in areas identified as susceptible to landslides and affected by environmental pollution;
- Promote measures that encourage street merchants to engage in formal indoor trade activities while utilizing coercive instruments against non-compliant citizens;
- Improve existing and increase public infrastructure such as roads, drainage network and public markets;
- Increase vegetation and greenness with the implementation of vertical urban gardening programs using the roof of houses and planting trees along the streets and in the hills. These would help increase the vegetative cover and prevent erosion.
- The transportation service needs a reinforcement of its capacity to monitor and control gas emission. Above all, as it is a customary usage in many developed countries, each vehicle should pass an inspection test once a year including a gas emission test. Vehicles that fail the inspection test from circulation should not be allowed to operate unless appropriate correction is

performed. The consolidation of the many individual operators of public transportation into consortium of operators would also contribute to decrease traffic density and in the same vein reduce pollution from traffic. The dislocation of street's merchants and the elimination of the current practice of using the street corners of large arteries as parking space or repair site should also alleviate traffic density and prevent the concentration of polluted gas that affect the ambient population;

- The institution in charge of sanitation needs to define appropriate localization and availability of dumpsters in relation to population distribution. The sanitation situation would greatly recover with the provision of more dumpsters in proportion with the needs of the neighborhoods and by ensuring regular collection of garbage. These interventions must be accompanied with public awareness and education messages as well as the adoption of coercive measures against those who refuse to comply.
- Since the holding capacity of the cemetery is exhausted, Port-au-Prince is in need of another cemetery in sync with the growth of the population. Thorough monitoring is needed to ensure proper handling of the coffins. In addition, a mechanism to protect the area of the cemetery against vandals should be put in place.
- The street markets phenomenon is a multi-faceted and complex problem that should be addressed cautiously. In several instances the police has intervened with muscular actions to displace the street merchants but without success. A good understanding of the problem is required before appropriate measures can be adopted. Street markets reflect a process of "informalization" of the economy that highlights the inability of the formal economy (such as manufacture) to absorb the jobs' supply available. It is also an indicator of pauperization of the population that has to make a living on a very fragile and derisory commercial asset. Brutally

depriving the street merchants of this livelihood without offering alternative would severely affect their livelihood. This phenomenon also represents an expression of the overpopulation of the metropolitan area mainly fueled by massive rural exodus. Finally, it is due to the weakness of the public institutions to manage space of the public domain. Any strategy to solve this issue should consider this backdrop and should include policies with both short-term and long-term goals.

VI.4.2 Preventive measures

The main goal of the preventive measures is to promote sustainability and avoid further replications of the environmental predicaments identified. To this effect, urban planners need to work conjointly with law-makers to elaborate and adopt environmental laws to prevent the depletion of resources. However, only a strong and stable government with high willingness and commitment for change can create the conditions required for the implementation of the identified strategies.

Since crowdedness represents the cornerstone of almost every single environmental problem identified in Port-au-Prince, it is imperative to adopt policies that have long-term socio-economical impacts that are likely to change the residents' status as well as those living in the back country so that they don't feel the urge to leave their village or city. Basically, the goal of these policies would be to counterbalance the push factors with pull factors that give most rural residents enough reasons to stay where they are (e.g. education, leisure, electricity, health, substantial source of income, security, etc.).

Another important milestone is to organize neighborhood's associations that persuade residents to take ownership of their neighborhoods. These local organizations are to be provided with appropriate training, collaboration and minimum financial support to ensure their

effectiveness. Finally, in addition to civic education to young students through school and public education of the entire population through any form of media, the last important aspect is to foster synergy through partnership between different stake holders, public, private, local, international organizations and other potential groups.

Regarding areas prone to natural disasters, the government should take appropriate measures to prevent further loss of lives and assets by displacing and relocating the population under threats.

VI.5 Limitations and propositions for improvements

In chapter III, population density needs to be analyzed over a larger extent including surrounding cities with which Port-au-Prince share the metropolitan areas. Another approach to population density would be the ambient population concept. Future works need to estimate ambient population and test it as dependent variable. Finally, urban structural change over time can be examined with data for several censuses. One main constraint for that is the availability of data. The population estimation model proposed in chapter IV needs to be validated in an urban area other than Port-au-Prince. Finally the UEQ model needs to include parameters such as waste and dust pollution as suggested. In addition, the measurement of some parameters can be refined by the inclusion of some sub-parameters contingent availability of data. Given the subjectivity-loaded of the ordinal approach, it is important to consider the objective measurement of some parameters included to the extent possible.

REFERENCES

Adrianse, C. C. M. 2007. Measuring residential satisfaction: a residential environmental satisfaction scale (RESS). J Housing Built Environ, 22, 287-304.

Agresti, A. 2002. Categorical Data Analysis. Gainesville, Florida: Wiley-Interscience.

Ali, S. A. & A. Tamura. 2003. Road traffic noise levels, restrictions and annoyance in Greater Cairo, Egypt. Applied Acoustics, 64, 815-823.

Alperovich, G. 1982. Density gradient and the identification of CBD. Urban Studies, 19, 313-320.

Amerigo, M. & J. I. Aragones. 1997. A theoretical and methodological approach to the study of residential satisfaction. Journal of Environmental Psychology, 17, 47-57.

Anderson, D. E. & P. N. Anderson (1973) Population estimates by humans and machines. *Photogrammetric Engineering & Remote Sensing*, 39**,** 147-154.

Artan, G. A., M. Restrepo & K. Asante. 2002. A flood early warning system for Southern Africa. In Pecora 15 and Land Satellite Information 4th Conference, ASPRS. Bethesda, Md.

Ayalew, L., H. Yamagishi & N. Ugawa. 2004. Landslide susceptibility maping using GIS-based weighted linear combination, the case in Tsugawa area of Agano River, Niigata Prefecture, Japan. Landslides, 1, 73-31.

Babcock, M. & B. Mitchell. 1980. Impact of flood hazard on residential property values in Galt (Cambridge), Ontario. Water Resources Bulletin, 16, 532-537.

Banerjee, D., S. K. Chakraborty, S. Bhattacharyya & A. Gangopadhyay. 2008. Modeling of road traffic noise in the industrial town of Asansol, India. Transportation Research Part D: Transport and Environment, 13, 539-541.

Bates, P. D. & A. P. J. De Roo. 2000. A simple raster-based model for flood inundation simulation. Journal of Hydrology, 236, 54-77.

Benn, H. P. 1995. Bus route evaluation standards. Transit Cooperative Research Program Synthesis of Transit Practice. Transportation Research Board, Washington, DC.

Berry, B. & H. Kim. 1993. Challenges to the monocentric model. Geographic Analysis, 25, 1-4.

Berry, B. J. L. & J. Kasarda. 1977. Contemporary Urban Ecology. New York: Macmillan.

Bonaiuto, M., A. Aiello, M. Perugini, M. Bonnes & A. P. Ercolani. 1999. Multidimensional perception of residential environment quality and neighborhood attachment in the urban environment. Journal of Environmental Psychology, 19, 331-352.

Bonaiuto, M., F. Fornara & M. Bonnes. 2003. Indexes of perceved residential environment quality and neighbourhood attachment in urban environments: a confirmation study on the city of Rome. Landscape and Urban Planning, 65, 41-52.

Bonaiuto, M., F. Fornara & M. Bonnes. 2006. Perceived residential environment quality in middle-and low-extension italian cities. Revue europeenne de psychologie appliquee, 56, 23-34.

Bonnes, M., M. Bonaiuto & A. P. Ercolani. 1991. Crowding and residential satisfaction in the urban environment - A contextual approach. Environment and Behavior, 23, 531-552.

Brewer, C. A. & L. Pickle. 2002. Evaluation of methods for classifying epidemiological data on chloropleth maps in series. Annals of the Association of American Geographers, 92, 662-681.

Burgess, E. 1925. The growth of the city. In The City, Park, R, Burgess, E. and Mackenzie, R., Eds. Chicago: University of Chicago Press.

Calixto, A., F. B. Diniz & P. H. T. Zannin. 2003. The statistical modeling of road traffic noise in an urban setting. Cities, 20, 23-29.

Canter, D. & K. Rees. 1982. A multivariate model of housing satisfaction. International Review of Applied Psychology, 31, 185-20.

Chan, Y.-K. 1999. Density, crowding, and factors intervening in their relationship: evidence from a hyperdense metropolis. Social Indicators Research, 48, 103-124.

Chang, C.-I. & D. C. Heinz (2000) Constrained subpixel target detection for remotely sensed imagery. *IEEE Transactions in Geoscience Remote Sensing,* 38**,** 1144-1159.

Clark, C. 1951. Urban population densities. Journal of the Royal Statistical Society, 114, 490-496.

Collins, W. G. & A. H. A. El-Beik (1971) Population census with the aid of aerial photographs: an experiment in the city of Leeds. *Photogrammetric Record,* 7**,** 16-26.

Cramer, V., S. Torgensen & E. Kringlen. 2004. Quality of life in a city: the effect of population density. Social Indicators Research, 69, 103-116.

Crowley, W. K. 1998. Modeling the Latin American city. Geographical Review, 88, 127-130.

Cummins, R. A. 1997. Assessing Quality of Life. In Quality of Life for People With Disabilities. Models, Research and Practice, ed. R. Brown. Cheltenham: Stanley Thornes.

Cummins, R. A. 2000. Objective and subjective quality of life: an interactive model. Social Indicators Research, 52, 55-72.

Dahmann, D. C. 1985. Assessments of neighborhood quality in Metropolitan America. Urban Affairs Review, 20, 511-535.

De Roo, A., J. Barredo, C. Lavalle, K. Bodis & R. Bonk. 2007. Potential Flood Hazard and Risk Mapping at Pan-European Scale In Digital Terrain Modelling: Lecture Notes in Geoinformation and Cartography, eds. R. J. Peckham & G. Jordan, 183-202. Springer Berlin Heidelberg.

Dempster, A. P. 1974. The direct use of likelihood for significance testing. In Proceedings of Conference on Foundational Questions in Statistical Inferences, 335-352. Department of Theoretical Statistics: University of Aarhus.

Denis, R. M. 2009. Port-au-Prince with Rachou Denis. <http://www.pikliz.com> (accessed on 24.9.09).

Dike, A. A. 1985. Environmental problems in Thirds World cties: A Nigerian example. Current Anthropology, 26, 501-505.

Dobson, J. E., E. A. Bright, P. R. Coleman, R. C. Durfee & B. A. Worley (2000) LandScan: A global population database for estimating populations at risk. *Photogrammetric Engineering and Remote Sensing,* 66**,** 849-857.

Dueker, K. & F. Horton. 1971. Toward geographic urban change detection systems with remote sensing inputs. In *Technical Papers, 37th Annual Meeting, American Society of Photogrammetry*, 204-218.

Elliott, P., D. J. Briggs, S. Morris, D. De Hoogh, C. Hurt & T. K. Jensen (2001) Risk of adverse birth outcomes in populations living near landfill sites. British Medical Journal, 323, 363-368.

English, P., R. Neutra, R. Scalf, M. Sullivan, L. Waller & L. Zhu. 1999. Examining associations between childhood asthma and traffic flow using a geographic information system. Environmental Health Perspectives, 1999, 761-767.

ESRI. 1996. ArcView GIS - The Geographic Information System for Everyone. Redlands, California: Environmental Systems Research Institute (ESRI).

Fang, Q., S. Harini & C. Yongwan (2010) Spatial autoregressive model for population estimation at the census block level using LIDAR-derived building volume information. *Cartography and Geographic Information Science,* 37**,** 239-257.

Felce, D. 1997. Defining and applying the concept of quality of life. Journal of Intellectual Disability Research, 41, 126-135.

Felce, D. & J. Perry. 1995. Quality of Life: Its Definition and Measurement. Research in Developmental Disabilities, 16, 51-74.

Feng, J., F. Wang & Y. Zhou. 2009. The spatial restructuration of population in metropolitan Beijing: toward polycentricity in the post-reform era. Urban Geography, 30, 779-802.

Ferdinando, F., M. Bonaiuto & M. Bonnes. 2010. Cross-Validation of Abbreviated Perceived Residential Environment Quality (PREQ) and Neighborhood Attachment (NA) Indicators. Environment and Behavior, 42, 171-196.

Ferguson, E. C., R. Maheswaran & M. Daly. 2004. Road-traffic pollution and asthma - using modeled exposure assessment for routine public health surveillance. International Journal of Health Geographics, 3:24, 1-7.

Field, A. 2005. Discovering statistics using SPSS. London: Sage Publications Ltd; 2nd Edition.

Fisher, P. & M. Langford. 1996. Modeling sensitivity to accuracy in classified imagery: a study of areal interpolation by dasymetric mapping. The Professional Geographer, 48, 299-309.

Fleury-Bahi, G., M.-L. Félonneau & M. Dorothée. 2008. Processes of Place Identificaion and Residential Satisfaction. Environment and Behavior, 40, 669-682.

Forster, B. C. (1985) An examination of some problems and solution in monitoring urban areas from satellite platforms. *Photogrammetric Engineering and Remote Sensing,* 49**,** 1693-1707.

Fotheringham, A. S., C. Brunsdon & M. Charlton. 2002. Geographically Weighted Regression: The analysis of spatially varying relationships. Chichester, UK.

Fox, J. 1984. Linear statistical models and related methods: With applications to social research. New York: John Wiley.

Fung, T. & W. Siu. 2000. Environmental quality and its changes, an analysis using NDVI. International Journal of Remote Sensing, 21, 1011-1024.

Galeon, F. A. (2008) Estimation of population in informal settlement communities using high resolution satellite image *The International Archives of the Photogrammetry, Remote Sensing and Spatial Information Sciences,* 37**,** 1377-1382.

Gall, M., B. J. Boruff & S. L. Cutter. 2007. Assessing Flood Hazard Zones in the Absence of Digital Floodplain Maps: Comparison of Alternative Approaches. Natural Hazards Review, 8, 12 pages.

Garcia-Mira, R., C. Arce & J. M. Sabucedo. 1997. Perceived quality of neighborhoods in a city in Northwest Spain: an individual differences scaling approach. Journal of Environmental Psychology, 17, 243-252.

Garrison, T. G. (2010) Remote sensing ancient Maya rural populations using QuickBird satellite imagery. *International Journal of Remote Sensing,* 31**,** 213-231.

Giannias, D. A. 1996. Quality of life in southern Ontario. Canadian Journal of Regional Science, 19, 213-223.

Gomez, F., L. Gil & J. Jabaloyes. 2004. Experimental investigation on the thermal comfort in the city: relationship with the green areas, interaction with the urban microclimate. Building and Environment, 39, 1077-1086.

Green, N. E. (1956) Aerial photographic analysis of residential neighborhoods: An evaluation of data accuracy. *Social Forces,* 35**,** 142-147.

Greene, R. P. & J. B. Pick. 2006. Exploring the Urban Community - A GIS approach. New Jersey: Prentice Hall series in GIS.

Griffin, E. & L. Ford. 1980. A Model of Latin American City Structure. Geographical Review, 70, 397-422.

Griffin, E. & L. Ford. 1993. Cities of Latin America. In Cities of the World: World Regional Urban Development, eds. S. D. Brunn & J. F. Williams, 25-265. HarperCollins, New York.

Griffith, D. 1981. Modeling urban population density in a multi-centered city. Journal of Urban Economics, 9, 298-310.

Guleid, A., H. M. Gadain, F. M. Muthusi & P. W. Muchiri. 2007. Improving Flood Forecasting and Early Warning in Somalia, Feasibility Study. Nairobi, Kenya: FAO-SWALIM.

Haas, B. K. 1999. A Multidisciplinary Concept Analysis of Quality of Life. Western Journal of Nursing Research, 21, 728-742.

Hagerty, M. R., R. A. Cummins, A. L. Ferriss, K. Land, A. C. Michalos, M. Peterson, A. Sharpe, M. J. Sirgy & J. Vogel. 2001. Quality of Life Indexes for National Policy: Review and Agenda for Research. Social Indicators Research, 55, 1-96.

Handal, P. J., P. W. Barling & E. Morrisy. 1981. Development of perceived and preferred measures of physical and social characteristics of the residential environment and their relationship to satisfaction. Journal of community Psychology, 9, 118-124.

Hardoy, J. E., D. Mitlin & D. Satterthwaite. 2001. Environmental problems in an urbanizing world. London and Sterling, VA: Earthscan Publications Ltd.

Hardoy, J. E. & D. Satterthwaite. 1991. Environmental problems of Third World cities: a global issue ignored? Public administration and development, 11, 341-361.

Harris, P., A. S. Fotheringham & M. Charlton. 2010. The use of geographically weighted regression for spatial prediction: an evalution of models using simulated data sets. Mathematical Geosciences, 42, 657-680.

Hartig, T. 2004. Restorative Environments. In: Spielberg, C. (Ed.), Encyclopedia of Applied Psychology Academic Press, Sand Diego USA, 3, 273-278.

Hartig, T. & C. Cooper-Marcus. 2006. Healing gardens - places for nature in health care. The Lancet, 372, 36-37.

Harvey, J. T. 2002a. Estimating census district populations from satellite imagery: some approaches and limitations. International Journal of Remote Sensing, 23, 2071-2095.

Harvey, J. T. 2002b. Population estimation models on individual TM pixels. Photogrammetric Engineering and Remote Sensing, 68, 1181-1192.

Heiken, G., R. H. Fakundiny & J. F. Sutter. 2003. Earth Science in the city: a reader. Washington, DC: American Geophysical Union.

Heikkika, E., P. Gordon, J. Kim, R. Peiser, H. Richardson & D. Dale-Johnson. 1989. What happened to the CBD-distance gradient?: Land values in a polycentric city. Environmment and Planning A, 21, 221-232.

Henderson, F. M. & Z.-G. Xia. 1997. SAR applications in human settlement detection, population estimation and urban land use pattern analysis: a status report. IEEE Transactions in Geosciences Remote Sensing, 35, 79-85.

Higgins, J. J. 2003. Introduction to Modern Nonparametric Statistics. Duxbury Press.

Hoek, G., B. Brunekreef, S. Goldbohm, P. Fischer & P. Van Den Brandt. 2002. Associations between mortality and indicators of traffic-related air pollution in the Netherlands: a cohort study. The Lancet, 360, 1203-1209.

Hoek, G., P. Fischer, P. Van Den Brandt, S. Sandra Goldbohm & B. Brunekreef. 2001. Estimation of long-term average exposure to outdoor air pollution for a cohort study on mortality. Journal of Exposure Analysis and Environmental Epidemiology, 11, 459-469.

Hopkins, W. G. 2000. A new View of Statistics. <http://www.sportsci.org/resource/stats/index.html > (accessed on 12.22.2010).

Howard, P. 1998. Environmental Scarcity and Conflict in Haiti: Ecology and Grievances in Haitiâ€™s Troubled Past and Uncertain Future. In Working paper 26-248, 59. Canadian International Development Agency.

Hoyt, H. 1939. The Structure and Growth of Residential Neighborhoods in American Cities. Washington, DC: USGPO.

Hsu, S. Y. (1971) Population estimation. *Photogrammetric Engineering* 37**,** 449-454.

Huang, Y. & Y. Leung. 2002. Analyzing regional industrialization in Jiangsu Province using Geographically Weighted Regression. Journal of Geographical Systems, 4, 233-249.

Hur, M. & H. Morrow-Jones. 2008. Factors that influence residents; satisfaction with neighborhoods. Environment and Behavior, 40, 619-635.

Hur, M., J. L. Nasar & B. Chun. 2009. Neighborhood satisfaction, physical and perceived naturalness and openness. Journal of Environmental Psychology, 30, 52-59.

IHSI. 2006. Recensement général de la population 2003. Port-au-Prince, Haiti: Institut Haitien de Statistiques et d'Informatiques.

Iisaka, J. & E. Hegedus (1981) Population estimatin from Landsat imagery. *Remote Sensing of Environment,* 12**,** 259-272.

Irrigaray Fernandez, C., T. F. Del Castillo, R. El Hamdouni & C. M. Montero. 1999. Verification of Landslide suceptibility mapping: a case study. Earth Surface Processes and Landforms, 24, 537-544.

Islam, M. M. & K. Sado. 2000. Flood hazard assessment in bangladesh using NOAA AVHRR data with geographical information system. Hydrological Processes, 14, 605-620.

Janse, A. J., R. J. Gemke, C. S. Uiterwaal, I. v. d. Tweel, J. L. Kimpen & G. Sinnema. 2004. Quality of Life: Patients and Doctors Don't Always Agree: a Meta-Analysis. Journal of Clinical Epidemiology, 57, 653-661.

Janssen, N. A. H., P. H. N. van Vliet, F. Aarts, H. Harssema & B. Bert. 2001. Assessment of exposure to traffic relatedair pollution of children attending schools near motorways. Atmospheric Environment, 35, 3875-3884.

Jenks, G. 1967. The data model concept in statistical mapping. International Yearbook of Cartography, 7, 186-190.

Jensen, J. R. 1983. Biophysical Remote Sensing. Annals of the Association of American Geographers, 73, 111-132.

Jensen, R., J. Gatrell, J. Boulton & B. Harper. 2004. Using Remote Sensing and Geographic Information Systems to Study Urban Quality of Life and Urban Forest Amenities. Ecology and Society, 9, 5.

Jerrett, M., A. Arain & P. Kanaroglou. 2005. A review and evaluation of intraurban air pollution exposure models. Journal of Exposure and Environmental Epidemiology, 15, 185-2004.

Jerrett, M., M. Sears, C. Giovis, R. Burnett, P. Kanaroglou, S. Elliott, S. Cakmak, P. Gossilin, Y. Bedard, J. Maclachlan & D. Cole. 2002. Intraurban Air Pollution Exposure and Asthma Prevalence in Hamilton, Canada. In The American Association of Geographerâ€™s Conference. Los Angeles, USA.

Ji, M. & J. R. Jensen. 1999. Effectiveness of subpixel analysis in detecting and quantifying urban imperviousness from Landsat Thematic Mapper imagery. Geocarto International, 14, 31-39.

Joseph, M. & F. Wang. 2010. Population Density Patterns in Port-Au-Prince, Haiti: A Model of Latin American City. Cities, 27, 127-136.

Joseph, M., L. Wang & F. Wang. 2012. Using Landsat Imagery and Census Data for Urban Population Density Modeling in Port-au-Prince, Haiti. GIScience & Remote Sensing, 49, 228-250.

Kaplan, S. 1995. The restorative benefit of nature: toward an integrative framework. Journal of Environmental Psychology, 15, 169-182.

Keene, O. N. 1995. The log transform is special. Statistics in Medicine, 14, 811-819.

Kelay, T. 2004. Integrating scientific and lay accounts of air pollution. Surrey, UK: University of Surrey.

Kelly, R. 2010. Harlan County landslide risk analysis, a geoprocessing task using ArcGIS Model Builder. In International Conference of GIS Users. San Diego, California: ESRI.

Kjellstrom, T. 2007. Our cities, our health, our future: Acting on social determinants for health equity in urban settings. 70. Kobe, Japan: WHO Centre for Health Development.

Kraus, S. P., L. W. Senger & J. M. Ryerson (1974) Estimating population from photographically determined residential land use types. *Remote Sensing of Environment,* 3**,** 35-42.

Ladd, H. F. & W. Wheaton. 1991. Causes and consequences of the changing urban form: introduction. Regional Science and Urban Economics 21, 157-162.

Lafortezza, R., G. Carrus, G. Sanesi & C. Davies. 2009. Benefits and well-being perceived by people visiting green spaces in periods of heat stress. Urban Forestry & Urban Greening, 8, 97-108.

Langford, M. 2006. Obtaining population estimates in non-census reporting zones: an evaluation of the 3-class dasymetric method. Computers, Environment and Urban Systems, 30, 161-180.

Langford, M., D. J. Maguire & D. J. Unwin. 1991. The areal interpolation problem: Estimating population using remote sensing within a GIS framework. Handling Geographical Information: Methodology and Potential Applications, 55-57.

Langford, M. & D. J. Unwin. 1994. Generating and mapping population density surfaces with a geographical information system. The Cartographic Journal, 31, 21-26.

Langholz, B., K. L. Ebi, D. C. Thomas, J. M. Peters & S. J. London. 2002. Traffic density and the risk of childhood leukemia in Los Angeles case-control study. Annals of Epidemiology, 2002, 482-487.

Leitmann, J., C. Bartone & J. Bernstein. 1992. Environmental management and urban development: issues and options for Third World cities. Environment and Urbanization, 4, 131-140.

Li, F., R. Wang, J. Pauluseen & X. Liu. 2005. Comprehensive concept planning of urban greening based on ecological principles: a case study in Beijing, China. Landscape and Urban Planning, 72, 325-336.

Li, G. & Q. Weng. 2005. Using Landsat ETM+ imagery to measure population density in Indianapolis, Indiana, USA. Photogrammetric Engineering and Remote Sensing, 71, 947-958.

Li, G. & Q. Weng. 2007. Measuring the quality of life in city of Indianapolis by integration of remote sensing and census data. International Journal of Remote Sensing, 28, 249-267.

Liu, X. 2003. Estimation of the spatial distribution of urban population using high spatial resolution satellite imagery. 175. Santa Barbara: University of California.

Liu, X., K. Clarke & M. Herold. 2006. Population Density and Image Texture: A comparison Study. Photogrammetric Engineering & Remote Sensing, 72, 187-196.

Lloyd, C. D. 2010. Nonstationary models for exploring and mapping monthly precipitation in the United Kingdom. International Journal of Climatology, 30, 390-405.

Lo, C. P. (1988) A raster approach to population estimation using high-altitude aerial and space photographs. *Remote Sensing of Environment,* 27**,** 59-71.

Lo, C. P. (1995) Automated population and dwelling unit estimation from high-resolution satellite images: a GIS approach. *International Journal of Remote Sensing,* 16**,** 1995.

Lo, C. P. (2001) Modeling the population of China using DMSP operational linescan system nighttime data. *Photogrammetric Engineering & Remote Sensing,* 67**,** 1037-1047.

Lo, C. P. (2002) Urban indicators of China from radiance-calibrated digital DMSP-OLS nighttime images. *Annals of the Association of American Geographers,* 92**,** 225-240.

Lo, C. P. 2008. Population estimation using Geographically Weighted Regression. GIScience & Remote Sensing, 45, 1548-1603.

Lo, C. P. & B. J. Faber. 1997. Integration of Landsat Thematic Mapper and Census Data for Quality of Life Assessment. Remote Sensing of the Environment, 62, 143-157.

Lo, C. P. & R. Welch (1977) Chinese urban population estimates. *Annals of the Association of American Geographers,* 67**,** 246-253.

Longley, P. A., M. F. Goodchild, D. J. Maguire & D. W. Rhind. 2005. Geographic Information Systems and Science. Wiley, 2nd edition.

Lotfi, S. & K. Solaimani. 2009. An assessment of urban quality of life by using analytic hierarchy process approach (Case study: comparative study of quality of life in the north of Iran). Journal of Social Sciences, 5, 123-133.

Lu, D. & Q. Weng (2006) Use of impervious surface in urban land-use classification. *Remote Sensing of Environment,* 102**,** 146-160.

Lu, D., Q. Weng & G. Li (2006) Residential population estimation using a remote sensing derived impervious surface approach. *International Journal of Remote Sensing,* 27**,** 3553-3570.

Lu, M. 1999. Determinants of residential satisfaction: ordered logit vs. regression models. Growth and Change, 30, 264-287

Lu, Z., J. IM, L. Quackenbush & K. Halligan (2010) Population estimation based on multi-sensor data fusion. *International Journal of Remote Sensing,* 31**,** 5587-5604.

Lynch, K. 1960. The Image of the City. Cambridge, MA: MIT Press.

Maheswaran, R. & P. Elliott. 2003. Stroke mortality associated with living near main roads in England and Wales: a geographical study. Stroke, 34, 2776-80.

Majumder, A. K., E. Hossain, N. Islam & I. Sarwar. 2007. Urban environmental quality mapping: a perception study on Chittagong Metropolitan City. Kathmandu University Journal of Science, Engineering and Technology, 1.

Marshall, J. D., T. E. Mckone, E. Deakin & W. W. Nazaroff. 2005. Inhalation of motor vehicle emissions: Effects of urban population and land area. Atmospheric Environment, 39, 283-295.

Mathieu, P., J. A. Constant, J. Noël & B. Piar. 2000. Cartes et étude de risques, de la vulnérabilité et des capacités de réponse en Haiti. Port-au-Prince, Haiti: OXFAM-GB.

McDonald, J. F. 1989. Econometric studies of urban population density: a survey. Journal of Urban Economics, 26, 361-385.

McDonald, J. F. & P. Prather. 1994. Suburban employment centers: The case of Chicago. Urban Studies, 31, 201-218.

Mercer. 2011. Mercer's 2011 Quality of Living ranking Highlights - Global. <http://www.mercer.com/articles/quality-of-living-survey-report-2011? (accessed on 04.01.2012).

Metropolitan-Studies-Group. 2010. Charlotte Neighborhood Quality of Life Study 2010 and Business Corridor Benchmarking Analysis. 247. Charlotte: University of North Carolina at Charlotte.

Mills, E. S. 1972. Studies in the structure of the urban economy. Baltimore: John Hopkins University.

Mills, E. S. & J. P. Tan. 1980. A comparison of urban population density functions in developed and developing countries. Urban Studies, 17, 313-321.

Mitchell, G., A. Namdeo & D. Kay. 2001. A new disease-burden method for estimating the impact of outdoor air quality on human health. Sci. Total Environ, 246, 153-164.

Mora, S. & W. G. Varhson. 1994. Macrozonation methodology for landslide hazard determination. Macrozonation methodology for landslide hazard determination, 31, 49-58.

Moser, G. 2009. Quality of life and sustainability: Toward person-environment congruity. Journal of Environmental Psychology, 29, 351-357.

MULTI-MENACE-HA. 2010. Analysis of Multiple Natural Hazards in Haiti. 63. Port-au-Prince, Haiti: Haitian Government.

Muth, R. 1969. Cities and Housing. Chicago: University of Chicago press.

Nafstad, P., L. L. Haheim, B. Oftedal, F. Gram, I. Holme, I. Hjermann & P. Leren. 2003.Lung cancer and air pollution: a 27-year follow-up of 16,209 Norwegian men. Thorax, 58, 1071-76.

Nichol, J. & M. S. Wong. 2009. Mapping urban environmental quality using satellite data and multiple parameters. Environment and Planning B: Planning and Design, 36, 170-185.

Nichol, J. E. & M. S. Wong. 2005. Modelling urban environmental quality in a tropical city. Landscape and Urban Planning, 73, 49-58.

Nikolopoulou, M. & K. Steemers. 2003. Thermal comfort and psychological adaptation as a guide for designing urban spaces. Energy and Buildings, 35, 95-101.

Norusis, M. 1983. Introductory statistics guide. New York: McGraw-Hill.

Nyambod, E. M. 2010. Environmental consequences of rapid urbanization: Bamenda City, Caomeroon. Journal of Environmental Protection, 1, 15-23.

Osarangi, T. 2002. Classification methods for spatial data representation. Working papers series, Paper 40.

Paez, A., T. Uchida & K. Miyamoto. 2002. A general framework for estimation and inference of geographically weighted regression models: 1. Location-specific kernel bandwidths and a test for locational heterogeneity. Environmental Planning, 34, 733-754.

Pamanikabud, P. & M. Tansatcha. 2003. Geographical information system for traffic noise analysis and forecasting with the appearance of barriers. Environmental Modelling & Software, 18, 959-973.

Pamuk, A. 2006. Mapping Global Cities - GIS Methods in Urban Analysis. Redlands, CA: ESRI Press.

Peters, J. C. 1998. HEC-HMS, Hydrologic Modeling Systems. Davis, CA: Hydrologic Engineering Center.

Porter, P. W. 1956. Population distribution and land use in Liberia. In *London school of Economics and Political Science*, 213. London, UK.

Prosperie, L. & R. Eyton (2000) The relationship between brightness values from a nighttime satellite image and Texas County population. *Southwestern Geographer,* 4**,** 16-29.

Pu, R., S. Landry & Q. Yu. 2009. Object-Based urban environment mapping with high spatial resolution Ikonos imagery. In ASPRS 2009 Annual Conference. Baltimore, Maryland.

Qiu, F., H. Sridharan & Y. Chun. 2010. Spatial autoregressive model for population estimation at the census block level using LIDAR-derived building volume information. Cartography and Geographic Information Science, 37, 239-257.

Qiu, F., K. Woller & R. Briggs (2003) Modeling urban population and regularization from airborne LIDAR point clouds. *Photogrammetric Engineering and Remote Sensing* 69**,** 1031-1042.

Radio Métropole, Haiti. 2003. Vers une catastrophe écologique nationale. <http://www.metropolehaiti.com> (accessed on 03.27.12)

Rahman, A., Y. Kumar, S. Fazal & S. Bhaskaran. 2011. Urbanization and quality or urban environment using remote sensing and GIS techniques in East Delhi-India. Journal of Geographic Information System, 3, 62-84.

Rashed, T., J. R. Weeks & M. S. Gadalla. 2001. Revealing the anatomy of cities through spectral mixture analysis of multispectral satellite imagery: a case study of the greater Cairo region, Egypt. Geocarto International, 16, 5-15.

Rehdanz, K. & D. Maddison. 2008. Local environmental quality and life-satisfaction in Germany. Ecological Economics, 64, 787-797.

Richman, B. T. 1994. Air pollution in the world's mega-cities. Environment, 36, 2-13.

Ridd, M. K. 1995 Exploring a V-I-S (vegetation-impervious surface-soil) model for urban ecosystem analysis through remote sensing: comparative anatomy for cities. International Journal of Remote Sensing, 16, 2165-2185.

Romero, H., A. Vásquez, C. Fuentes, M. Salgado, A. Schmidt & E. Banzhaf. 2012. Assessing urban environmental segregation (UES). The case of Santiago de Chile. Ecological Indicators, 23.

Saaty, T. L. 2005. Analytic Hierarchy Process. In Encyclopedia of Biostatistics. John Wiley & Sons, Ltd.

Sahsuvaroglu, T., M. Jerrett, M. R. Sears, R. McConnell, N. Finkelstein, A. Arain, B. Newbold & R. Burnett. 2009. Spatial analysis of air pollution and childhood asthma in Hamilton, Canada: comparing exposure methods in sensitive subgroups. Environmental Health, 8, 8-14.

Sanesi, G., R. Lafortezza, M. Bonnes & C. Giuseppe. 2006. Comparison of two different approaches for assessing the psychological and social dimensions of green spaces. Urban Forestry & Urban Greening, 5, 121-129.

Scawthorn, C., N. Blais, H. Seligson, E. Tate, E. Mifflin, W. Thomas, J. Murphy & C. Jones. 2006. HAZUS-MH flood loss estimation methodology. Part 1: Overview and flood hazard characterization. Natural Hazards Review, 7, 60-70.

Schaefer, K. A. 1990. The effect of floodplain designation/regulations on residential property values: a case study in North York, Ontario. Canadian Water Resources Journal, 15, 1-14.

Schalock, R. L. 1996. Reconsidering the Conceptualisation and Measurement of Quality of Life' in Schalock. In Quality of Life, Vol 1, Conceptualization and Measurement, ed. R. L. Washington: American Association on Mental Retardation

Schikowski, T., D. Sugiri, U. Ranft, U. Gehring, J. Heinrich, H.-E. Wichmann & U. Krämer. 2005. Long-term air pollution exposure and living close to busy roads are associated with COPD in women. Respiratory Research, 6:152.

Schweitzer, L. & J. Zhou. 2010. Neighborhood air quality, respiratory health, anv vulnerable populations in compact and sprawled regions. Journal of the American Planning Association, 76, 363-371.

Sengupta, S. K., C. Kamath, D. Poland & J. A. H. Futterman. 2003. Detecting human settlements in satellite images. Livermore, Ca: Laurence Livermore National Laboratory.

Shafer, C. S., B. Koo Lee & S. Turner. 2000. A tale of three greenway trails: user perceptions related to quality of life. Landscape and Urban Planning, 49, 163-178.

Shashua-Bar, L. & M. E. Hoffman. 2003. Vegetation as a climatic component in the design of an urban street. An empirical model for predicting the cooling effect of urban gree areas with trees. Energy and Buildings, 31, 221-235.

Shaw, G. & D. Wheeler. 1994. Statistical techniques in geographical analysis. New York: Wiley.

Shookner, M. 1997. The Quality of Life in Ontario. 20. Ontario: Ontario Social Development Council and Social Planning Network of Ontario.

Shroeder, M. A. 1990. Diagnosing and dealing with multicollinearity. Western Journal of Nursing Research, 12, 175-187.

Simon, L. J. 2004. Detecting multicollinearity using variance inflation factors. The Pennsylvania State University.

Small, K. A. & S. Song. 1994. Population and employment densities: Structure and change. Journal of Urban Economics, 36, 292-313.

Stutz, F. P. & B. Warf. 2007. The world economy: geography, business, development. Upper Saddle River: Prentice Hall.

Sutton, P. 1997. Modeling population density with nighttime satellite imagery and GIS. Computers, Environment, and Urban System, 21, 227-244.

Sutton, P., D. Roberts, C. Elvidge & K. Baugh. 2001. Census from Heaven: An estimate of the global human population using night-time satellite imagery. International Journal of Remote Sensing, 22, 9-22.

Sutton, P., D. Roberts, C. Elvidge & H. Meij. 1997. A comparison of nighttime satellite imagery and population density for the continental United States. Photogrammetric Engineering and Remote Sensing, 63, 1303-1313.

Szalai, A. 1980. The meaning of comparative research on the quality of life. In Szalai, A., Andrews, F. (Eds), The Quality of Life Sage Beverly Hills, 7-24.

Testa, M. A. 1996. Assessment of Quality-of-Life Outcomes. New England Journal of Medicine, 334, 835-840.

Tobin, G. A. & B. E. Montz. 1988. Catastrophic Flooding and the Response of the Real Estate Market. The Social Science Journal, 25, 167-177.

Tobin, G. A. & B. E. Montz. 1990. Response of the Real Estate Market to Frequent Flooding: The Case of Des Plaines, illinois. Bulletin of the Illinois Geographical Society, 32, 11-21.

Tobin, G. A. & B. E. Montz. 1994. The flood hazard and dynamics of the urban residential land market. Water Resources Bulletin, 30, 673-685.

Tobler, W. R. (1969) Satellite confirmation of settlement size coefficients. *Area*, 1**,** 30-34

Tobler, W. R. 1970. A computer movie simulating urban growth in the Detroit region. Economic Geography, 46, 234-240.

Tralli, D. M., R. G. Blom, V. Zlotnicki, A. Donnellan & D. L. Evans. 2005. Satellite remote sensing of earthquake, volcano, flood, landslide and coastal inundation hazards. ISPRS Journal of Photogrammetry and Remote Sensing, 59, 185-198.

Tzeng, G.-H., S.-H. Tsaur, Y.-D. Laiw & S. Opricovic. 2002. Multicriteria analysis of environmental quality in Taipei: public preferences and improvement strategies. Journal of Environmental Management, 65, 109-120.

Ulrich, R. S. 1984. View through a window may influence recovery from surgery. Science, 244, 420-421.

United Nations. 2003. World urbanization prospects. The 2003 revision - Data Tables and Highlights. New York: Economic and Social Affairs.

UNEP. 1996. International Source Book on Environmentally Sound Technologies for Municipal Solid Waste Management. UNEP Technical Publications.

USEPA. 1981. Noise effects handbook - A desk reference to health and welfare effects of noise. Fort Walton Beach, Fl: National Association of Noise Control Officials.

Van Kamp, I. V., K. Leidelmeijer, G. Marsman & A. de Hollander. 2003. Urban environmental quality and human well-being - Towards a conceptual framework and demarcation of concepts; a literature study. Landscape and Urban Planning, 65, 5-18.

Van Leeuwen, E. S., R. Vreeker & C. A. Rodenburg. 2006. A framework for quality of life assessment of urban gree areas in Europe: an application to District Park Reudnitz Leipzig. International Journal of Environmental Technology and Management, 6, 111-122.

Van Vliet, P., M. Knape, J. de Hartog, N. Janssen, H. Hendrik & B. Brunekreef. 1997. Motor Vehicle Exhaust and Chronic Respiratory Symptoms in Children Living near Freeways. Environmental Research, 74, 122-132.

Venn, A., S. Lewis, M. Cooper, R. Hubbard, I. Hill, R. Boddy, M. Bell & J. Britton. 2000. Local road traffic activity and the prevalence, severity, and persitence of wheeze in school children: combined cross sectional and longitudinal study. Occupational Environmental Medicine, 57, 152-158.

Venn, A. J., S. A. Lewis, M. Cooper, R. Hubbard & J. Britton. 2001. Living near a main road and the risk of wheezing illness in children. American Journal of Respiratory Critical Care Medicine, 164, 2177-2180.

Verluis, A. H. 1994. Methodology for predicting vehicle emissions on motorways and their impact on air quality in the Netherlands Science of The Total Environment, 146-147, 359-364.

Wade, T. G., J. D. Wickham, N. Zacarelli & K. H. Riitters. 2009. A multi-scale method of mapping urban influence. Environmental Modelling & Software, 24, 1252-1256.

Walton, D., S. J. Murray & J. A. Thomas. 2008. Relationships between population density and the perceived quality of neighborhood. Social Indicators Research, 89, 405-420.

Wang, F. 2006. Quantitative Methods and Application in GIS. Boca Raton, FL: Taylor & Francis.

Wang, F. & Y. Meng. 1999. Analyzing urban population change patterns in Shenyang, China 1982-1990: Density Function and spatial association approaches. Geographic Information Sciences, 5, 121-130.

Wang, F. & Y. Zhou. 1999. Modeling urban population densities in Beijing 1982-1990: Suburbanization and its Causes. Urban Studies, 36, 271-287.

Webster, C. J. 1996. Population and dwelling unit estimates from space. Third World Planning Review, 18, 155-176.

Weng, Q. & D. A. Quattrochi (2007) Urban Remote Sensing. *Landscape and Urban Planning*, 99**,** 259-260.

WHO. 1998. WHOQOL - Measuring quality of life. 15. Division of Mental Health and Prevention of Substance Abuse.

WHO. 2007. Our cities, our health, our future: Acting on social determinants for health equity in urban settings. ed. W. C. f. H. Development, 70. Kobe, Japan: WHO Kobe Centre.

WHOQOL-Group. 1995. The World Health Organization Quality of Life Assessment (WHOQOL): Position Paper From the World Health Organization'. Social Science and Medicine, 41, 1403-1409.

Wilhelm, M. & B. Ritz. 2003. Residential Proximity to Traffic and Adverse Birth Outcomes in Los Angeles County, California, 1994-1996. Environmental Health Perspectives, 111, 207-216.

Wilkinson, P., P. Elliott, C. Grundy, G. Shaddick, B. Thakrar, P. Walls & S. Falconer. 1999. Case-control study of hospital admission with asthma in children aged 5-14 years: relation with road traffic in North West London. Thorax, 54, 1070-1074.

Wu, C. (2004) Normalized spectral mixture analysis for monitoring urban composition using ETM+ imagery. *Remote Sensing of Environment*, 93**,** 480-492.

Wu, C. & A. T. Murray. 2003. Estimating impervious surface distribution by spectral mixture analysis. Remote Sensing of Environment, 84, 493-505.

Wu, C. & A. T. Murray. 2005. A cokriging method for estimating population density in urban areas. Computers, Environment and Urban Systems, 29, 558-579.

Wu, C. & A. T. Murray. 2007. Population estimation using Landsat Enhanced Thematic Mapper Imagery. Geographical Analysis, 39, 26-43.

Wu, S.-S., L. Wang & X. Qiu (2008) Incorporating GIS building data and census housing statistics for sub-block level population estimation. *The Professional Geographer,* 60**,** 121-135.

Wu, S., X. Qiu & L. Wang. 2005. Population estimation methods in GIS and Remote Sensing: A review. GIScience & Remote Sensing, 42, 80-96.

Yoshida, T., Y. Osada, T. Kawaguchi, Y. Hoshiyama, K. Yoshida & K. Yamamoto. 1997. Effects of road traffic noise on inhabitants of Tokyo. Journal of Sound and Vibration, 205, 517-522.

Young, O. C., C. Kil Jin & C. U. Choi. 2010. The comparative research of landslide susceptibility mapping using FR, AHP, LR, ANN. In International Conference of GIS Users. San Diego, California: ESRI.

Yu, D. & C. Wu (2004) Understanding Population Segregation from Landsat ETM+ Imagery: A Geographically Weighted Regression Approach. *Giscience & Remote Sensing,* 41**,** 187-206.

Yuan, Y., R. M. Smith & W. F. Limp. 1997. Remodeling census population with spatial information from Landsat TM imagery. Computers Environment and Urban Systems, 21, 245-258.

Zou, B., J. G. Wilson, F. B. Zhang & Y. Zeng. 2009. An emission-weighted proximity model for air pollution exposure assessment. Science of the Total Environment, 407, 4939-4945.

APPENDICES

Appendix I : Figures

Figure 32 : Top: Port-au-Prince, H. Truman Boulevard, south, occupied by a slum. Bottom: Cap-Haitian, north section of boulevard, a common place used for relaxation.

Figure 33 : Old and broken coffin exposed to plain sky in the cemetery of Port-au-Prince

Appendix II: Table

Table 8 : Parameters used in the model and processing

Domains	Sub-domains	Parameters	Sub-parameters	Operationalization
Group I Physical Domain	Environmental amenity	Greenness	Vegetation fraction	Obtained from V-I-S with LSMA
	Environmental pollution	Traffic gas emission	Elevation	0-240 meters (Classification with NB Jenks)
			Distance from roads	Up to 200 meters
			Building density	Impervious fraction (Classification with NB Jenks)
			Traffic density	Traffic density field based on road types and usage obtained from Google Earth images observation at peak hours
		Traffic noise	Distance from roads	Up to 500 meters
			Building density	Impervious fraction (Classification with NB Jenks)
			Traffic density	Traffic density field based on road types and usage obtained from Google earth images observation at peak hours
		Water pollution	Distance to waterways	Up to 400 meters
			Habitat density	(Classification with NB Jenks)
			Elevation	0-240 meters (Classification with NB Jenks)
			Slope	0-50%

Table 8 continued

Domains	Sub-Domains	Parameters	Sub-parameters	Operationalization
Group I Physical Domain (Cont.)	Environmental pollution (Cont.)	Coastal pollution	Distance to coast	Up to 1000 meters
			Habitat density	Classification with NB Jenks
			Land use	
			Waterways near the coast	Proximity and concentration (waterways length by coast section) of waterways to coast
Group II Public Domain		Slums		Slums and 200 meters buffer
		Public markets		300 meters buffer around lines and polygons
		Cemetery		400 meters
Group III Natural Hazards Domain		Flood probability	Floodplains	Difference between terrain height and river height for a 100-year event
				Distance thresholds within floodplains up to 500 meters
				Elevation thresholds up to 50 meters
		Landslide susceptibility	Slope	>= 20%
			Habitat density	Classification with NB Jenks
			Distance to water	50 meters
			Distance to roads	50 meters
		Coastal Surge		Difference between ground elevation and sea level for an event that could raise sea water up to 5 meters above ground

Appendix III: UEQ Model Builder

Appendix-III-a : Model global view

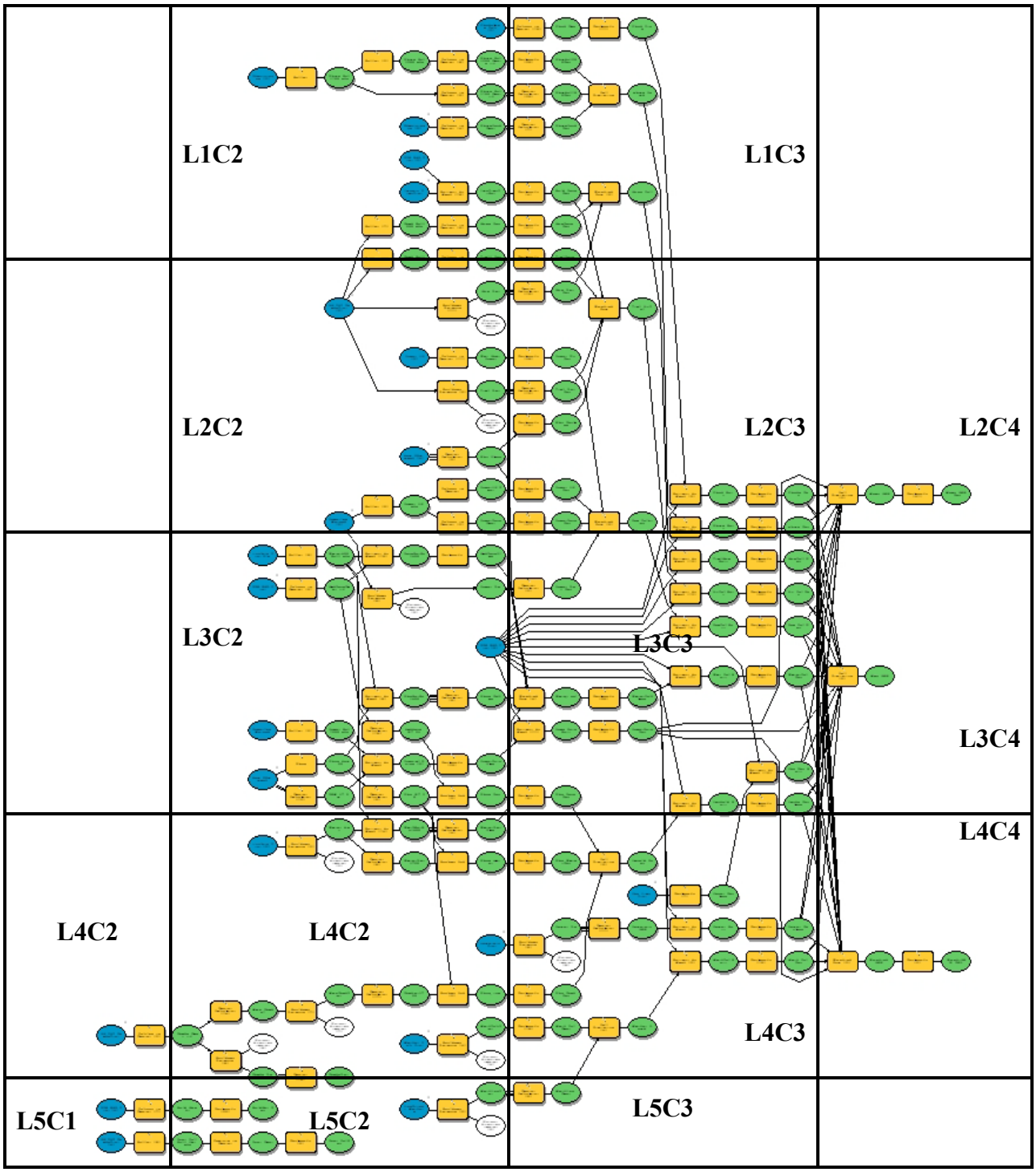

LiCj stands for Line i & Column j corresponding to the label of the detailed grids in the following pages.

Appendix-III-b: Model detailed view

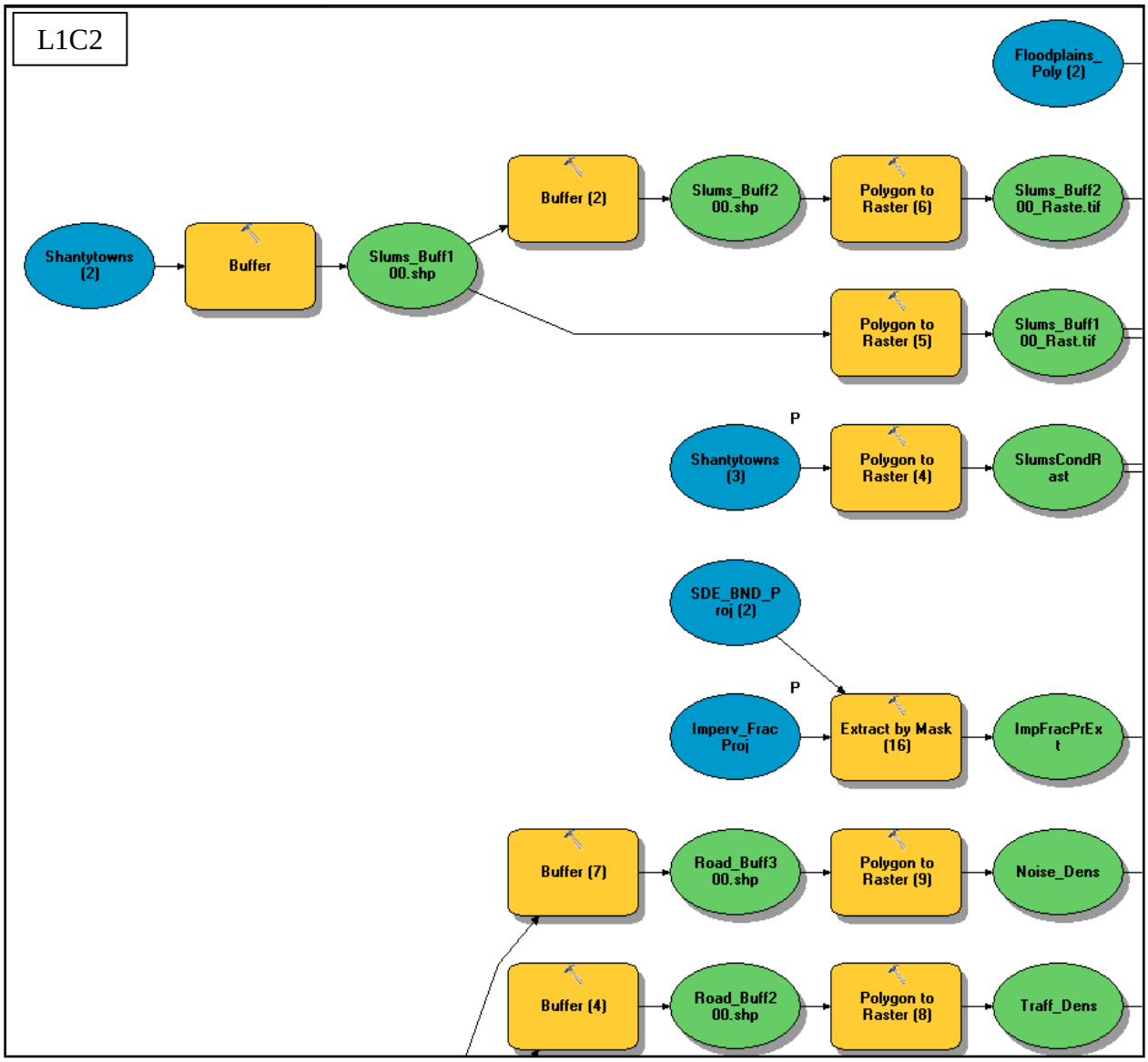

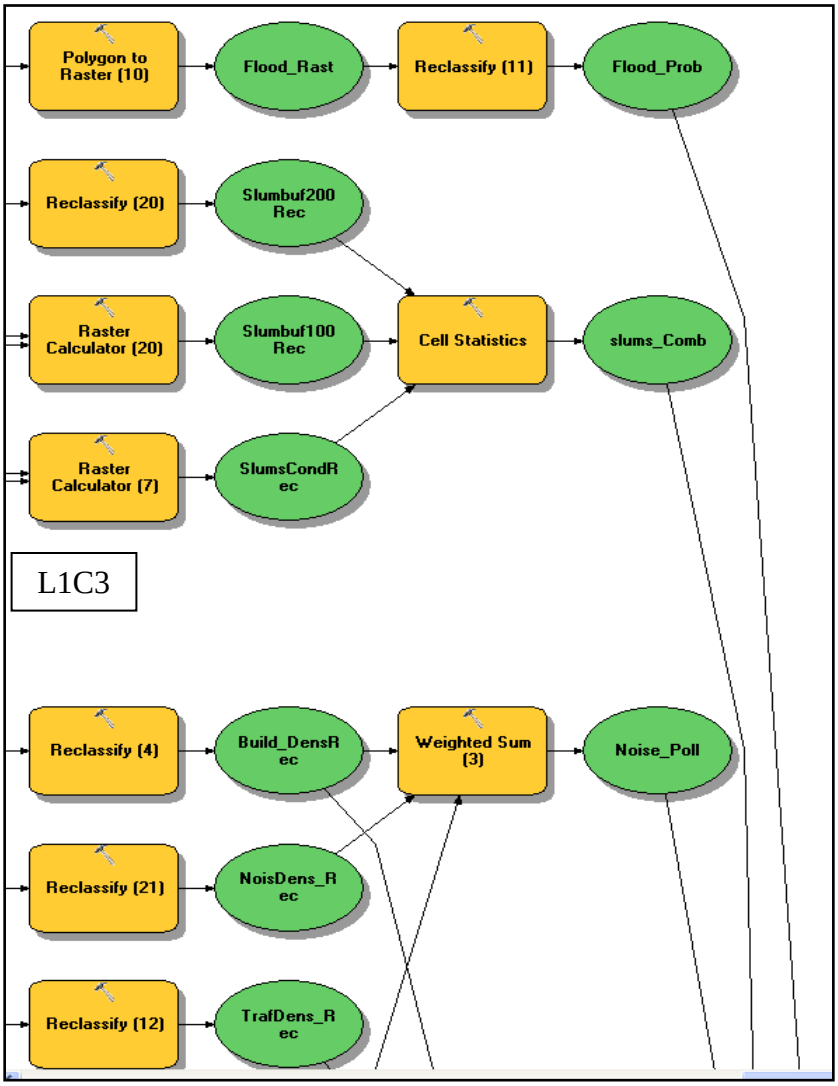
Polygon to Raster (10)
Flood_Rast
Reclassify (11)
Flood_Prob
Reclassify (20)
Slumbuf200 Rec
Raster Calculator (20)
Slumbuf100 Rec
Cell Statistics
slums_Comb
Raster Calculator (7)
SlumsCondRec
L1C3
Reclassify (4)
Build_DensRec
Weighted Sum (3)
Noise_Poll
Reclassify (21)
NoisDens_Rec
Reclassify (12)
TrafDens_Rec

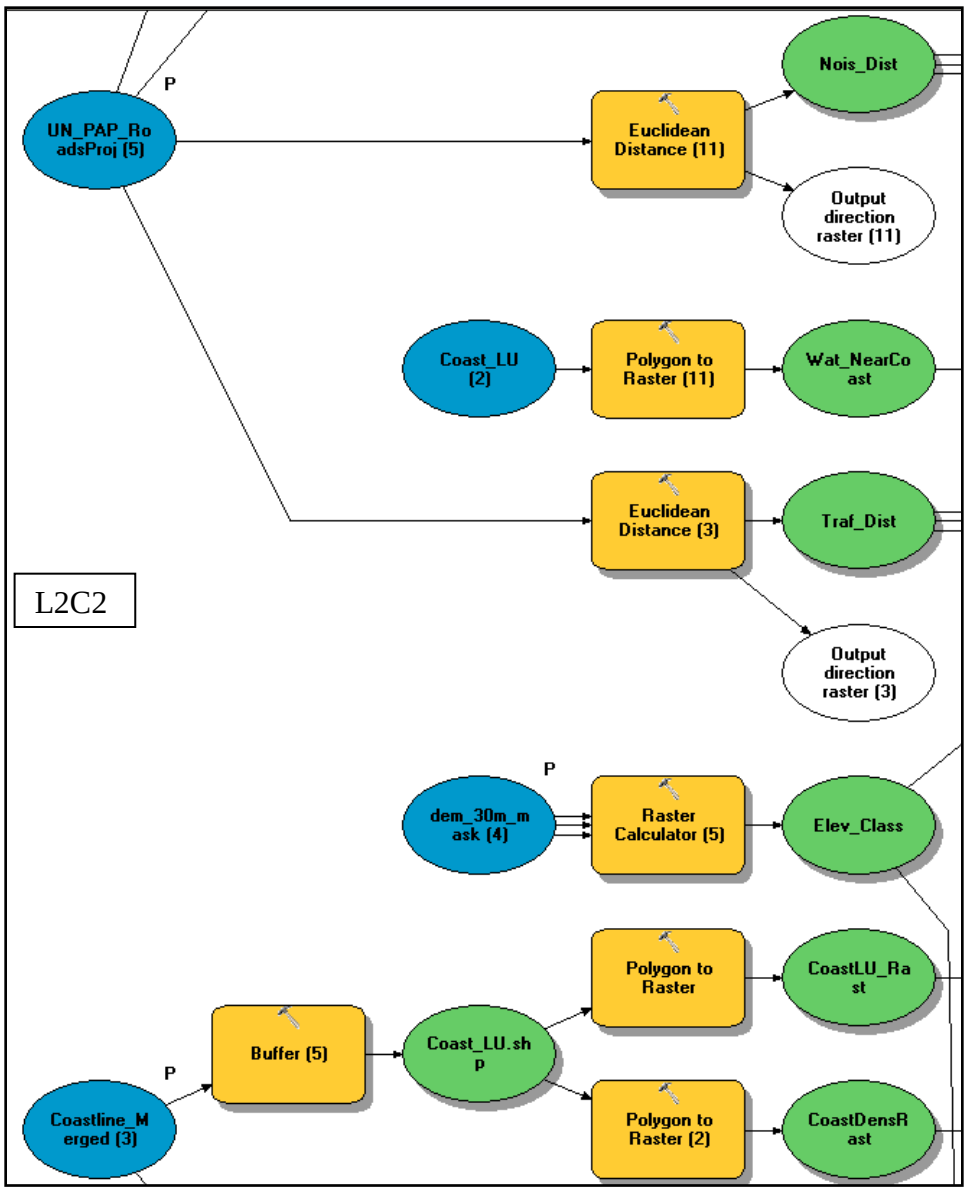
P
UN_PAP_RoadsProj (5)
Euclidean Distance (11)
Nois_Dist
Output direction raster (11)
Coast_LU (2)
Polygon to Raster (11)
Wat_NearCoast
Euclidean Distance (3)
Traf_Dist
L2C2
Output direction raster (3)
P
dem_30m_mask (4)
Raster Calculator (5)
Elev_Class
Polygon to Raster
CoastLU_Rast
P
Buffer (5)
Coast_LU.shp
Coastline_Merged (3)
Polygon to Raster (2)
CoastDensRast

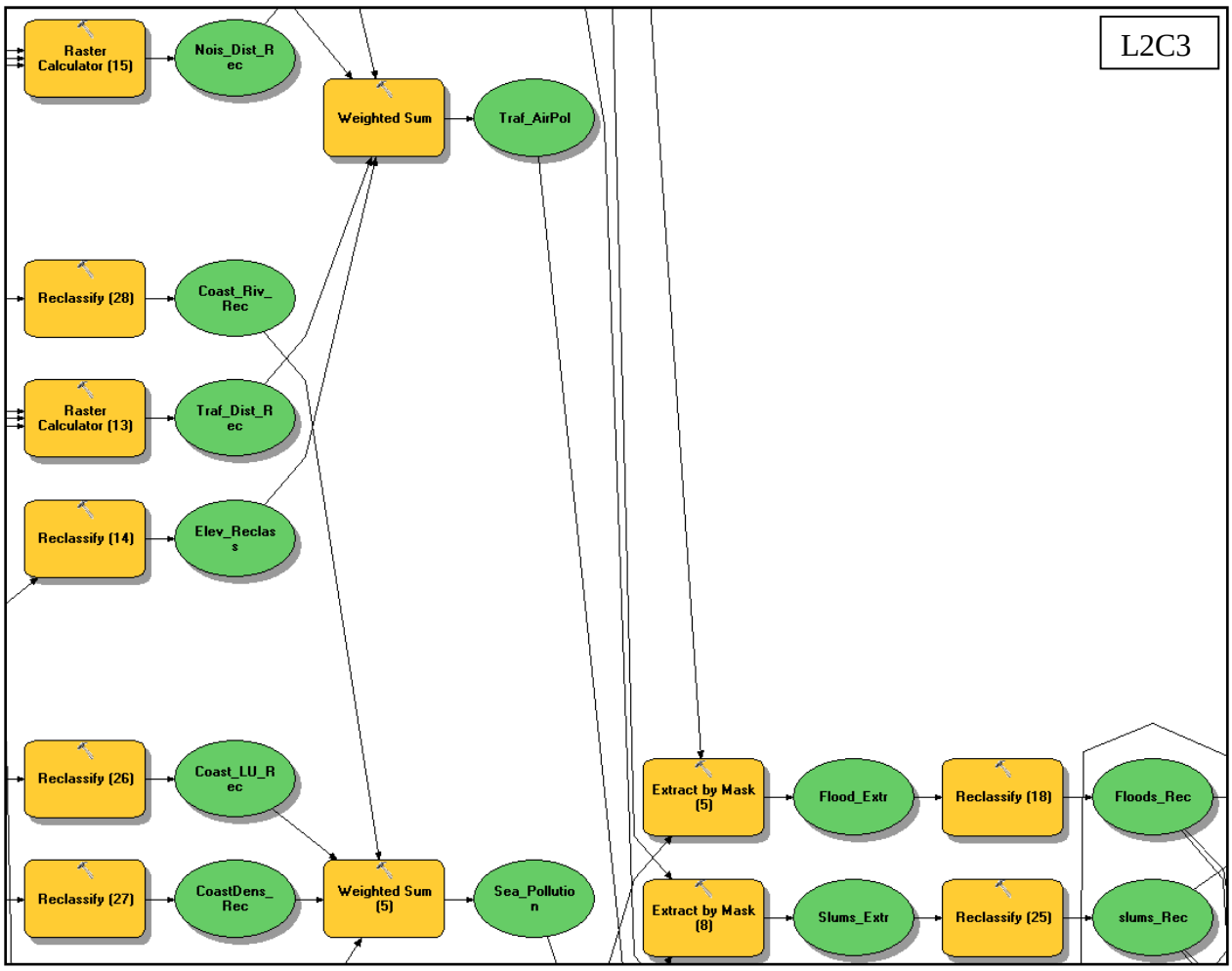
L2C3
Raster Calculator (15)
Nois_Dist_Rec
Weighted Sum
Traf_AirPol
Reclassify (28)
Coast_Riv_Rec
Raster Calculator (13)
Traf_Dist_Rec
Reclassify (14)
Elev_Reclass
Reclassify (26)
Coast_LU_Rec
Reclassify (27)
CoastDens_Rec
Weighted Sum (5)
Sea_Pollution
Extract by Mask (5)
Flood_Extr
Reclassify (18)
Floods_Rec
Extract by Mask (8)
Slums_Extr
Reclassify (25)
slums_Rec

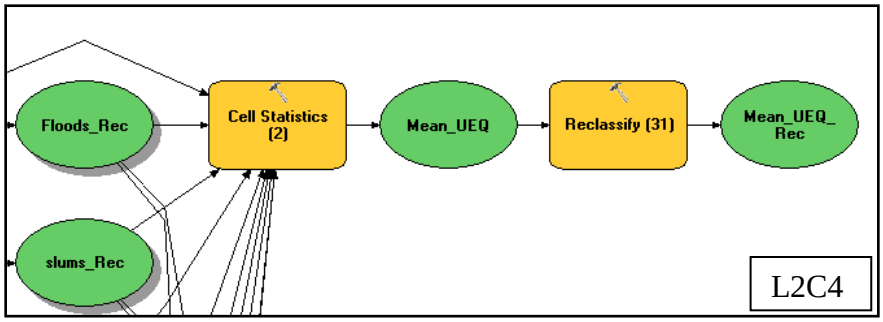
Floods_Rec
Cell Statistics (2)
Mean_UEQ
Reclassify (31)
Mean_UEQ_Rec
slums_Rec
L2C4

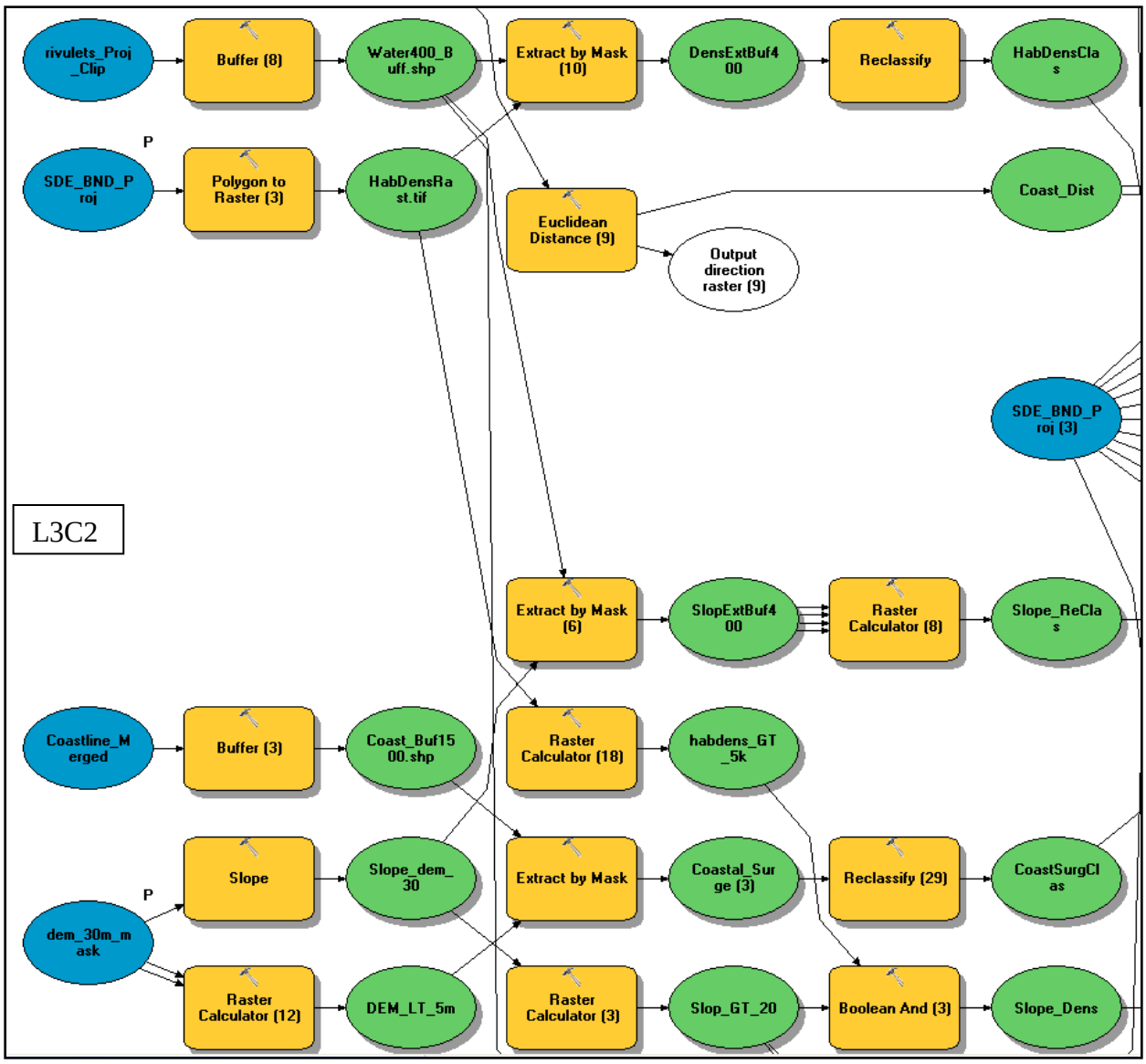
rivulets_Proj_Clip
Buffer (8)
Water400_Buff.shp
Extract by Mask (10)
DensExtBuf400
Reclassify
HabDensClas
SDE_BND_Proj
P
Polygon to Raster (3)
HabDensRast.tif
Euclidean Distance (9)
Coast_Dist
Output direction raster (9)
SDE_BND_Proj (3)
L3C2
Extract by Mask (6)
SlopExtBuf400
Raster Calculator (8)
Slope_ReClas
Coastline_Merged
Buffer (3)
Coast_Buf1500.shp
Raster Calculator (18)
habdens_GT_5k
Slope
Slope_dem_30
Extract by Mask
Coastal_Surge (3)
Reclassify (29)
CoastSurgClas
dem_30m_mask
P
Raster Calculator (12)
DEM_LT_5m
Raster Calculator (3)
Slop_GT_20
Boolean And (3)
Slope_Dens

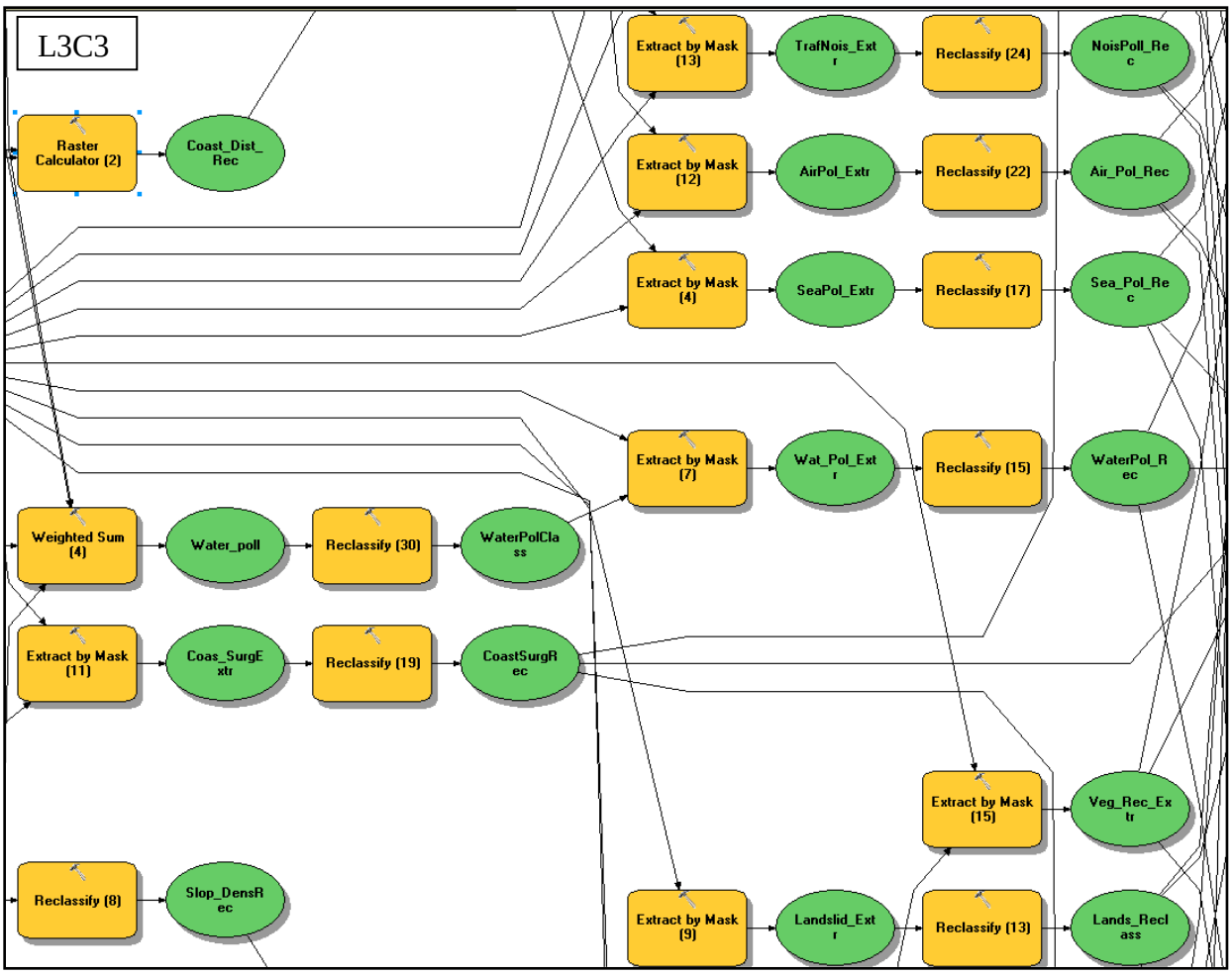
L3C3
Raster Calculator (2)
Coast_Dist_Rec
Extract by Mask (13)
TrafNois_Extr
Reclassify (24)
NoisPoll_Rec
Extract by Mask (12)
AirPol_Extr
Reclassify (22)
Air_Pol_Rec
Extract by Mask (4)
SeaPol_Extr
Reclassify (17)
Sea_Pol_Rec
Extract by Mask (7)
Wat_Pol_Extr
Reclassify (15)
WaterPol_Rec
Weighted Sum (4)
Water_poll
Reclassify (30)
WaterPolClass
Extract by Mask (11)
Coas_SurgExtr
Reclassify (19)
CoastSurgRec
Extract by Mask (15)
Veg_Rec_Extr
Reclassify (8)
Slop_DensRec
Extract by Mask (9)
Landslid_Extr
Reclassify (13)
Lands_Reclass

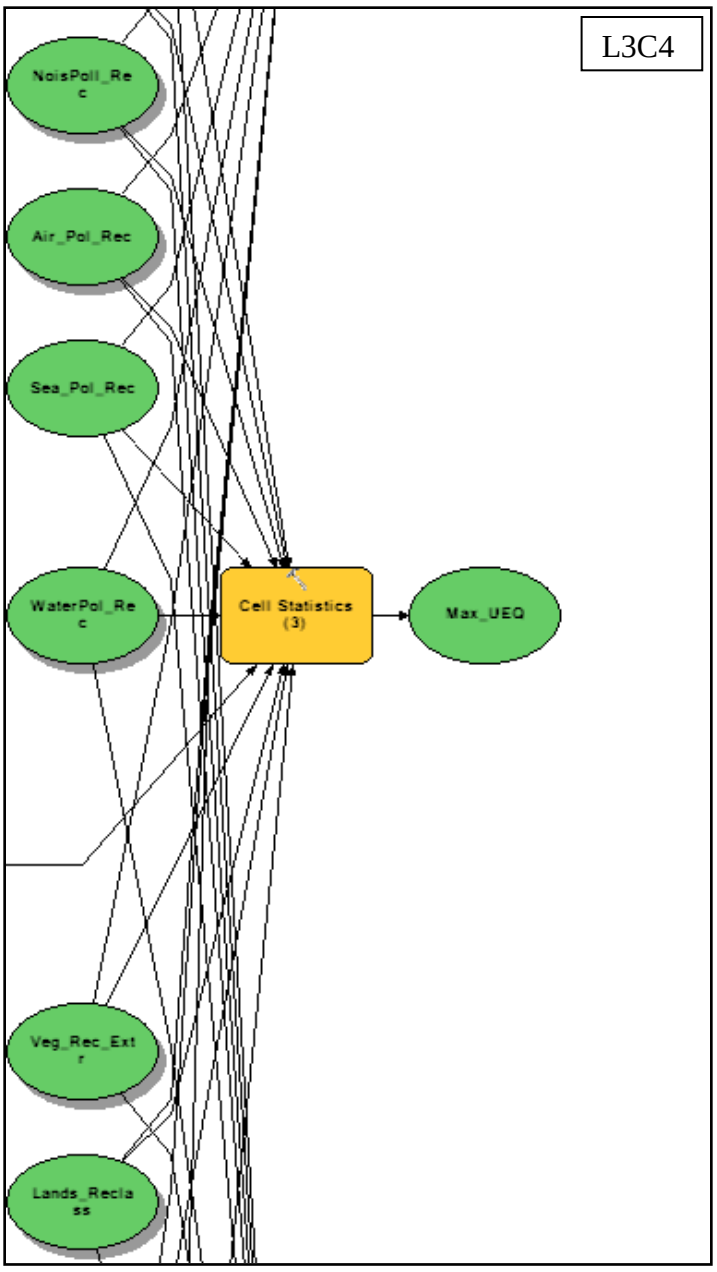
L3C4
NoisPoll_Rec
Air_Pol_Rec
Sea_Pol_Rec
WaterPol_Rec
Cell Statistics (3)
Max_UEQ
Veg_Rec_Extr
Lands_Reclass

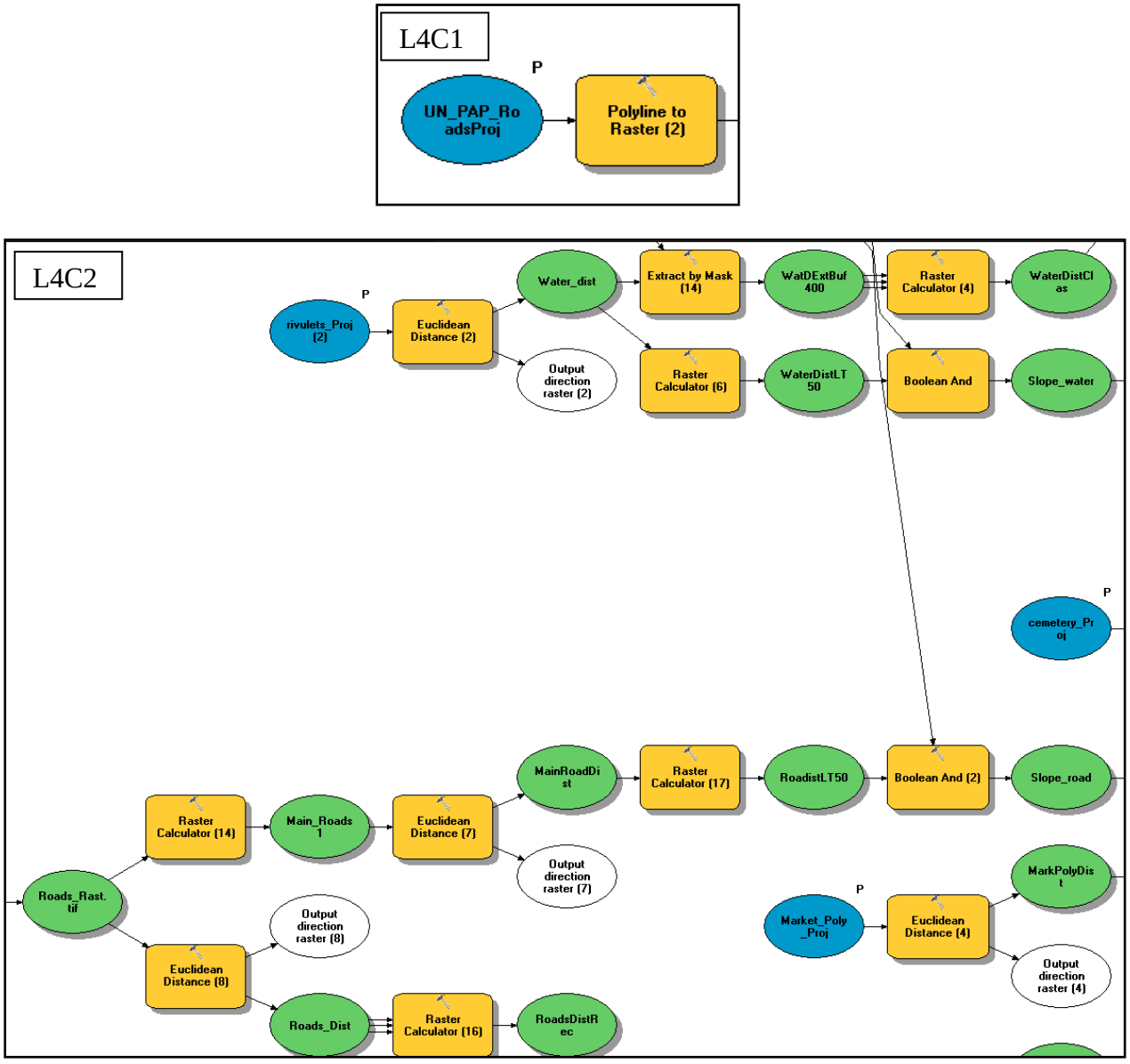
L4C1
P
UN_PAP_RoadsProj
Polyline to Raster (2)
L4C2
P
rivulets_Proj (2)
Euclidean Distance (2)
Water_dist
Output direction raster (2)
Extract by Mask (14)
Raster Calculator (6)
WatDExtBuf 400
WaterDistLT 50
Raster Calculator (4)
Boolean And
WaterDistClas
Slope_water
P
cemetery_Proj
Raster Calculator (14)
Main_Roads 1
Euclidean Distance (7)
MainRoadDist
Output direction raster (7)
Raster Calculator (17)
RoadistLT50
Boolean And (2)
Slope_road
Roads_Rast.tif
Euclidean Distance (8)
Output direction raster (8)
Roads_Dist
Raster Calculator (16)
RoadsDistRec
P
Market_Poly_Proj
Euclidean Distance (4)
MarkPolyDist
Output direction raster (4)

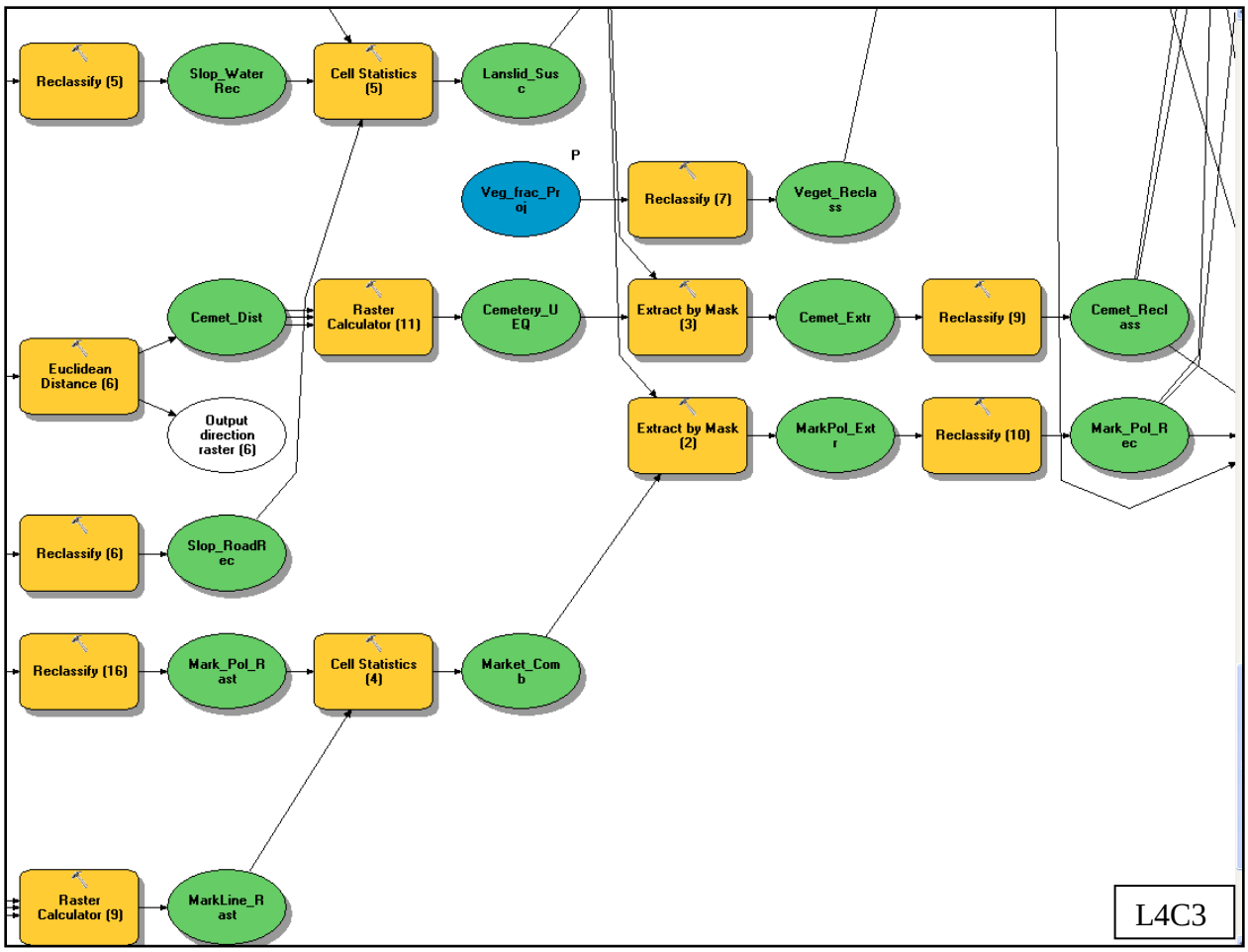
Reclassify (5)
Slop_Water Rec
Cell Statistics (5)
Lanslid_Susc
Veg_frac_Proj
Reclassify (7)
Veget_Reclass
Cemet_Dist
Raster Calculator (11)
Cemetery_UEQ
Extract by Mask (3)
Cemet_Extr
Reclassify (9)
Cemet_Reclass
Euclidean Distance (6)
Output direction raster (6)
Extract by Mask (2)
MarkPol_Extr
Reclassify (10)
Mark_Pol_Rec
Reclassify (6)
Slop_RoadRec
Reclassify (16)
Mark_Pol_Rast
Cell Statistics (4)
Market_Comb
Raster Calculator (9)
MarkLine_Rast
L4C3

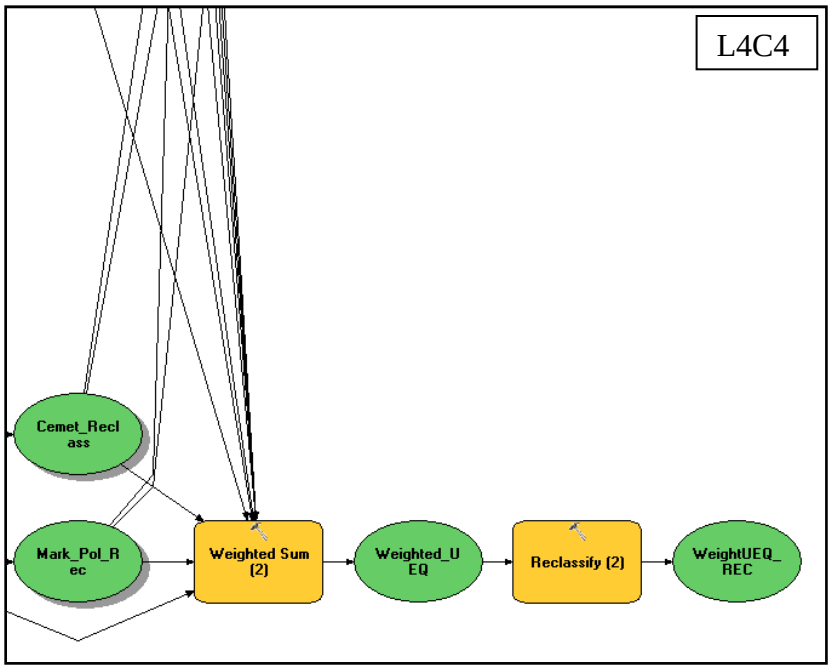
L4C4
Cemet_Reclass
Mark_Pol_Rec
Weighted Sum (2)
Weighted_UEQ
Reclassify (2)
WeightUEQ_REC

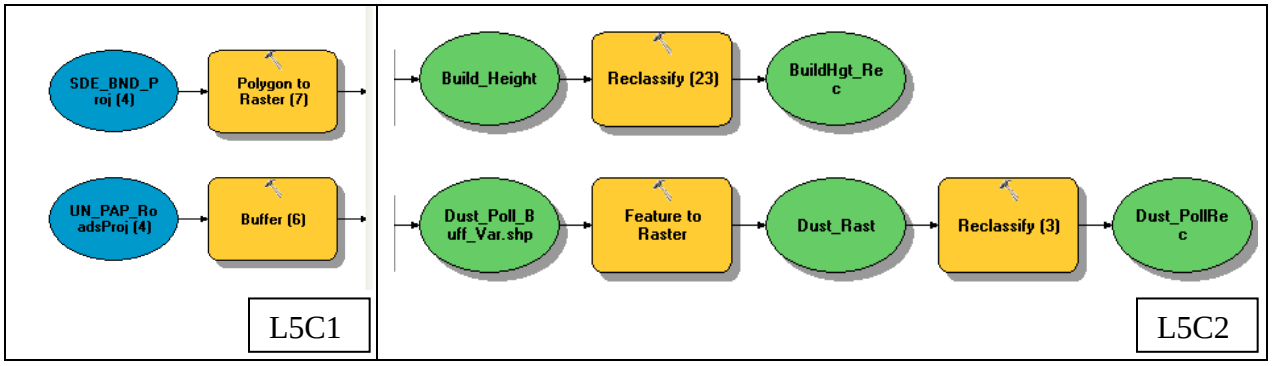
SDE_BND_Proj (4)
Polygon to Raster (7)
UN_PAP_RoadsProj (4)
Buffer (6)
L5C1
Build_Height
Reclassify (23)
BuildHgt_Rec
Dust_Poll_Buff_Var.shp
Feature to Raster
Dust_Rast
Reclassify (3)
Dust_PollRec
L5C2

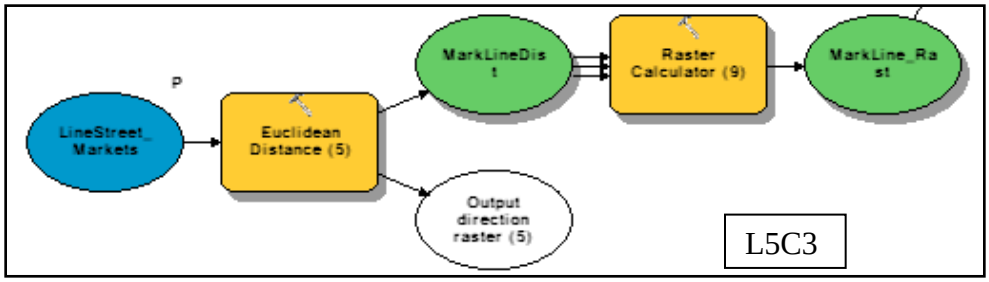
P
LineStreet_Markets
Euclidean Distance (5)
MarkLineDist
Output direction raster (5)
Raster Calculator (9)
MarkLine_Rast
L5C3

Appendix IV: UEQ Model Python Script

```
# UEQ_Script.py
# Created on: 2012-05-23 16:00:28.00000
#   (generated by ArcGIS/ModelBuilder)
# Usage: UEQ_Script <rivulets_Proj__2_> <dem_30m_mask> <SDE_BND_Proj>
<LineStreet_Markets> <cemetery_Proj> <Veg_frac_Proj>
<Coastline_Merged__3_> <Market_Poly_Proj> <UN_PAP_RoadsProj>
<dem_30m_mask__4_> <Imperv_FracProj> <UN_PAP_RoadsProj__5_>
<Shantytowns__3_>
# Description:
# Model built to assess the environmental quality of Port-au-Prince, Haiti
from multiple parameters.
# ---------------------------------------------------------------------------

# Import arcpy module
import arcpy

# Check out any necessary licenses
arcpy.CheckOutExtension("spatial")

# Set Geoprocessing environments
arcpy.env.scratchWorkspace = "C:\\Temp_Work\\Summer-
Fall_2011\\Paper_3.Data\\Intermediate_output"
arcpy.env.outputCoordinateSystem = ""
arcpy.env.extent = "777213.689602015 2048755.22666333 785664.268421347
2054658.29067428"
arcpy.env.cellSize = "30"
arcpy.env.mask = ""
arcpy.env.workspace = "C:\\Temp_Work\\Summer-
Fall_2011\\Paper_3.Data\\PAP_UEQ.mdb"

# Script arguments
rivulets_Proj__2_ = arcpy.GetParameterAsText(0)
if rivulets_Proj__2_ == '#' or not rivulets_Proj__2_:
    rivulets_Proj__2_ = "C:\\Temp_Work\\Summer-
Fall_2011\\Paper_3.Data\\PAP_UEQ.mdb\\rivulets_Proj" # provide a default
value if unspecified

dem_30m_mask = arcpy.GetParameterAsText(1)
if dem_30m_mask == '#' or not dem_30m_mask:
    dem_30m_mask = "C:\\Temp_Work\\Summer-
Fall_2011\\Paper_3.Data\\PAP_UEQ.mdb\\dem_30m_mask" # provide a default
value if unspecified

SDE_BND_Proj = arcpy.GetParameterAsText(2)
if SDE_BND_Proj == '#' or not SDE_BND_Proj:
    SDE_BND_Proj = "C:\\Temp_Work\\Summer-
Fall_2011\\Paper_3.Data\\PAP_UEQ.mdb\\SDE_BND_Proj" # provide a default
value if unspecified

LineStreet_Markets = arcpy.GetParameterAsText(3)
if LineStreet_Markets == '#' or not LineStreet_Markets:
```

```
    LineStreet_Markets = "C:\\Temp_Work\\Summer-
Fall_2011\\Paper_3.Data\\PAP_UEQ.mdb\\LineStreet_Markets" # provide a
default value if unspecified

cemetery_Proj = arcpy.GetParameterAsText(4)
if cemetery_Proj == '#' or not cemetery_Proj:
    cemetery_Proj = "C:\\Temp_Work\\Summer-
Fall_2011\\Paper_3.Data\\PAP_UEQ.mdb\\cemetery_Proj" # provide a default
value if unspecified

Veg_frac_Proj = arcpy.GetParameterAsText(5)
if Veg_frac_Proj == '#' or not Veg_frac_Proj:
    Veg_frac_Proj = "C:\\Temp_Work\\Summer-
Fall_2011\\Paper_3.Data\\PAP_UEQ.mdb\\Veg_frac_Proj" # provide a default
value if unspecified

Coastline_Merged__3_ = arcpy.GetParameterAsText(6)
if Coastline_Merged__3_ == '#' or not Coastline_Merged__3_:
    Coastline_Merged__3_ = "C:\\Temp_Work\\Summer-
Fall_2011\\Paper_3.Data\\PAP_UEQ.mdb\\Coastline_Merged" # provide a
default value if unspecified

Market_Poly_Proj = arcpy.GetParameterAsText(7)
if Market_Poly_Proj == '#' or not Market_Poly_Proj:
    Market_Poly_Proj = "C:\\Temp_Work\\Summer-
Fall_2011\\Paper_3.Data\\PAP_UEQ.mdb\\Market_Poly_Proj" # provide a
default value if unspecified

UN_PAP_RoadsProj = arcpy.GetParameterAsText(8)
if UN_PAP_RoadsProj == '#' or not UN_PAP_RoadsProj:
    UN_PAP_RoadsProj = "C:\\Temp_Work\\Summer-
Fall_2011\\Paper_3.Data\\PAP_UEQ.mdb\\UN_PAP_RoadsProj" # provide a
default value if unspecified

dem_30m_mask__4_ = arcpy.GetParameterAsText(9)
if dem_30m_mask__4_ == '#' or not dem_30m_mask__4_:
    dem_30m_mask__4_ = "C:\\Temp_Work\\Summer-
Fall_2011\\Paper_3.Data\\PAP_UEQ.mdb\\dem_30m_mask" # provide a default
value if unspecified

Imperv_FracProj = arcpy.GetParameterAsText(10)
if Imperv_FracProj == '#' or not Imperv_FracProj:
    Imperv_FracProj = "C:\\Temp_Work\\Summer-
Fall_2011\\Paper_3.Data\\PAP_UEQ.mdb\\Imperv_FracProj" # provide a default
value if unspecified

UN_PAP_RoadsProj__5_ = arcpy.GetParameterAsText(11)
if UN_PAP_RoadsProj__5_ == '#' or not UN_PAP_RoadsProj__5_:
    UN_PAP_RoadsProj__5_ = "C:\\Temp_Work\\Summer-
Fall_2011\\Paper_3.Data\\PAP_UEQ.mdb\\UN_PAP_RoadsProj" # provide a
default value if unspecified

Shantytowns__3_ = arcpy.GetParameterAsText(12)
if Shantytowns__3_ == '#' or not Shantytowns__3_:
```

```
    Shantytowns__3_ = "C:\\Temp_Work\\Summer-
Fall_2011\\Paper_3.Data\\PAP_UEQ.mdb\\Shantytowns" # provide a default
value if unspecified

# Local variables:
Roads_Rast_tif = UN_PAP_RoadsProj
Main_Roads1 = Roads_Rast_tif
MainRoadDist = Main_Roads1
RoadistLT50 = MainRoadDist
Slope_road = RoadistLT50
Slop_RoadRec = Slope_road
Lanslid_Susc = Slop_RoadRec
Landslid_Extr = Lanslid_Susc
Lands_Reclass = Landslid_Extr
Weighted_UEQ = Lands_Reclass
WeightUEQ_REC = Weighted_UEQ
Mean_UEQ = Lands_Reclass
Mean_UEQ_Rec = Mean_UEQ
Max_UEQ = Lands_Reclass
Output_direction_raster__7_ = Main_Roads1
Roads_Dist = Roads_Rast_tif
RoadsDistRec = Roads_Dist
Output_direction_raster__8_ = Roads_Rast_tif
Cemet_Dist = cemetery_Proj
Cemetery_UEQ = Cemet_Dist
Cemet_Extr = Cemetery_UEQ
Cemet_Reclass = Cemet_Extr
Output_direction_raster__6_ = cemetery_Proj
MarkLineDist = LineStreet_Markets
MarkLine_Rast = MarkLineDist
Market_Comb = MarkLine_Rast
MarkPol_Extr = Market_Comb
Mark_Pol_Rec = MarkPol_Extr
Output_direction_raster__5_ = LineStreet_Markets
Coast_LU_shp = Coastline_Merged__3_
CoastLU_Rast = Coast_LU_shp
Coast_LU_Rec = CoastLU_Rast
Sea_Pollution = Coast_LU_Rec
SeaPol_Extr = Sea_Pollution
Sea_Pol_Rec = SeaPol_Extr
CoastDensRast = Coast_LU_shp
CoastDens_Rec = CoastDensRast
Coast_Dist = Coastline_Merged__3_
Output_direction_raster__9_ = Coastline_Merged__3_
Water_dist = rivulets_Proj__2_
WaterDistLT50 = Water_dist
Slope_water = WaterDistLT50
Slop_WaterRec = Slope_water
WatDExtBuf400 = Water_dist
WaterDistClas = WatDExtBuf400
Water_poll = WaterDistClas
WaterPolClass = Water_poll
Wat_Pol_Extr = WaterPolClass
WaterPol_Rec = Wat_Pol_Extr
```

```
Output_direction_raster__2_ = rivulets_Proj__2_
HabDensRast_tif = SDE_BND_Proj
habdens_GT_5k = HabDensRast_tif
Slope_Dens = habdens_GT_5k
Slop_DensRec = Slope_Dens
DensExtBuf400 = HabDensRast_tif
HabDensClas = DensExtBuf400
Slope_dem_30 = dem_30m_mask
Slop_GT_20 = Slope_dem_30
SlopExtBuf400 = Slope_dem_30
Slope_ReClas = SlopExtBuf400
DEM_LT_5m = dem_30m_mask
Coastal_Surge__3_ = DEM_LT_5m
CoastSurgClas = Coastal_Surge__3_
Coas_SurgExtr = CoastSurgClas
CoastSurgRec = Coas_SurgExtr
Elev_Class = dem_30m_mask__4_
Elev_Reclass = Elev_Class
Traf_AirPol = Elev_Reclass
AirPol_Extr = Traf_AirPol
Air_Pol_Rec = AirPol_Extr
SlumsCondRast = Shantytowns__3_
SlumsCondRec = SlumsCondRast
slums_Comb = SlumsCondRec
Slums_Extr = slums_Comb
slums_Rec = Slums_Extr
MarkPolyDist = Market_Poly_Proj
Mark_Pol_Rast = MarkPolyDist
Output_direction_raster__4_ = Market_Poly_Proj
ImpFracPrExt = Imperv_FracProj
Build_DensRec = ImpFracPrExt
Noise_Poll = Build_DensRec
TrafNois_Extr = Noise_Poll
NoisPoll_Rec = TrafNois_Extr
Traf_Dist = UN_PAP_RoadsProj__5_
Traf_Dist_Rec = Traf_Dist
Output_direction_raster__3_ = UN_PAP_RoadsProj__5_
Road_Buff200_shp = UN_PAP_RoadsProj__5_
Traff_Dens = Road_Buff200_shp
TrafDens_Rec = Traff_Dens
Road_Buff300_shp = UN_PAP_RoadsProj__5_
Noise_Dens = Road_Buff300_shp
NoisDens_Rec = Noise_Dens
Nois_Dist = UN_PAP_RoadsProj__5_
Nois_Dist_Rec = Nois_Dist
Output_direction_raster__11_ = UN_PAP_RoadsProj__5_
Veget_Reclass = Veg_frac_Proj
Veg_Rec_Extr = Veget_Reclass
Shantytowns__2_ = "C:\\Temp_Work\\Summer-
Fall_2011\\Paper_3.Data\\PAP_UEQ.mdb\\Shantytowns"
UN_PAP_RoadsProj__4_ = "C:\\Temp_Work\\Summer-
Fall_2011\\Paper_3.Data\\PAP_UEQ.mdb\\UN_PAP_RoadsProj"
Coastline_Merged = "C:\\Temp_Work\\Summer-
Fall_2011\\Paper_3.Data\\PAP_UEQ.mdb\\Coastline_Merged"
```

```
SDE_BND_Proj__3_ = "C:\\Temp_Work\\Summer-
Fall_2011\\Paper_3.Data\\PAP_UEQ.mdb\\SDE_BND_Proj"
SDE_BND_Proj__4_ = "C:\\Temp_Work\\Summer-
Fall_2011\\Paper_3.Data\\PAP_UEQ.mdb\\SDE_BND_Proj"
Floodplains_Poly__2_ = "C:\\Temp_Work\\Summer-
Fall_2011\\Paper_3.Data\\PAP_UEQ.mdb\\Floodplains_Poly"
rivulets_Proj_Clip = "C:\\Temp_Work\\Summer-
Fall_2011\\Paper_3.Data\\PAP_UEQ.mdb\\rivulets_Proj_Clip"
SDE_BND_Proj__2_ = "C:\\Temp_Work\\Summer-
Fall_2011\\Paper_3.Data\\PAP_UEQ.mdb\\SDE_BND_Proj"
Coast_LU__2_ = "Coast_LU"
Dust_Poll_Buff_Var_shp = "C:\\Temp_Work\\Summer-
Fall_2011\\Paper_3.Data\\Intermediate_output\\Dust_Poll_Buff_Var.shp"
Coast_Dist_Rec = "C:\\Temp_Work\\Summer-
Fall_2011\\Paper_3.Data\\Intermediate_output\\Coast_Dist_Rec"
Dust_Rast = "C:\\Temp_Work\\Summer-
Fall_2011\\Paper_3.Data\\Intermediate_output\\Dust_Rast"
Dust_PollRec = "C:\\Temp_Work\\Summer-
Fall_2011\\Paper_3.Data\\Intermediate_output\\Dust_PollRec"
Slums_Buff100_shp = "C:\\Temp_Work\\Summer-
Fall_2011\\Paper_3.Data\\Intermediate_output\\Slums_Buff100.shp"
Slums_Buff200_shp = "C:\\Temp_Work\\Summer-
Fall_2011\\Paper_3.Data\\Intermediate_output\\Slums_Buff200.shp"
Slums_Buff100_Rast_tif = "C:\\Temp_Work\\Summer-
Fall_2011\\Paper_3.Data\\Intermediate_output\\Slums_Buff100_Rast.tif"
Slums_Buff200_Raste_tif = "C:\\Temp_Work\\Summer-
Fall_2011\\Paper_3.Data\\Intermediate_output\\Slums_Buff200_Raste.tif"
Slumbuf100Rec = "C:\\Temp_Work\\Summer-
Fall_2011\\Paper_3.Data\\Intermediate_output\\Slumbuf100Rec"
Coast_Buf1500_shp = "C:\\Temp_Work\\Summer-
Fall_2011\\Paper_3.Data\\Intermediate_output\\Coast_Buf1500.shp"
Slumbuf200Rec = "C:\\Temp_Work\\Summer-
Fall_2011\\Paper_3.Data\\Intermediate_output\\Slumbuf200Rec"
Build_Height = "C:\\Temp_Work\\Summer-
Fall_2011\\Paper_3.Data\\Intermediate_output\\Build_Height"
Flood_Rast = "C:\\Temp_Work\\Summer-
Fall_2011\\Paper_3.Data\\Intermediate_output\\Flood_Rast"
Flood_Prob = "C:\\Temp_Work\\Summer-
Fall_2011\\Paper_3.Data\\Intermediate_output\\Flood_Prob"
BuildHgt_Rec = "C:\\Temp_Work\\Summer-
Fall_2011\\Paper_3.Data\\Intermediate_output\\BuildHgt_Rec"
Wat_NearCoast = "C:\\Temp_Work\\Summer-
Fall_2011\\Paper_3.Data\\Intermediate_output\\Wat_NearCoast"
Flood_Extr = "C:\\Temp_Work\\Summer-
Fall_2011\\Paper_3.Data\\Intermediate_output\\Flood_Extr"
Floods_Rec = "C:\\Temp_Work\\Summer-
Fall_2011\\Paper_3.Data\\PAP_UEQ.mdb\\Floods_Rec"
Water400_Buff_shp = "C:\\Temp_Work\\Summer-
Fall_2011\\Paper_3.Data\\Intermediate_output\\Water400_Buff.shp"
Coast_Riv_Rec = "C:\\Temp_Work\\Summer-
Fall_2011\\Paper_3.Data\\Intermediate_output\\Coast_Riv_Rec"

# Process: Euclidean Distance (2)
```

```
arcpy.gp.EucDistance_sa(rivulets_Proj__2_, Water_dist, "", "30",
Output_direction_raster__2_)

# Process: Euclidean Distance (4)
arcpy.gp.EucDistance_sa(Market_Poly_Proj, MarkPolyDist, "", "30",
Output_direction_raster__4_)

# Process: Euclidean Distance (5)
arcpy.gp.EucDistance_sa(LineStreet_Markets, MarkLineDist, "", "30",
Output_direction_raster__5_)

# Process: Buffer (6)
arcpy.Buffer_analysis(UN_PAP_RoadsProj__4_, Dust_Poll_Buff_Var_shp,
"Dust_Buff", "FULL", "ROUND", "NONE", "")

# Process: Feature to Raster
arcpy.FeatureToRaster_conversion(Dust_Poll_Buff_Var_shp, "Dust_Cond",
Dust_Rast, "30")

# Process: Reclassify (3)
arcpy.gp.Reclassify_sa(Dust_Rast, "VALUE", "1 4;2 3;NODATA 1",
Dust_PollRec, "DATA")

# Process: Euclidean Distance (6)
arcpy.gp.EucDistance_sa(cemetery_Proj, Cemet_Dist, "", "30",
Output_direction_raster__6_)

# Process: Polyline to Raster (2)
arcpy.PolylineToRaster_conversion(UN_PAP_RoadsProj, "Traf_Dens",
Roads_Rast_tif, "MAXIMUM_LENGTH", "NONE", "30")

# Process: Raster Calculator (14)
arcpy.gp.RasterCalculator_sa("Con(\"%Roads_Rast.tif%\", 1,\"\", \"Value<=
2\")", Main_Roads1)

# Process: Euclidean Distance (7)
arcpy.gp.EucDistance_sa(Main_Roads1, MainRoadDist, "", "30",
Output_direction_raster__7_)

# Process: Euclidean Distance (8)
arcpy.gp.EucDistance_sa(Roads_Rast_tif, Roads_Dist, "", "30",
Output_direction_raster__8_)

# Process: Raster Calculator (16)
arcpy.gp.RasterCalculator_sa("Con(\"%Roads_Dist%\"
<=100,1,Con(\"%Roads_Dist%\" <= 200,2,Con(\"%Roads_Dist%\" <= 300,3,4)))",
RoadsDistRec)

# Process: Euclidean Distance (9)
arcpy.gp.EucDistance_sa(Coastline_Merged__3_, Coast_Dist, "", "30",
Output_direction_raster__9_)

# Process: Polygon to Raster (4)
```

```
arcpy.PolygonToRaster_conversion(Shantytowns__3_, "Conditions",
SlumsCondRast, "MAXIMUM_AREA", "NONE", "30")

# Process: Raster Calculator (7)
arcpy.gp.RasterCalculator_sa("Con(\"%SlumsCondRast%\" ==
1,1,Con(\"%SlumsCondRast%\" == 2,2,4))", SlumsCondRec)

# Process: Buffer
arcpy.Buffer_analysis(Shantytowns__2_, Slums_Buff100_shp, "100 Meters",
"OUTSIDE_ONLY", "ROUND", "NONE", "")

# Process: Polygon to Raster (5)
arcpy.PolygonToRaster_conversion(Slums_Buff100_shp, "Conditions",
Slums_Buff100_Rast_tif, "MAXIMUM_AREA", "NONE", "30")

# Process: Raster Calculator (20)
arcpy.gp.RasterCalculator_sa("Con(\"%Slums_Buff100_Rast.tif%\" ==
1,2,Con(\"%Slums_Buff100_Rast.tif%\" == 2,3,4))", Slumbuf100Rec)

# Process: Buffer (2)
arcpy.Buffer_analysis(Slums_Buff100_shp, Slums_Buff200_shp, "Dist_Buff2",
"OUTSIDE_ONLY", "ROUND", "NONE", "")

# Process: Polygon to Raster (6)
arcpy.PolygonToRaster_conversion(Slums_Buff200_shp, "Conditions",
Slums_Buff200_Raste_tif, "MAXIMUM_AREA", "NONE", "30")

# Process: Reclassify (20)
arcpy.gp.Reclassify_sa(Slums_Buff200_Raste_tif, "VALUE", "1 3;2 4;NODATA
5", Slumbuf200Rec, "DATA")

# Process: Cell Statistics
arcpy.gp.CellStatistics_sa("C:\\Temp_Work\\Summer-
Fall_2011\\Paper_3.Data\\Intermediate_output\\SlumsCondRec;C:\\Temp_Work\\
Summer-
Fall_2011\\Paper_3.Data\\Intermediate_output\\Slumbuf100Rec;C:\\Temp_Work\
\Summer-Fall_2011\\Paper_3.Data\\Intermediate_output\\Slumbuf200Rec",
slums_Comb, "MINIMUM", "DATA")

# Process: Extract by Mask (8)
arcpy.gp.ExtractByMask_sa(slums_Comb, SDE_BND_Proj__3_, Slums_Extr)

# Process: Reclassify (25)
arcpy.gp.Reclassify_sa(Slums_Extr, "VALUE", "1 2 4;3 3;4 2;5 1",
slums_Rec, "DATA")

# Process: Raster Calculator (12)
arcpy.gp.RasterCalculator_sa("Con(\"%dem_30m_mask%\",
\"%dem_30m_mask%\",\"\", \"Value<= 5\")", DEM_LT_5m)

# Process: Buffer (3)
arcpy.Buffer_analysis(Coastline_Merged, Coast_Buf1500_shp, "1500 Meters",
"FULL", "ROUND", "ALL", "")
```

```
# Process: Extract by Mask
arcpy.gp.ExtractByMask_sa(DEM_LT_5m, Coast_Buf1500_shp, Coastal_Surge__3_)

# Process: Reclassify (29)
arcpy.gp.Reclassify_sa(Coastal_Surge__3_, "Value", "0.67998182773590088
1.7248649718239903 1;1.7248649718239903 2.8203069777227938
2;2.8203069777227938 3.7977783060632646 3;3.7977783060632646
4.9943380355834961 4;NODATA 4", CoastSurgClas, "DATA")

# Process: Extract by Mask (11)
arcpy.gp.ExtractByMask_sa(CoastSurgClas, SDE_BND_Proj__3_, Coas_SurgExtr)

# Process: Reclassify (19)
arcpy.gp.Reclassify_sa(Coas_SurgExtr, "VALUE", "0.67998182773590088
1.7248649718239903 4;1.7248649718239903 2.8203069777227938
3;2.8203069777227938 3.7977783060632646 2;3.7977783060632646
4.9943380355834961 1", CoastSurgRec, "DATA")

# Process: Extract by Mask (16)
arcpy.gp.ExtractByMask_sa(Imperv_FracProj, SDE_BND_Proj__2_, ImpFracPrExt)

# Process: Reclassify (4)
arcpy.gp.Reclassify_sa(ImpFracPrExt, "Value", "-1.4988010832439613e-015
0.030776413157580836 1;0.030776413157580836 0.092329239472745461
2;0.092329239472745461 0.18081142730079452 3;0.18081142730079452
0.98999999999999999 4;1 1065098961 NODATA", Build_DensRec, "DATA")

# Process: Euclidean Distance (3)
arcpy.gp.EucDistance_sa(UN_PAP_RoadsProj__5_, Traf_Dist, "", "30",
Output_direction_raster__3_)

# Process: Raster Calculator (13)
arcpy.gp.RasterCalculator_sa("Con(\"%Traf_Dist%\" <=
50,4,Con(\"%Traf_Dist%\" <= 100,3,Con(\"%Traf_Dist%\" <= 200,2,1)))",
Traf_Dist_Rec)

# Process: Buffer (4)
arcpy.Buffer_analysis(UN_PAP_RoadsProj__5_, Road_Buff200_shp, "200
Meters", "FULL", "ROUND", "LIST", "OBJECTID;Traf_Dens")

# Process: Polygon to Raster (8)
arcpy.PolygonToRaster_conversion(Road_Buff200_shp, "Traf_Dens",
Traff_Dens, "MAXIMUM_AREA", "NONE", "30")

# Process: Reclassify (12)
arcpy.gp.Reclassify_sa(Traff_Dens, "VALUE", "1 4;2 3;3 2;4 1;NODATA 1",
TrafDens_Rec, "DATA")

# Process: Raster Calculator (5)
arcpy.gp.RasterCalculator_sa("Con(\"%dem_30m_mask (4)%\" <=
60,1,Con(\"%dem_30m_mask (4)%\" <= 143,2,Con(\"%dem_30m_mask (4)%\" <=
240,3, 4)))", Elev_Class)

# Process: Reclassify (14)
```

```
arcpy.gp.Reclassify_sa(Elev_Class, "VALUE", "1 4;1 2 3;2 3 2;3 4 1;NODATA
1", Elev_Reclass, "DATA")

# Process: Weighted Sum
arcpy.gp.WeightedSum_sa("C:\\Temp_Work\\Summer-
Fall_2011\\Paper_3.Data\\Intermediate_output\\Build_DensRec VALUE
0.228;C:\\Temp_Work\\Summer-
Fall_2011\\Paper_3.Data\\Intermediate_output\\Traf_Dist_Rec VALUE
0.287;C:\\Temp_Work\\Summer-
Fall_2011\\Paper_3.Data\\Intermediate_output\\TrafDens_Rec VALUE
0.304;C:\\Temp_Work\\Summer-
Fall_2011\\Paper_3.Data\\Intermediate_output\\Elev_Reclass VALUE 0.18",
Traf_AirPol)

# Process: Extract by Mask (12)
arcpy.gp.ExtractByMask_sa(Traf_AirPol, SDE_BND_Proj__3_, AirPol_Extr)

# Process: Reclassify (22)
arcpy.gp.Reclassify_sa(AirPol_Extr, "Value", "0.99900001287460327
1.8887343993410468 1;1.8887343993410468 2.5209140949882567
2;2.5209140949882567 3.0594375394284725 3;3.0594375394284725
3.9960000514984131 4", Air_Pol_Rec, "DATA")

# Process: Buffer (7)
arcpy.Buffer_analysis(UN_PAP_RoadsProj__5_, Road_Buff300_shp, "300
Meters", "FULL", "ROUND", "LIST", "OBJECTID;Traf_Dens")

# Process: Polygon to Raster (9)
arcpy.PolygonToRaster_conversion(Road_Buff300_shp, "Traf_Dens",
Noise_Dens, "MAXIMUM_AREA", "NONE", "30")

# Process: Reclassify (21)
arcpy.gp.Reclassify_sa(Noise_Dens, "VALUE", "1 4;2 3;3 2;4 1;NODATA 1",
NoisDens_Rec, "DATA")

# Process: Euclidean Distance (11)
arcpy.gp.EucDistance_sa(UN_PAP_RoadsProj__5_, Nois_Dist, "", "30",
Output_direction_raster__11_)

# Process: Raster Calculator (15)
arcpy.gp.RasterCalculator_sa("Con(\"%Nois_Dist%\" <=
100,4,Con(\"%Nois_Dist%\" <= 300,3,Con(\"%Nois_Dist%\" <= 500,2,1)))",
Nois_Dist_Rec)

# Process: Weighted Sum (3)
arcpy.gp.WeightedSum_sa("C:\\Temp_Work\\Summer-
Fall_2011\\Paper_3.Data\\Intermediate_output\\Build_DensRec VALUE
0.268;C:\\Temp_Work\\Summer-
Fall_2011\\Paper_3.Data\\Intermediate_output\\NoisDens_Rec VALUE
0.372;C:\\Temp_Work\\Summer-
Fall_2011\\Paper_3.Data\\Intermediate_output\\Nois_Dist_Rec VALUE 0.36",
Noise_Poll)

# Process: Extract by Mask (13)
```

```
arcpy.gp.ExtractByMask_sa(Noise_Poll, SDE_BND_Proj__3_, TrafNois_Extr)

# Process: Reclassify (24)
arcpy.gp.Reclassify_sa(TrafNois_Extr, "Value", "1.2680000066757202
2.0790625046938658 1;2.0790625046938658 2.6126562533900142
2;2.6126562533900142 3.0928906272165477 3;3.0928906272165477 4 4",
NoisPoll_Rec, "DATA")

# Process: Buffer (8)
arcpy.Buffer_analysis(rivulets_Proj_Clip, Water400_Buff_shp, "400 Meters",
"FULL", "ROUND", "NONE", "")

# Process: Extract by Mask (14)
arcpy.gp.ExtractByMask_sa(Water_dist, Water400_Buff_shp, WatDExtBuf400)

# Process: Raster Calculator (4)
arcpy.gp.RasterCalculator_sa("Con(\"%WatDExtBuf400%\" <=
200,1,Con(\"%WatDExtBuf400%\"
<=200,2,Con(\"%WatDExtBuf400%\"<=400,3,4)))", WaterDistClas)

# Process: Polygon to Raster (3)
arcpy.PolygonToRaster_conversion(SDE_BND_Proj, "Hab_Dens",
HabDensRast_tif, "CELL_CENTER", "NONE", "30")

# Process: Extract by Mask (10)
arcpy.gp.ExtractByMask_sa(HabDensRast_tif, Water400_Buff_shp,
DensExtBuf400)

# Process: Reclassify
arcpy.gp.Reclassify_sa(DensExtBuf400, "VALUE", "0 4072 4;4072 9559 3;9559
17811 2;17811 65000 1", HabDensClas, "DATA")

# Process: Slope
arcpy.gp.Slope_sa(dem_30m_mask, Slope_dem_30, "PERCENT_RISE", "1")

# Process: Extract by Mask (6)
arcpy.gp.ExtractByMask_sa(Slope_dem_30, Water400_Buff_shp, SlopExtBuf400)

# Process: Raster Calculator (8)
arcpy.gp.RasterCalculator_sa("Con(\"%SlopExtBuf400%\" <= 5,1,
Con(\"%SlopExtBuf400%\" <= 15,2, Con(\"%SlopExtBuf400%\" <=
25,3,Con(\"%SlopExtBuf400%\" <=50,4,5))))", Slope_ReClas)

# Process: Weighted Sum (4)
arcpy.gp.WeightedSum_sa("C:\\Temp_Work\\Summer-
Fall_2011\\Paper_3.Data\\Intermediate_output\\WaterDistClas VALUE
0.15;C:\\Temp_Work\\Summer-
Fall_2011\\Paper_3.Data\\Intermediate_output\\HabDensClas VALUE
0.25;C:\\Temp_Work\\Summer-
Fall_2011\\Paper_3.Data\\Intermediate_output\\Elev_Class VALUE
0.35;C:\\Temp_Work\\Summer-
Fall_2011\\Paper_3.Data\\Intermediate_output\\Slope_ReClas VALUE 0.25",
Water_poll)
```

```
# Process: Reclassify (30)
arcpy.gp.Reclassify_sa(Water_poll, "VALUE", "1 1.8960937224328518
4;1.8960937224328518 2.4894530791789293 3;2.4894530791789293
3.0828124359250069 2;3.0828124359250069 4.0999999046325684 1;NODATA 1",
WaterPolClass, "DATA")

# Process: Extract by Mask (7)
arcpy.gp.ExtractByMask_sa(WaterPolClass, SDE_BND_Proj__3_, Wat_Pol_Extr)

# Process: Reclassify (15)
arcpy.gp.Reclassify_sa(Wat_Pol_Extr, "VALUE", "1 1;2 2;3 3;4 4",
WaterPol_Rec, "DATA")

# Process: Raster Calculator (2)
arcpy.gp.RasterCalculator_sa("Con(\"%Coast_RivDist%\" <=
300,1,Con(\"%Coast_RivDist%\" <= 500,2, Con(\"%Coast_RivDist%\" <= 700,3,
Con(\"%Coast_RivDist%\" <= 1000, 4,5))))", Coast_Dist_Rec)

# Process: Buffer (5)
arcpy.Buffer_analysis(Coastline_Merged__3_, Coast_LU_shp, "Buffer",
"FULL", "ROUND", "NONE", "")

# Process: Polygon to Raster
arcpy.PolygonToRaster_conversion(Coast_LU_shp, "Coastal_LU", CoastLU_Rast,
"CELL_CENTER", "NONE", "30")

# Process: Reclassify (26)
arcpy.gp.Reclassify_sa(CoastLU_Rast, "VALUE", "1 1;2 2;3 3;4 4;NODATA 4",
Coast_LU_Rec, "DATA")

# Process: Polygon to Raster (2)
arcpy.PolygonToRaster_conversion(Coast_LU_shp, "Hab_Dens", CoastDensRast,
"CELL_CENTER", "NONE", "30")

# Process: Reclassify (27)
arcpy.gp.Reclassify_sa(CoastDensRast, "VALUE", "1 1;2 2;3 3;4 4;NODATA 4",
CoastDens_Rec, "DATA")

# Process: Polygon to Raster (11)
arcpy.PolygonToRaster_conversion(Coast_LU__2_,
"Coast_Int_Wat_Stats.SUM_Shape_Length", Wat_NearCoast, "CELL_CENTER",
"NONE", "30")

# Process: Reclassify (28)
arcpy.gp.Reclassify_sa(Wat_NearCoast, "Value", "0 1000 3;1001 3000 2;3001
8000 1;NODATA 4", Coast_Riv_Rec, "DATA")

# Process: Weighted Sum (5)
arcpy.gp.WeightedSum_sa("C:\\Temp_Work\\Summer-
Fall_2011\\Paper_3.Data\\Intermediate_output\\Coast_Dist_Rec VALUE
0.2;C:\\Temp_Work\\Summer-
Fall_2011\\Paper_3.Data\\Intermediate_output\\Coast_LU_Rec VALUE
0.3;C:\\Temp_Work\\Summer-
Fall_2011\\Paper_3.Data\\Intermediate_output\\CoastDens_Rec VALUE
```

```
0.3;C:\\Temp_Work\\Summer-
Fall_2011\\Paper_3.Data\\Intermediate_output\\Coast_Riv_Rec VALUE 0.2",
Sea_Pollution)

# Process: Extract by Mask (4)
arcpy.gp.ExtractByMask_sa(Sea_Pollution, SDE_BND_Proj__3_, SeaPol_Extr)

# Process: Reclassify (17)
arcpy.gp.Reclassify_sa(SeaPol_Extr, "VALUE", "1 1.5874999649822712
4;1.5874999649822712 2.7874998934566975 3;2.7874998934566975
3.7874998338520527 2;3.7874998338520527 4.1999998092651367 1",
Sea_Pol_Rec, "DATA")

# Process: Raster Calculator (3)
arcpy.gp.RasterCalculator_sa("Con(\"%Slope_dem_30%\" >= 20,1)",
Slop_GT_20)

# Process: Raster Calculator (6)
arcpy.gp.RasterCalculator_sa("Con(\"%Water_dist%\"  <=  50,1)",
WaterDistLT50)

# Process: Boolean And
arcpy.gp.BooleanAnd_sa(Slop_GT_20, WaterDistLT50, Slope_water)

# Process: Reclassify (5)
arcpy.gp.Reclassify_sa(Slope_water, "VALUE", "1 1;NODATA 4",
Slop_WaterRec, "DATA")

# Process: Raster Calculator (17)
arcpy.gp.RasterCalculator_sa("Con(\"%MainRoadDist%\" <=  50,1)",
RoadistLT50)

# Process: Boolean And (2)
arcpy.gp.BooleanAnd_sa(Slop_GT_20, RoadistLT50, Slope_road)

# Process: Reclassify (6)
arcpy.gp.Reclassify_sa(Slope_road, "VALUE", "1 2;NODATA 4", Slop_RoadRec,
"DATA")

# Process: Raster Calculator (18)
arcpy.gp.RasterCalculator_sa("Con(\"%HabDensRast.tif%\" >= 5000,1)",
habdens_GT_5k)

# Process: Boolean And (3)
arcpy.gp.BooleanAnd_sa(Slop_GT_20, habdens_GT_5k, Slope_Dens)

# Process: Reclassify (8)
arcpy.gp.Reclassify_sa(Slope_Dens, "VALUE", "1 3;NODATA 4", Slop_DensRec,
"DATA")

# Process: Cell Statistics (5)
arcpy.gp.CellStatistics_sa("C:\\Temp_Work\\Summer-
Fall_2011\\Paper_3.Data\\Intermediate_output\\Slop_WaterRec;C:\\Temp_Work\
\Summer-
```

```
Fall_2011\\Paper_3.Data\\Intermediate_output\\Slop_RoadRec;C:\\Temp_Work\\
Summer-Fall_2011\\Paper_3.Data\\Intermediate_output\\Slop_DensRec",
Lanslid_Susc, "MINIMUM", "DATA")

# Process: Extract by Mask (9)
arcpy.gp.ExtractByMask_sa(Lanslid_Susc, SDE_BND_Proj__3_, Landslid_Extr)

# Process: Reclassify (13)
arcpy.gp.Reclassify_sa(Landslid_Extr, "VALUE", "1 4;1 2 3;2 3 2;3 4 1",
Lands_Reclass, "DATA")

# Process: Reclassify (16)
arcpy.gp.Reclassify_sa(MarkPolyDist, "Value", "0 100 1;100 200 2;200 300
3;300 5000 4;NODATA 4", Mark_Pol_Rast, "DATA")

# Process: Raster Calculator (9)
arcpy.gp.RasterCalculator_sa("Con(\"%MarkLineDist%\" <= 100,1,
Con(\"%MarkLineDist%\" <= 200,2,Con(\"%MarkLineDist%\" <= 300,3,4)))",
MarkLine_Rast)

# Process: Cell Statistics (4)
arcpy.gp.CellStatistics_sa("C:\\Temp_Work\\Summer-
Fall_2011\\Paper_3.Data\\Intermediate_output\\Mark_Pol_Rast;C:\\Temp_Work\
\Summer-Fall_2011\\Paper_3.Data\\Intermediate_output\\MarkLine_Rast",
Market_Comb, "MINIMUM", "DATA")

# Process: Extract by Mask (2)
arcpy.gp.ExtractByMask_sa(Market_Comb, SDE_BND_Proj__3_, MarkPol_Extr)

# Process: Reclassify (10)
arcpy.gp.Reclassify_sa(MarkPol_Extr, "VALUE", "1 4;2 3;3 2;4 1",
Mark_Pol_Rec, "DATA")

# Process: Raster Calculator (11)
arcpy.gp.RasterCalculator_sa("Con(\"%Cemet_Dist%\" <=
200,1,Con(\"%Cemet_Dist%\" <= 300,2,Con(\"%Cemet_Dist%\" <= 400,3,4)))",
Cemetery_UEQ)

# Process: Extract by Mask (3)
arcpy.gp.ExtractByMask_sa(Cemetery_UEQ, SDE_BND_Proj__3_, Cemet_Extr)

# Process: Reclassify (9)
arcpy.gp.Reclassify_sa(Cemet_Extr, "VALUE", "1 4;1 2 3;2 3 2;3 4 1",
Cemet_Reclass, "DATA")

# Process: Polygon to Raster (10)
arcpy.PolygonToRaster_conversion(Floodplains_Poly__2_, "Flood_Prob",
Flood_Rast, "CELL_CENTER", "NONE", "30")

# Process: Reclassify (11)
arcpy.gp.Reclassify_sa(Flood_Rast, "VALUE", "1 4;2 3;3 2;4 1;NODATA 1",
Flood_Prob, "DATA")

# Process: Extract by Mask (5)
```

```
arcpy.gp.ExtractByMask_sa(Flood_Prob, SDE_BND_Proj__3_, Flood_Extr)

# Process: Reclassify (18)
arcpy.gp.Reclassify_sa(Flood_Extr, "VALUE", "1 1;2 2;3 3;4 4", Floods_Rec,
"DATA")

# Process: Reclassify (7)
arcpy.gp.Reclassify_sa(Veg_frac_Proj, "Value", "-2.2204460492503131e-015
0.11322939395904348 4;0.11322939395904348 0.31626141071319391
3;0.31626141071319391 0.53491127490997126 2;0.53491127490997126
0.999542236328125 1", Veget_Reclass, "DATA")

# Process: Extract by Mask (15)
arcpy.gp.ExtractByMask_sa(Veget_Reclass, SDE_BND_Proj__3_, Veg_Rec_Extr)

# Process: Weighted Sum (2)
arcpy.gp.WeightedSum_sa("C:\\Temp_Work\\Summer-
Fall_2011\\Paper_3.Data\\PAP_UEQ.mdb\\slums_Rec VALUE
0.1019;C:\\Temp_Work\\Summer-
Fall_2011\\Paper_3.Data\\PAP_UEQ.mdb\\CoastSurgRec VALUE
0.0685;C:\\Temp_Work\\Summer-
Fall_2011\\Paper_3.Data\\PAP_UEQ.mdb\\Air_Pol_Rec VALUE
0.0942;C:\\Temp_Work\\Summer-
Fall_2011\\Paper_3.Data\\PAP_UEQ.mdb\\NoisPoll_Rec VALUE
0.0918;C:\\Temp_Work\\Summer-
Fall_2011\\Paper_3.Data\\PAP_UEQ.mdb\\WaterPol_Rec VALUE
0.1012;C:\\Temp_Work\\Summer-
Fall_2011\\Paper_3.Data\\PAP_UEQ.mdb\\Sea_Pol_Rec VALUE
0.0949;C:\\Temp_Work\\Summer-
Fall_2011\\Paper_3.Data\\PAP_UEQ.mdb\\Lands_Reclass VALUE
0.0802;C:\\Temp_Work\\Summer-
Fall_2011\\Paper_3.Data\\PAP_UEQ.mdb\\Mark_Pol_Rec VALUE
0.0872;C:\\Temp_Work\\Summer-
Fall_2011\\Paper_3.Data\\PAP_UEQ.mdb\\Cemet_Reclass VALUE
0.0716;C:\\Temp_Work\\Summer-
Fall_2011\\Paper_3.Data\\PAP_UEQ.mdb\\Floods_Rec VALUE
0.0965;C:\\Temp_Work\\Summer-
Fall_2011\\Paper_3.Data\\PAP_UEQ.mdb\\Veg_Rec_Extr VALUE 0.1121",
Weighted_UEQ)

# Process: Reclassify (2)
arcpy.gp.Reclassify_sa(Weighted_UEQ, "VALUE", "1.0001000165939331
1.6215031240135431 1;1.6215031240135431 2.0327257686294615
2;2.0327257686294615 2.498778099194169 3;2.498778099194169
3.3394999504089355 4", WeightUEQ_REC, "DATA")

# Process: Polygon to Raster (7)
arcpy.PolygonToRaster_conversion(SDE_BND_Proj__4_, "Build_Height",
Build_Height, "MAXIMUM_AREA", "NONE", "30")

# Process: Reclassify (23)
arcpy.gp.Reclassify_sa(Build_Height, "VALUE", "1 4;2 3;3 2;4 1;NODATA 1",
BuildHgt_Rec, "DATA")
```

```
# Process: Cell Statistics (2)
arcpy.gp.CellStatistics_sa("C:\\Temp_Work\\Summer-
Fall_2011\\Paper_3.Data\\PAP_UEQ.mdb\\Floods_Rec;C:\\Temp_Work\\Summer-
Fall_2011\\Paper_3.Data\\PAP_UEQ.mdb\\slums_Rec;C:\\Temp_Work\\Summer-
Fall_2011\\Paper_3.Data\\PAP_UEQ.mdb\\NoisPoll_Rec;C:\\Temp_Work\\Summer-
Fall_2011\\Paper_3.Data\\PAP_UEQ.mdb\\CoastSurgRec;C:\\Temp_Work\\Summer-
Fall_2011\\Paper_3.Data\\PAP_UEQ.mdb\\Air_Pol_Rec;C:\\Temp_Work\\Summer-
Fall_2011\\Paper_3.Data\\PAP_UEQ.mdb\\WaterPol_Rec;C:\\Temp_Work\\Summer-
Fall_2011\\Paper_3.Data\\PAP_UEQ.mdb\\Sea_Pol_Rec;C:\\Temp_Work\\Summer-
Fall_2011\\Paper_3.Data\\PAP_UEQ.mdb\\Lands_Reclass;C:\\Temp_Work\\Summer-
Fall_2011\\Paper_3.Data\\PAP_UEQ.mdb\\Cemet_Reclass;C:\\Temp_Work\\Summer-
Fall_2011\\Paper_3.Data\\PAP_UEQ.mdb\\Mark_Pol_Rec;C:\\Temp_Work\\Summer-
Fall_2011\\Paper_3.Data\\PAP_UEQ.mdb\\Veg_Rec_Extr", Mean_UEQ, "MEAN",
"DATA")

# Process: Reclassify (31)
arcpy.gp.Reclassify_sa(Mean_UEQ, "Value", "1 1.3636363744735718
1;1.3636363744735718 1.8181818723678589 2;1.8181818723678589
2.2727272510528564 3;2.2727272510528564 3.1818182468414307
4;3.1818182468414307 129830184 5", Mean_UEQ_Rec, "DATA")

# Process: Cell Statistics (3)
arcpy.gp.CellStatistics_sa("C:\\Temp_Work\\Summer-
Fall_2011\\Paper_3.Data\\PAP_UEQ.mdb\\Floods_Rec;C:\\Temp_Work\\Summer-
Fall_2011\\Paper_3.Data\\PAP_UEQ.mdb\\slums_Rec;C:\\Temp_Work\\Summer-
Fall_2011\\Paper_3.Data\\PAP_UEQ.mdb\\NoisPoll_Rec;C:\\Temp_Work\\Summer-
Fall_2011\\Paper_3.Data\\PAP_UEQ.mdb\\CoastSurgRec;C:\\Temp_Work\\Summer-
Fall_2011\\Paper_3.Data\\PAP_UEQ.mdb\\Air_Pol_Rec;C:\\Temp_Work\\Summer-
Fall_2011\\Paper_3.Data\\PAP_UEQ.mdb\\WaterPol_Rec;C:\\Temp_Work\\Summer-
Fall_2011\\Paper_3.Data\\PAP_UEQ.mdb\\Sea_Pol_Rec;C:\\Temp_Work\\Summer-
Fall_2011\\Paper_3.Data\\PAP_UEQ.mdb\\Lands_Reclass;C:\\Temp_Work\\Summer-
Fall_2011\\Paper_3.Data\\PAP_UEQ.mdb\\Cemet_Reclass;C:\\Temp_Work\\Summer-
Fall_2011\\Paper_3.Data\\PAP_UEQ.mdb\\Mark_Pol_Rec;C:\\Temp_Work\\Summer-
Fall_2011\\Paper_3.Data\\PAP_UEQ.mdb\\Veg_Rec_Extr", Max_UEQ, "MAXIMUM",
"DATA")
```

Appendix V: Surveys

Appendix V-a: Experts' Survey

As an experienced professional, researcher or professor acquainted with the urban environment of Port-au-Prince, I am requesting your input to help weighing parameters affecting the quality of the environment in Port-au-Prince. Your participation will me complete my dissertation as Ph.D. candidate in Urban Geography at Louisiana State University in Baton Rouge, LA. Your answers will be used to generate an urban environmental quality (UEQ) index for Port-au-Prince, which will then be mapped.

Your participation is greatly appreciated.

Myrtho Joseph, Ph.D. candidate

What is your current occupation?
What is your major? (e.g. B.S./M.S./Ph.D. in environmental management, environmental studies, agronomy, water resources, natural resources, economy, civil engineering, geography, urban planning, public policies, urban architecture, sanitation, disaster management or any related field.

On a scale of 1 to 10, with 1 meaning extremely low and 10 extremely high, how would you rate these variables in relation to their impact on air pollution from traffic?

Parameters	1	2	3	4	5	6	7	8	9	10
Traffic Density										
Building Height										
Building Density										
Elevation										

On a scale of 1 to 10, with 1 meaning extremely low and 10 extremely high, how would you rate these variables in relation to their impact on noise pollution from traffic?

Parameters	1	2	3	4	5	6	7	8	9	10
Traffic Density										
Building Height										
Building Density										

On a scale of 1 to 10 with 1 meaning very low and 10 extremely important, how would you rate these parameters regarding their impact on environmental quality in Port-au-Prince?

Parameters	Scale									
	1	2	3	4	5	6	7	8	9	10
Vegetation/Greenness										
Crowdedness										
Solid waste										
Public markets										
Gas emission from traffic										
Noise pollution from traffic										
Polluted waterways										
The cemetery										
Flood-prone areas										
Landslide susceptibility										
Polluted seacoast										
Coastal surge/Tsunami										
Shanty towns										

Other (Please specify)

Appendix V-b: Professional profile and educational background of the experts

Experts	Occupation	Education Level
1.	Director of promotion and environmental education and durable development (DPREEDD)	B.S. in Civil Engineering M.S. Tourism & town planning, M.S. in Public Entities Management Ph.D. candidate in Town Planning and Development
2.	Environmental compliance specialist	M.S. in Navigation and Related Applications
3.	Research and Teaching Assistant	M.S. in Environmental Sciences
4.	Teacher-Researcher at Quisqueya University	Ph.D. in Urban Hydrology
5.	Graduate student	Ph.D. in Human Geography
6.	North-East program unit manager – Plan-International	M.S. in Agronomy
7.	Water, sanitation & hygiene division manager	B.S. in Civil Engineering M.S. in Environmental Management
8.	Energy & environment management specialist	M.S. in Energy and Environmental Management
9.	NGO's coordinator	B.S in Civil Engineering
10.	Agronomist	B.S. in Agronomy
11.	Civil Engineering and Environment	Ph.D. candidate in Environmental Hydrology
12.	Director of Water Quality & Environment Laboratory at Quisqueya University	Ph.D. in Urban Sanitation and Environment
13.	Finance & Management	M.S. in Urban Planning
14.	Development projects manager	M.S. in Natural Resources and Environment Management
15.	Engineer-Agronomist	M.S. in Urban Planning
16.	Food security management	B.S. in Agronomy

Appendix V-c: Lay-persons survey (English version)

Having lived in this neighborhood before the January 2010 earthquake, we solicit your participation to this survey which objective is to evaluate the conditions of the environment in your neighborhood. The information you provide will allow us to define and map a general index of environmental quality for Port-au-Prince.

We sincerely thank you for your participation.

Longitude ☐ Latitude ☐

1-1. SDE number

☐

1-2. Survey number

☐

2. Have you lived in this neighborhood before the earthquake ? (If yes, continue the survey ; otherwise stop and find the next qualified respondent)

Yes	No
☐	☐

3. Gender

Male	Female
☐	☐

4. Age

18-25	26-35	36-45	46-55	56-65	>65	Don't know
☐	☐	☐	☐	☐	☐	☐

5. What is your highest education level?

Never attended schol	Elementary school	A few years in middle school	At least 11th grade	Professional school	Some undergraduate studies	Completed university	At least a masters' Degree	No answer
☐	☐	☐	☐	☐	☐	☐	☐	☐

6. What are the general conditions of the neighborhood where you live?

Very bad	Bad	Fair	Good	Very good
1	2	3	4	5
☐	☐	☐	☐	☐

7. On a scale of 1 to 5 with one meaning very bad and 5 very good (9: not applicable or not a problem), how do you qualify your neighborhood regarding the following aspects:

	1	2	3	4	5	9
1) Vegetation (Greenness)						
2) Crowdedness						
3) Solid waste						
4) Public markets						
5) Gas emission from traffic						
6) Noise pollution from traffic						
7) Polluted waterways						
8) Proximity to the cemetery						
9) Living in flood-prone areas						
10) Living in zones susceptible to landslide						
11) Living near the polluted seacoast						
12) Coastal surge (Tsunami)						
13) Shantytowns						

Other (Provide details, please.)

Appendix V-d: Lay-persons survey (French version)

Ayant vécu dans ce quartier avant le tremblement de terre, nous sollicitons votre participation à cette enquête visant à évaluer les conditions de l'environnement dans votre quartier de résidence. Les informations fournies permettront de définir un indice général des conditions de l'environnement à Port-au-Prince, qui sera ensuite reproduit sur une carte géographique.

Merci infiniment de votre participation.

Longitude ☐ Latitude ☐

1-1. Numéro de la section d'énumération (SDE)

☐

1-2. Numéro du questionnaire

☐

2. Avez-vous vécu dans ce quartier avant le tremblement de terre? (Si oui, continuer l'enquête, sinon, terminer)

Oui	Non
☐	☐

3. Quel est votre sexe?

Homme	Femme
☐	☐

4. Quel est votre age?

18-25	26-35	36-45	46-55	56-65	>65	Ne sait pas
☐	☐	☐	☐	☐	☐	☐

5. Quel est votre plus haut niveau d'éducation?

N'a jamais fréquenté l'école	Ecole primaire	Quelques années en secondaire	Bac, au moins première partie	Ecole professionnelle	Quelques années à l'université	Achevé l'université	Au moins une maîtrise	Pas de réponse
☐	☐	☐	☐	☐	☐	☐	☐	☐

6. Dans quelle condition générale se trouve le quartier dans lequel vous vivez?

Très mauvaise	Mauvaise	Passable	Bonne	Très bonne
1	2	3	4	5
☐	☐	☐	☐	☐

7. Sur une échelle de 1 à 5 1 signifiant très mauvaise et 5 très bonne (9 pas applicable, ou ce n'est pas un problème), comment est la qualité de votre quartier en ce qui a trait aux aspects suivants:

	1	2	3	4	5	9
1) Vegetation, espace vert						
2) Trop de gens entassés dans le quartier						
3) Exposition aux ordures ménagères et autres fatras						
4) Marchés publics						
5) Pollution de l'air à cause du traffic						
6) Bruit provenant du traffic						
7) Proximité d'une rivière ou d'un ruisseau						
8) Proximité du cimetière de Port-au-Prince						
9) Risques d'inondations						
10) Risques de glissement de terrains (éboulement)						
11) Proximité de la mer polluée						
12) Marée montante ou raz-de-marée						
13) Proximité d'une bidonville						

Autres (donnez des détails svp)

Appendix VI: Permission to include published articles in the dissertation

Subject:RE: Publication authorization request
From: Andrew Bond (abond@bellpub.com)
To: myrthoj0101@yahoo.com;
Cc: JOHNJ@mailbox.sc.edu;
Date: Sunday, May 20, 2012 1:28 PM

Dear Myrtho Joseph,

As an authorized agent of Bellwether Publishing, Ltd. (the copyright holder of GIScience & Remote Sensing), I hereby grant your request to insert the paper “Using Landsat Imagery and Census Data for Urban Population Density Modeling in Port-au-Prince, Haiti” (published in the March-April 2012 issue of GIScience & Remote Sensing) in your dissertation. Should you need any additional information and/or assistance in this matter, please contact me directly.

Sincerely,

Andrew Bond

Managing Editor

Bellwether Publishing, Ltd.

8640 Guilford Road, Suite 200

Columbia, MD 21046

Phone: 410-290-3870

Fax: 410-290-8726

Email: abond@bellpub.com

ELSEVIER LICENSE
TERMS AND CONDITIONS

May 21, 2012

This is a License Agreement between Myrtho Joseph ("You") and Elsevier ("Elsevier") provided by Copyright Clearance Center ("CCC"). The license consists of your order details, the terms and conditions provided by Elsevier, and the payment terms and conditions.

All payments must be made in full to CCC. For payment instructions, please see information listed at the bottom of this form.

Supplier: Elsevier Limited
The Boulevard,Langford Lane
Kidlington,Oxford,OX5 1GB,UK

Registered Company Number: 1982084

Customer name: Myrtho Joseph

Customer address:2245 College Dr Baton Rouge, LA 70808

License number: 2912091002104

License date: May 18, 2012

Licensed content publisher: Elsevier

Licensed content publication: Cities

Licensed content title: Population density patterns in Port-au-Prince, Haiti: A model of Latin
American city?

Licensed content author: Myrtho Joseph,Fahui Wang

Licensed content date: June 2010

Licensed content volume number: 27

Licensed content issue number: 3

Number of pages: 10

Start Page: 127

End Page: 136

Type of Use: reuse in a thesis/dissertation

Portion: full article

Format: both print and electronic

Are you the author of this Elsevier article? Yes

Will you be translating? No

Order reference number: MJ1stpaper

Title of your thesis/dissertation :

URBAN POPULATION DENSITY AND ENVIRONMENTAL QUALITY IN PORT-AU-PRINCE,

HAITI: A GEOSTATISTICAL ANALYSIS

Expected completion date: Jul 2012

Estimated size (number of pages): 150

Elsevier VAT number: GB 494 6272 12

Permissions price: 0.00 USD

VAT/Local Sales Tax: 0.0 USD / 0.0 GBP

Total: 0.00 USD

VITA

Myrtho Joseph was born in 1968 in Plaisance, located in Haiti's north department. Trained in Economics and Statistics at undergraduate level, his 10 years of work experience in data analysis and in cartography and several short seminars received in GIS in the US during these 10 years developed his interest for the fields of Geography and Environmental Sciences. Deeply concerned with the deterioration of the urban and rural environment in Haiti, he has decided to pursue graduate studies in Geography and Environment. With the support of a Fulbright scholarship he completed a Master of Sciences in Natural Resources Information Science in 2007 at the University of Arizona. Then he moved to Baton Rouge to pursue a Ph.D. in Human Geography with a focus on Urban Geography.